NG-8.4 Low-Quality Natural Gas Sulfur Removal/Recovery

CONTRACT INFORMATION

Contract Number	DE-AC21-92MC29470
Contractor	CNG Research Company CNG Tower / 625 Liberty Avenue Pittsburgh, Pennsylvania 15222-3199
Contractor Project Manager	David A Damon (412) 227 1464
Principal Investigators	Lawrence A Siwajek Acrion Technologies, Inc 9099 Bank Street / Cleveland, Ohio 44125 (216) 573 1185
	Bruce W Klint BOVAR Inc, Western Research 1313 44th Avenue / Calgary, Alberta T2E 6L5 (403) 291 1313
METC Project Manager	Harold D Shoemaker (304) 291 4715
Period of Performance	October 1, 1992 - August 31, 1993
Schedule/Milestones	

FY93 Base Program Schedule

	O	N	D	J	F	M	A	M	J	J	A	S
NEPA Draft Report	✓	✓				✓					✓	
Conceptual Process Designs	✓	✓	✓	✓	✓	✓	✓	✓				
Experimental Research Plan	✓	✓	✓	✓	✓	✓	✓	✓			✓	
Task 2 Draft and Final Reports					✓	✓	✓	✓			✓	

OBJECTIVES

1. Develop conceptual process designs and economics for large scale (200 MMSCFD) treatment of low quality natural gas having high carbon dioxide content (>10%) and hydrogen sulfide.
2. Construct an experimental research plan for the Optional Program.

BACKGROUND

Low Quality Natural Gas (LQNG)

Natural gas is generally categorized as low quality if its acid gas content or inert content is above the minimum specifications of a natural gas transmission company. Pipeline specifications for acid gas content are usually a maximum of ¼ grain H_2S per 100 SCF (4 ppm H_2S) and less than 2%

CO_2. Hugman's [1] definition of low quality gas appears as suitable as any other: "*. . . any volume of gas containing levels of carbon dioxide above 2 percent or of nitrogen above 4 percent or gas with carbon dioxide plus nitrogen above 4 percent, or significant (more than trace) quantities of H_2S.*"

Motivation to Tap LQNG Reserves

Increased use of natural gas (methane) in the domestic energy market will force the development of large domestic non-producing gas reserves now considered low quality.

New Federal regulations embodied in the Clean Air Act of 1990, Title III and Title V, are creating strong new market opportunities for natural gas. These include natural gas co-firing and reburn in coal-fired power plants to help reduce SO_2 and NOx emissions; natural gas fired turbines for peak-shaving and on-site generation of electrical power and steam; and natural gas as an alternative clean transportation fuel. The American Gas Association forecasts these new markets will increase the annual demand for natural gas by 2 TCF, more than 13% of current production. To meet these anticipated gas supply demands, domestic production of natural gas must begin to exploit the large reserves of low quality gas available but not now produced for technical, economic, or environmental reasons.

Target LQNG

The target high acid gas LQNG for processing with the CFZ-CNG-Claus Process contains more than 10% CO_2, is contaminated with H_2S, possibly COS and other sulfur compounds, and may contain nitrogen and other inerts such as helium. Conventional gas treatment in the form of amine based chemical solvents, physical solvents, and newer membrane based processes, is accustomed to processing LQNG contaminated with only modest levels of acid gas, e.g., up to several percent of H_2S and CO_2. With the possible exception of physical absorption processes such as Selexol, existing technologies do not now process high acid gas LQNG in an economic, environmentally acceptable manner.

The major proven non-producing reserve of high acid gas LQNG is located in the LaBarge reservoir of southwestern Wyoming; the amount of gas is large, dwarfing all other proven reserves combined. Estimates place the LaBarge reservoir recoverable gas at 167 TCF (trillion cubic feet), of which at least 33 TCF is methane. The LaBarge reservoir is high in CO_2 and prone to other contaminants such as H_2S, COS, N_2 and He [1,2]

The CFZ/CNG-Claus process is designed to treat the relatively large quantity of LQNG containing >10% CO_2 which may also contain either or both of H_2S and COS and which cannot be economically treated on a large scale by other known technologies.

LQNG Production Barriers

There are many technical and economic barriers which now prevent the up-grade of LQNG to pipeline standards [3] These include but are not limited to:

- removal of H_2S to pipeline specification of 4 ppm H_2S;
- removal of N_2 to increase heating value, decrease transportation cost;
- regeneration of separating agents [4];
- degradation of polymeric membrane materials;
- poor selectivity for CH_4 in presence of acid gases, or for H_2S in presence of CO_2;
- separation of isolated acid gases into pure CO_2 and concentrated H_2S;
- recovery of sulfur from separated H_2S;
- dissipation of high CO_2 partial pressure available in high-CO_2 LQNG;
- recompression of CO_2 for commodity use or sales.

The above list mentions explicitly only the three major contaminants (aside from water) of LQNG: nitrogen, hydrogen sulfide, and carbon dioxide. The presence of additional contaminants, especially sulfur species such as carbonyl sulfide (COS) and mercaptans (RSH), increases the difficulty of treating LQNG.

CFZ-CNG LQNG Process

The technology comprises four process technologies integrated to produce pipeline methane from LQNG by efficient separation of relatively large amounts of hydrogen sulfide and carbon dioxide. These process technologies are:

- Exxon's Controlled Freeze Zone (CFZ) Process
- CNG's Liquid CO_2 Absorption of Sulfur Contaminants
- CNG's Triple-Point Crystallization (TPC) Process, and
- CNG's High Pressure Sulfur Recovery Process (HPSRU).

Exxon developed the CFZ process to separate methane from acid gases in a single cryogenic distillation operation. CNG Research Company developed the TPC process to purify carbon dioxide and concentrate hydrogen sulfide by alternately freezing and melting CO_2 at or near its triple point conditions (-69.9° F, 75.1 psia). The CNG HPSRU combines the high initial conversion obtained in a Claus thermal reactor with recycle of unconverted H_2S to effectively remove all sulfur components in the HPSRU feed gas. Liquid CO_2 is used to absorb sulfur compounds from HPSRU tail gas, and can be used to absorb sulfur containing contaminants from LQNG in a process variant which does not use CFZ to separate methane from acid gases.

The conceptual designs developed in the Base Program separate hydrogen sulfide and large amounts of carbon dioxide (>20%) from methane, convert hydrogen sulfide to elemental sulfur, produce a substantial portion of the carbon dioxide as EOR or food grade CO_2, and vent residual CO_2 virtually free of contaminating sulfur containing compounds.

CFZ-CNG Process Features

Controlled Freeze Zone

- Acid gas removal in single distillation step,
- No solvents or additives necessary,
- Contaminant insensitivity,
- High pressure acid gas,
- Synergy with cryogenic NRU, LNG product,
- Non-corrosive process streams.

Liquid Carbon Dioxide Contaminant Absorption

- Attractive physical properties (density/viscosity/mol weight),
- Favorable contaminant equilibrium,
- High stage efficiency,
- No solvents or additives necessary, available from raw gas,
- Not combustible

Triple-Point Crystallization

- Concentrated hydrogen sulfide,
- Commercially pure LCO_2 for market or absorption of H_2S
- Sharp separation of trace contaminants
- No solvents or additives necessary,
- Direct contact heat exchange,
- Small pressure changes cause phase changes.

CNG High Pressure Claus Sulfur Recovery

- Claus thermal stage at elevated pressure,
- Eliminates catalytic stages, tail gas unit, and incinerator,
- Oxygen or enriched air,
- No solvents or additives necessary,
- High sulfur recovery, low sulfur emissions.

PROJECT DESCRIPTION

The project comprises a Base Program and an Optional Program. The Base Program, with objectives outlined above, was completed August 31, 1993 with submission of the Task 2 Final Report. The Optional Program has not begun. The project goal is to further develop and demonstrate two of the component technologies of the CFZ-CNG Process: 1) pilot-scale triple-point crystallization of carbon dioxide, producing commercially pure carbon dioxide from contaminated carbon dioxide at the rate of 25 ton/day, and 2) bench-scale modified high pressure Claus technology, recovering elemental sulfur from hydrogen sulfide at the rate of 200 lb/day.

RESULTS AND DISCUSSION

A complete discussion of Base Program results is contained in Task 2 Final Report [5] and Research Plan [6], Contract DE-AC21-92MC29470. The following is condensed from these reports.

CFZ Process

The Controlled Freeze Zone (CFZ) Process is a cryogenic technology for the separation of carbon dioxide from natural gas by distillation. CFZ is a proprietary process developed and wholly owned by Exxon Production Research Company [7]. The CFZ concept has been successfully demonstrated in a 600 MSCFD pilot plant at Clear Lake, near Houston, Texas [8,9]. CFZ is the most fully developed of the component technologies comprising the CFZ-CNG LQNG Process. As such, further development of Exxon's CFZ process is not a contract objective, and no DOE funds are allocated for that purpose.

Natural gas processing involves the separation and recovery of valuable hydrocarbon components, and the removal of undesirable components such as H_2S, CO_2 and water. Low temperature physical separations, based on turbo-expander and Joule-Thomson (J-T) operations, and direct fractionation are the preferred methods for processing natural gas whenever possible. However, cryogenic fractionation of a gas containing more than about 5% CO_2 can lead to solidification of CO_2 at an intermediate point in a cryogenic demethanizer rendering such tower inoperative [10]. Thus alternative technologies, using solvents or freeze-prevention additives, have been utilized in the past. The CFZ process, in contrast, achieves a direct cryogenic separation of methane and CO_2. In an otherwise conventional distillation tower, solid CO_2 is confined to a special section of the tower, *the CFZ section*, specifically designed to control the formation and melting of solid CO_2.

TPC Process

Acid gas removal from gases with a high CO_2 to H_2S ratio requires the separation of CO_2 and H_2S to produce a CO_2 byproduct or vent stream free of sulfur compounds and a concentrated H_2S Claus feed. Distillation of CO_2 and H_2S to produce a pure CO_2 product is not practical due to the low relative volatility of CO_2 to H_2S and high CO_2 purity requirements at the pure CO_2 end (top) of the distillation column.

The continuous triple point crystallizer separates pure carbon dioxide from a variety of contaminants such as H_2S, COS, CH_3SH and hydrocarbons. The process has been developed and patented by Consolidated Natural Gas Company (CNG Research Company) [11,12,13,14,15,16]. The crystallizer operates at or near the triple point of CO_2. Solid CO_2 crystals are formed by adiabatic flashing at pressures slightly *below* the CO_2 triple point, and melted by adiabatic contact with CO_2 vapor at pressures slightly *above* the CO_2 triple point. No solid CO_2 is formed on heat exchange surfaces by indirect heat exchange; all solid CO_2 is formed and melted by direct contact heat exchange.

Experimental operation of a laboratory crystallizer has demonstrated that a very high degree of separation can be achieved in a single stage of crystallization. Experimentally measured separation factors, the ratios of contaminant concentrations in the flash zone (solid forming) to the melt zone, are 1000 to 1500 for H_2S and over 3000 for COS [16]. Pure CO_2 containing less than 1 ppm by volume H_2S has been produced by triple point crystallization from contaminated CO_2 mixtures. In this particular low quality natural gas processing application, two stages of triple point crystallization produce pure CO_2 and a concentrated H_2S product.

The triple point crystallizer has been tested extensively in the laboratory at bench-scale (up to 6-inch vessel diameters) [16]. With the laboratory bench-scale equipment continuous runs of up to 72 hours duration were achieved and terminated routinely. A large scale flash vessel (18-inch diameter) built to test rates of solid carbon dioxide production and slurry pumping characteristics was operated in continuous runs of up to 40 hours duration at production rates of 25 tons of solid CO_2 per day [17]. No unusual wear or abrasion on the slurry pump was observed after many tests totaling hundreds of hours. Slurries of 25 wt% solid CO_2 were routinely pumped.

HPSRU Process

A new sulfur recovery process [18] based on the Claus thermal reaction, with no catalytic stages or conventional tailgas cleanup, is made possible by TPC's ability to separate hydrogen sulfide and other contaminants from carbon dioxide. The high pressure sulfur recovery unit (HPSRU) comprises four operations: 1) Claus thermal reaction to convert hydrogen sulfide to sulfur, 2) waste heat exchange and sulfur condensation, 3) hydrogenation of sulfur and SO_2 in the Claus reactor effluent to hydrogen sulfide, and 4) quench and dehydration. All hydrogen sulfide is recycled to the TPC which concentrates acid gases by rejecting carbon dioxide and other inert species such as nitrogen

To recover 99+% sulfur, the conventional Claus plant normally comprises a thermal reactor, several catalytic reactors in series, and a tail gas cleanup unit . As noted by Hyne [19], "more than 50% of the conversion of hydrogen sulfide to elemental sulphur takes place in the front end reaction furnace; (while the) downstream components do no more than convert that part of the sour gas feed stream that is not converted to product sulphur in the front end reaction furnace." The high conversion of hydrogen sulfide to sulfur achieved in the front end reaction furnace is achieved at relatively modest cost -- about 20% of the total Claus plant capital cost. The downstream components, which accomplish roughly 40% of hydrogen sulfide conversion to sulfur, account for about 80% of the capital cost.

The new HPSRU process retains the high recovery/low cost of the Claus thermal reactor, but eliminates the low recovery/high cost catalytic stages and tailgas cleanup unit. Unreacted hydrogen sulfide is recycled to the thermal reactor inlet via the TPC section; this tail gas recycle approach enables essentially 100% sulfur recovery, free of thermodynamic and kinetic limitations imposed by the Claus reaction.

Aside from the Claus thermal reactor, the remaining equipment is more conventional. Concern for corrosion should be limited to the quench tower where liquid water and hydrogen sulfide are present. However, quench towers performing comparable service are presently used in the SCOT and Beavon tail gas cleanup processes. Also, sulfur dioxide, which is much more acidic in aqueous solution than hydrogen sulfide, is not present in the quench tower because of upstream hydrogenation.

Contaminant Absorption with Liquid CO_2

Sulfur contaminants in the HPSRU tail gas, H_2S and COS, are absorbed with pure liquid CO_2 from the TPC. These sulfur contaminants are recycled to the TPC. Liquid CO_2's low molecular weight (44) and high density (1.18 g/cm^3 at -70° F) provide high absorption capacity per unit volume of solvent. Liquid CO_2's low viscosity (0.25 cp at -70° F) promotes high stage efficiency. Liquid CO_2 absorption of H_2S and COS has been measured experimentally in a pilot absorption unit processing 20 MCFD of gas [16].

Liquid CO_2 is an effective absorbent for removal of contaminants from raw gas streams which contain CO_2. Favorable contaminant equilibrium data has been measured for many compounds which contain sulfur, chlorine, or an aromatic ring structure. Liquid CO_2 absorption efficiently cleans landfill gas because of its high CO_2 content and the many, often unknown, contaminants which are present [20].

Conceptual CFZ-CNG LQNG Process

The integrated process is shown in Figure 1. After dehydration and cooling the feed gas is sent to the CFZ tower which separates the CH_4 and other light components such as He and N_2 from CO_2, H_2S and other trace heavy components such as COS and C_2H_6. If the CH_4 overhead product contains significant amounts of N_2 it is sent to a cryogenic nitrogen rejection unit (NRU). The CO_2 rich bottoms product is sent to the TPC section of the process.

The TPC section contains an absorber-stripper which strips out small amounts of CH_4 (approximately 1%) and C_2H_6 carried over in the CFZ bottoms. H_2S in the vent stripping gas is re-absorbed with clean liquid CO_2 from the crystallizer. The vent gas also contains the inert components N_2, argon, and hydrogen brought to the TPC with the HPSRU recycle stream. The stripped CO_2 is sent to the TPC which produces

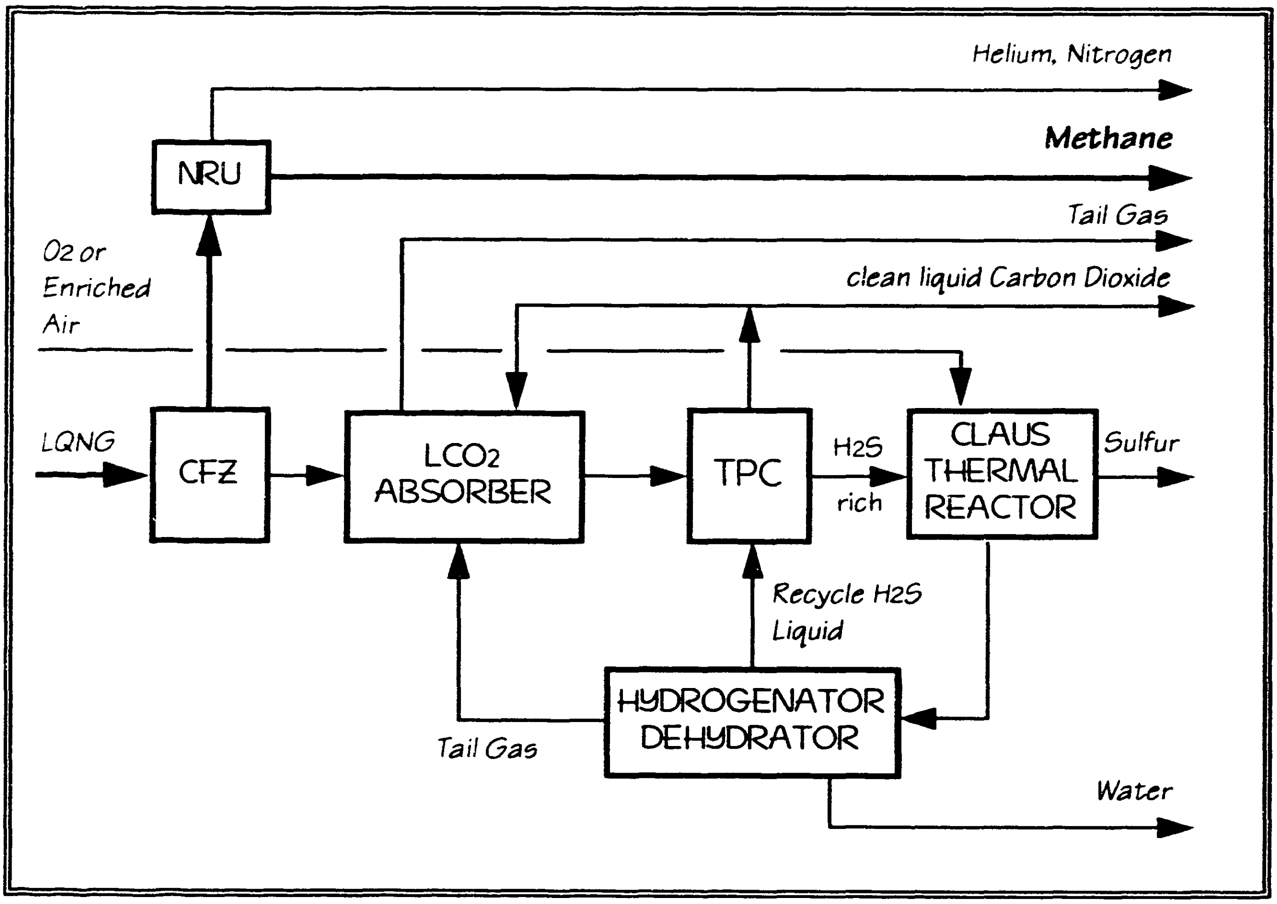

Figure 1. Conceptual CFZ/CNG Claus LQNG Treatment Process

pure CO_2 and a CO_2 stream concentrated in H_2S. Pure CO_2 product can be used for EOR or commodity CO_2 applications. H_2S rich TPC product is further enriched by stripping out CO_2 and is sent to the Claus plant. Tail gas from the HPSRU is returned to the TPC for reconcentration of the unreacted H_2S.

Two feed gas mixtures, each 200 million SCF/day, were studied having CO_2 contents covering a wide range of process applicability. One case is a high CO_2 gas now processed at Exxon's Shute Creek facility near LaBarge, Wyoming. The feed gas for the second case is a lower CO_2 content generic subquality gas. These crude gas streams are more fully described below.

The LaBarge case examines treatment of LQNG produced from the LaBarge field in southwestern Wyoming. The formation is estimated to contain 167 TCF of low Btu raw gas [1]. This crude gas is characterized below in Table 1. The product slate includes methane (pipeline gas), elemental sulfur, helium, and EOR grade carbon dioxide. The CFZ methane product has 50 ppm CO_2 and less than 4 ppm H_2S (¼ grain/SCF). The low CO_2 content of the methane prevents formation of solid CO_2 in the cryogenic NRU. The final methane product specification after nitrogen and helium rejection and recompression is 97% CH_4 at 1000 psia. The EOR-grade liquid CO_2 product, at 2000 psia, contains less than 16 ppm H_2S.

The generic case examines treatment of LQNG with composition shown in Table 1. Product specifications for the generic case include a methane product with 4 ppm H_2S (¼ grain/SCF) and less than 2% CO_2 (0.25% CO_2 is achieved as dictated by the controlling spec on H_2S). In the design of this case, no market was assumed to exist for CO_2. Pipeline methane and a small stream of elemental sulfur are the only salable products produced from this generic subquality gas.

Process economics, evaluated for high and low product price scenarios, were developed on the basis of a breakeven allowance per MSCF of raw gas, i.e., the raw gas cost per MSCF at which plant net revenues become zero. Plant net revenue is positive for raw gas cost below the breakeven allowance, negative above. Breakeven allowances range from 20¢ to \$2.14/MSCF of raw gas for low and high product price scenarios, assuming a simple five year capital payout. Capital and operating costs estimated for the conceptual process compare favorably with costs derived for the Selexol process treating low quality LaBarge gas [21]. Comparable breakeven allowances derived for the Selexol process are 8¢ and 73¢.

Conclusions

Low quality natural gas processing with the integrated CFZ/CNG Claus process is feasible for low quality natural gas containing 10% or more of CO_2, *and any amount of* H_2S. The CNG Claus process requires a minimum CO_2 partial pressure in the feed gas of about 100 psia (15% CO_2 for a 700 psia feed gas) and also can handle any amount of H_2S. The process is well suited for handling a variety of trace contaminants usually associated with low quality natural gas and Claus sulfur recovery.

The integrated process can produce high pressure carbon dioxide at purities required by end use markets, including food grade CO_2. The ability to economically co-produce high pressure CO_2 as a commodity with significant revenue potential frees process economic viability from total reliance on pipeline gas, and extends the range of process applicability to low quality gases with relatively low methane content.

Gases with high acid gas content and high CO_2 to H_2S ratios can be economically processed by the CFZ/CNG Claus and CNG Claus processes. The large energy requirements for regeneration make chemical solvent processing prohibitive. The cost of Selexol physical solvent processing of the LaBarge gas is significantly greater than the CNG/CNG Claus and CNG Claus processes.

Table 1. Gas Compositions and Process Conditions

	Case 1: LaBarge		Case 2: Generic	
Specie:	mol%	lb mol/hr	mol%	lb mol/hr
CH_4	20.50	4,494	80.50	17,679
CO_2	66.50	14,578	19.00	4,172
H_2S	5.00	1,096	0.50	110
N_2	7.35	1,644		
COS	0.05	10		
C_2H_6	0.01	2		
He	0.60	132		
TOTAL	100.00	21,956	100.00	21,961
Pressure	1,060 psia		715 psia	
Temperature	60° F		90° F	
Gas Flow	200 MMSCF/day		200 MMSCF/day	
Water	10 lb/MMSCF		75 lb/MMSCF	
Claus Plant	High Pressure Oxygen		High Pressure Oxygen	
Oxygen	90% O_2 210 Ton/day		90% O_2 21 Ton/day	
EOR CO_2	16 ppm H_2S 2,000 psia		None	
Methane	50 ppm CO_2 undetectable H_2S 40 MMSCFD		0.25% CO_2 4 ppm H_2S 160 MMSCFD	
Sulfur	375 LT/day 99.9% recovery		38 LT/day 99.9% recovery	
CO_2 Vent	16 ppm H_2S 13 Ton H_2S/yr		16 ppm H_2S 8.5 Ton H_2S/yr	

FUTURE WORK

A complete one-stage TPC will be operated in the Optional Program to determine the production rate of commercially pure CO_2. The TPC will incorporate a submerged bed design to melt solid CO_2 by condensing CO_2 gas. Determination of this rate will allow assessment of TPC's applicability for minimum maintenance, remote site service for LQNG processing. TPC demonstration is planned at a scale of 25 ton/day.

The HPSRU design is based on an equilibrium model of the thermal reactor. The model has been shown valid for many systems with a similar array of reacting components. Reaction kinetics may have an effect on conversion efficiency, reaction temperature and the extent of side reactions such as hydrogen or carbon monoxide formation. These effects will be quantified by operation of a bench-scale reactor in the Optional Program. The HPSRU scale will be 200 lb sulfur/day.

REFERENCES

1. Hugman, R.H., E.H. Vidas, and P.S. Springer, "Chemical Composition of Discovered and Undiscovered Natural Gas in the Lower 48 United States," GRI Contract 5088-222-1745, GRI 90/0248, November, 1990.
2. Meyer, Howard S., Presentation, Chemical Process Research Department, Gas Research Institute, October 3, 1990.
3. Kohl, Arthur, and Fred Riesenfeld, *Gas Purification*, Gulf Publishing Company, Houston, 1974.
4. Rosseau, R.W., et al, "Regeneration of Physical Solvents in Conditioning Gases from Coal," in *Acid and Sour Gas Treating*, Stephen A. Newman, Ed., Gulf Publishing Company, Houston, 1985, p 131.
5. Cook, W. Jeffrey, Marina Neyman, Wm R. Brown, Bruce W. Klint, Larry Kuehn, John O'Connell, Harold Paskall, and Peter Dale "TASK 2 REPORT, Low Quality Natural Gas Sulfur Removal/Recovery," US Department of Energy, Morgantown Energy Technology Center, Contract DE-AC21-92MC29470, August 16, 1993.
6. Siwajek, Lawrence A., Clark C. Turner, Sheldon Asnien, Bruce W. Klint, Larry Kuehn, John O'Connell, Harold Paskall, and Peter Dale, "RESEARCH PLAN, Low Quality Natural Gas Sulfur Removal/Recovery," US Department of Energy, Morgantown Energy Technology Center, Contract DE-AC21-92MC29470, August 16, 1993.
7. Valencia, J. A. and Denton, R. D., "Method and Apparatus for Separating Carbon Dioxide and Other Acid Gases from Methane by the Use of Distillation and a Controlled Freeze Zone", U.S. Patent 4,533,372, August 6, 1985.
8. Victory D. J., and J. A. Valencia, "The CFZ Process: Direct Methane-Carbon Dioxide Factionation," *Hydrocarbon Processing*, 66 (5) 1987.
9. Haut, R. C., et. al., "Development and Application of the Controlled Freeze Zone Process," SPE Production Engineering, p 265, August 1989.
10. Donnelly, H. G. and Katz, D. L., "Phase Equilibria in the Carbon Dioxide - Methane System", *Ind & Eng Chem*. Vol. 46, No. 3, p. 511, March 1954.
11. Brown, W.R., et al, "Gas Separation Process," U.S. Patent 4,270,937, June 2, 1981.
12. Brown, W.R., et al, "Gas Separation Process," U.S. Patent 4,581,052, April 8, 1986.
13. Brown, W.R., et al, "Gas Separation Process," U.S. Patent 4,609,388, September 2, 1986.
14. Brown, W.R., Cook, W.J., et al, "Crystallization Process," U.S. Patent 4,623,372, November 18, 1986.
15. Brown, W.R., et al, "Triple-Point Crystallization Separates and Concentrates Acid Gases," presented at AIChE Spring National Meeting, March 27-31, 1983, Houston, Texas.
16. Siwajek, L.A., et al, "CNG Acid Gas Removal Process," Final Technical Report, US Department of Energy, Morgantown Energy Technology Center, Contract DE-AC21-83MC20230, July, 1986.
17. Siwajek, L.A., Brown, W.R., et. al., "CNG Gas Separation Process," Final Technical Report, Gas Research Institute Contract 5086-222-1429, September 1988.
18. Hise, Ralph E., and Jeffrey Cook, "Sulfur Recovery Process," US Patent 5,021,232, June 4, 1991.

19. Hyne, J.B., "Design and Chemistry of Front End Reaction Furnaces," *Canadian Gas Journal*, March-April 1972, pp 12-16.

20. Siwajek, Lawrence. A., Clark C. Turner, W. Jeffrey Cook, and William R. Brown, "Landfill Gas Recovery for Compressed Natural Gas Vehicles and Food Grade Carbon Dioxide," SBIR Phase I Final Report, Contract No DE-FG02-91ER81223, May 4, 1992.

21. Johnson, John E., and Arthur C. Homme, Jr., "Selexol Solvent Process Reduces Lean, High-CO2 Natural Gas Treating Costs," Paper 65c, AIChE 1983 Summer National Meeting, Denver, August 29, 1983.

NG-8.5 Application of Rotating Contactor to Natural Gas Processing

CONTRACT INFORMATION

Contract Number	DE-FC21-92MC28178
Contractor	Institute of Gas Technology 3424 South State Street Chicago, Illinois 60616
Contractor Project Manager	Anthony L. Lee
Principal Investigators	James T. Semrau
METC Project Manager	Harold D. Shoemaker
Period of Performance	October 1, 1992 to September 30, 1995
Schedule and Milestones	FY93 PROGRAM SCHEDULE

	S	O	N	D	J	F	M	A	M	J	J	A
NEPA			═	═								
Field Experiment Site Selection					═	═	═	═	═	═	═	═
Field Experiment Skid Unit Design and Preliminary Economic Evaluations					═	═	═	═	═	═	═	═
Fluid Dynamic Studies				═	═	═	═	═	═	═	═	═
Mass Transfer Coefficient Studies				═	═	═	═	═	═	═	═	═
Data Analysis and Reports				═	═	═	═	═	═	═	═	═

OBJECTIVES

The objective of the U.S. Department of Energy (DOE) and Gas Research Institute (GRI) program entitled "Evaluation of High-Efficiency Gas-Liquid Contactors for Natural Gas Processing" is to evaluate the potential of rotating gas-liquid contactors for natural gas processing by expanding the currently available database. This expansion is leading to commercial demonstration of this technology to environments representative of those typically encountered in the natural gas processing industry. Operational and reliability concerns will be addressed while generating pertinent engineering data relating to the mass-transfer process.

BACKGROUND INFORMATION

Description of Rotating Contactor Technology and Its Benefits

A rotary contactor is a mass transfer device which uses a rotating bed of high surface area and high voidage packing to promote intense gas-liquid mixing and disengagement. The heart of the device is a donut or annular shaped rotor filled with a special reticulated metal packing. Figure 1 depicts the spinning rotor which produces an acceleration at its "eye" or center of about 100 times the standard gravitational acceleration. Gas or vapor enters via a nozzle in the casing and is forced inward through the rotating packing. There it comes into intimate contact with the liquid, which, having been distributed at the "eye" of the packing annulus, is forced outward by centrifugal force. The gas or vapor leaves from the center of the machine, while the liquid impinges of the casing walls and is drained from the casing.

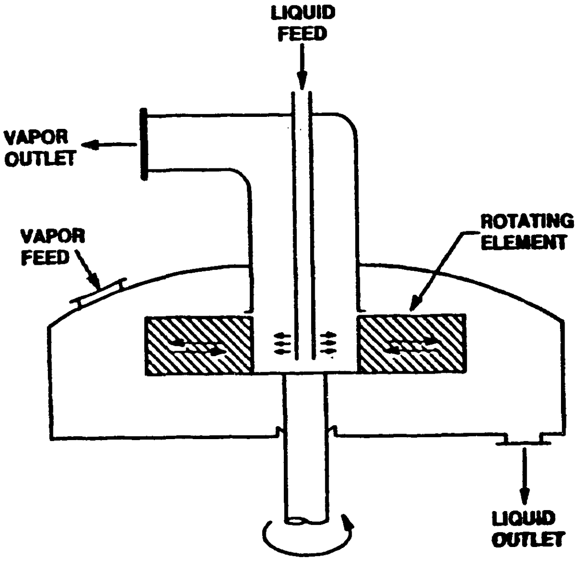

Figure 1. Rotating Contactor

The high gravitational acceleration allows for large increases in the superficial gas velocity and the area of packing as demonstrated by Sherwood Correlation shown in Figure 2. These factors result in dramatic reductions in height equivalent to a theoretical stage, HETP, which equates to reducing packing volumes two orders of magnitude, significantly reducing the weight and volume of any containment vessel.

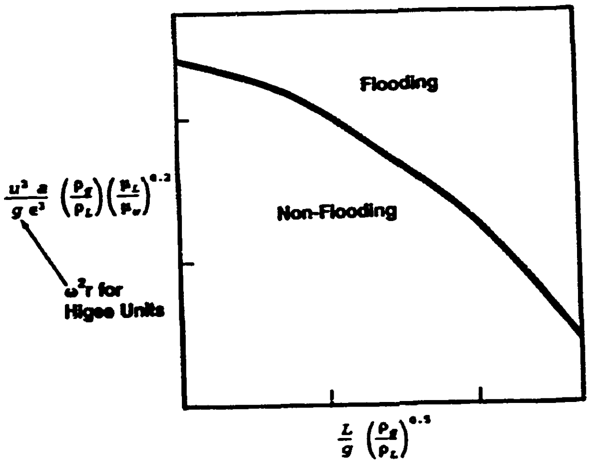

Figure 2. Sherwood Correlation

Figure 3 shows a typical rotating contactor rotor packing. The through put capacity of these units is determined by the flow area, $2\pi R \times L$. Capacity limits can be changed by adjusting the rotor inner diameter, R_1, the axial length, L, or both. The "Height of Packing" is simply the thickness of the packing, R_0-R_1. Flooding is calculated at the "eye" where the flow area and the gravitational acceleration are lowest.

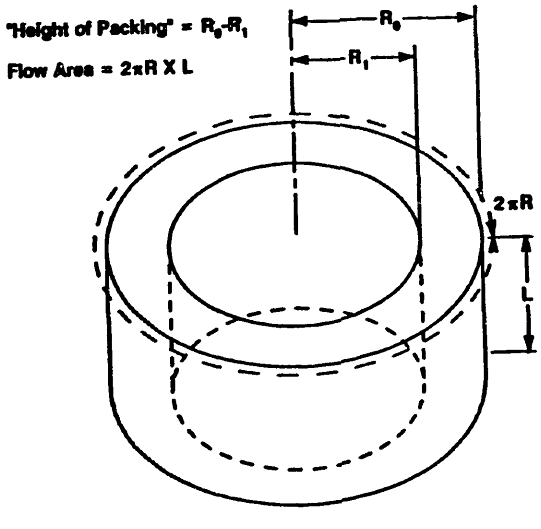

Figure 3. Rotor

The "Height of a Transfer Unit," HTU, for conventional packed columns is measured in feet; however, the HTU for rotating contactors is measured in centimeters. For example, a gas processing duty requiring a conventional packed column diameter of 4.5 feet and an overall height of 45 feet (715 cubic feet packing) could conceivably be accomplished using a rotor with outer diameter, R_0, of 39 inches, an inner diameter, R_1, of 14 inches and an axial length L of 18 inches having 10 cubic feet packing.

Based on preliminary evaluations, the benefits of rotary contactors over conventional mass transfer devices include:

- Small size, low profile
- Low weight
- Short contact time
- Low liquid hold-up
- Insensitive to motion or orientation
- Rapidly attains steady state
- Quickly emptied and cleaned
- Easily transported.

Brief History of Rotating Contactor Development

The rotating contactor was first conceived by Colin Ramshaw of Imperial Chemical Industrie (ICI) of Great Britain in the mid-1970's. ICI's original work demonstrated the validity of using the Sherwood Correlation to predict flooding in enhanced gravity contactors. ICI built and successfully demonstrated a commercial size distillation unit in the early 1980's.

Subsequently, ICI realized that it was not the preferred type of organization to market rotating contactor technology, so in 1984 Glitsch, Inc. was selected and granted exclusive rights to market ICI rotating contactor technology on a worldwide basis. In 1985, Glitsch sold a commercial unit to the U.S. Coast Guard to air-strip aromatics from ground water at atmospheric pressure. Later, Glitsch sold two more commercial air-stripping units, very similar to the Coast Guard unit.

In 1986, Fluor Technology, Inc. joined Glitsch to develop the rotating contactor for selective H_2S removal. In 1987, tests were run at an El Paso Natural Gas Company facility in New Mexico. Although results were encouraging, MDEA loadings obtained with the rotating contactor in the 0.7 to 0.9 range, CO_2 pickup was higher than expected. After careful review, it was concluded that additional development was needed before commercialization.

Subsequent to the El Paso tests (under a joint program by Chevron, Statoil, and Glitsch), a test skid was moved to a Chevron facility in Louisiana where the rotary unit was tested in two other process applications: a DEA system for CO_2 removal and a TEG system for dehydration of natural gas.

In 1988, GRI contracted with Glitsch and Fluor Daniel (partners with Glitsch for selective applications) for a four phase fast track commercial development program for selective applications. Preliminary analysis of the program, currently in Phase 2, indicates that with the current packing, rotor configuration, and using MDEA as the solvent, the system will not achieve the desired specifications needed to make it economically attractive. Subsequently, GRI has deferred the planned Phase 3, Field Experiment. They have taken the program out of a fast commercialization track and have identified a need for a technology based program for centrifugal contactors.

In 1990, Glitsch built and installed a rotating contactor distillation skid at University of Texas' Separation Research Project. Some of the Phase 2, GRI/Glitsch/ Fluor Daniel work, was contracted to the university, and the unit has performed well in distillation applications.

Summary of Prior Work Findings

After ICI's original experimental work demonstrated the validity of using the Sherwood Correlation in predicting flooding in enhanced gravity contactors, computer models were developed for hydraulic capability, pressure drop, power requirements and packing characteristics.

Glitsch Inc. has successfully demonstrated air-stripping of volatile organics from water in three commercial scale rotary strippers.

Although the selectivity for acid gas removal has not been fully realized in rotary contactors, bulk removal of both H_2S and CO_2 have successfully demonstrated, the former at El Paso Natural Gas, which had loadings in the 0.7 to 0.9 mol/mol range, and the latter at Chevron, which processed up to 20 million SCFD of gas containing up to 7 mole percent CO_2. Dehydration of natural gas was also demonstrated at the Chevron facility. In general, it was found that the product gas closely approached equilibrium with the incoming glycol stream, so performance was limited by the incoming glycol quality.

Phase 2 of the development program, GRI/Glitsch/Fluor, produced correlations for liquid hold-up, residence time over the packing, as well as droplet size and "time of flight" in the annulus. An internal hydraulic drive system was successfully tested to replace the conventional external electric motor drive which requires a double mechanical sealing system for high pressure applications.

The impact of using a rotating contactor on transfer unit height is apparent from the results of distillation experiments carried out at the University of Texas. Comparative tests using a packed bed unit and the rotary contactor using cyclohexane/n-heptane show transfer heights of approximately 2.5 centimeters compared to 1.25 to 2 feet for the packed column.

Potential Applications of Rotating Contactor Technology for Gas Processing

The rotating contactor has a number of special features that differ significantly from more conventional mass-transfer devices. Some of these features include:

- Small Size
- Low Weight
- Insensitivity to Motion
- Short Residence Times.

These characteristics make rotating contactors ideal for offshore applications. Factors which make offshore operations very capital intensive are:

- Depth of Water
- Weather Conditions
- The Weight and Size of the Equipment to be Placed on the Rig.

The first two factors are, of course, outside the control of the designer, but for the third factor, significant economies in size and weight of equipment can have overall cost implications for the structure that far outweigh the cost of the equipment itself. Design problems such as a column having to pass through multiple decks (creating the need for a cantilevered design), center of gravity and motion effects can be reduced or even eliminated use rotating contactors. Since rotating contactors are unaffected by motion operations can be carried out on floating platforms or converted crude carriers and at sea conditions that would be impossible, or at the least very difficult, with conventional equipment.

Listed below are some of the significant process applications that can be encountered in offshore operation (or onshore) and in which rotating contactors can be used with advantage.

1. Stabilization of crude or condensate – Careful consideration because formation of stable emulsions must be avoided.
2. Gas dehydration, both bulk dehydration and super dehydration.
3. Bulk carbon dioxide removal (with or without hydrogen sulfide present).
4. Selective H_2S removal.
5. Seawater deaeration.
6. Hydrocarbon separation – C_3/C_4 splitting.

7. Methanol recovery – Separation and recovery of methanol injected to suppress hydrate formation.
8. Air separation – The production of nitrogen suitable for reinjection in enhanced oil recovery.

PROJECT DESCRIPTION

Project Approach

The objective of this proposed program is to evaluate the potential of rotating gas-liquid contactors for natural gas processing by expanding the currently available database. The overall program consists of eight tasks. A brief summary of each follows.

Task 1. National Environmental Policy Act (NEPA). This task is for the generating and processing the documentation required to satisfy NEPA requirements for conducting laboratory studies of the rotating contactor technology.

Task 2. Field Experiment Site Selection. Organizations now involved in natural gas processing will be solicited for the purpose of identifying a site where a field validation can be performed.

Task 3. Field Experimental Skid Unit Design and Preliminary Economic Evaluation. IGT will purchase equipment and services from Glitsch, Inc. This includes a fully integrated skid with sufficient instrumentation so the rotating contactors performance can be fully characterized. This characterization includes reliability studies of mechanical aspects of the rotating contactor, including seals, bearings, lubrication, and mechanical drives.

This task also includes the techno-economic evaluations needed to compare rotating contactor technology to existing gas processing technologies.

Task 4. Project Review. This is a review of data collected through the fluid dynamic studies, Task 6, by the Technical Management Committee for this program consisting of GRI, DOE, Glitsch, and IGT.

Task 5. Field Site NEPA. Similar to Task 1, all the necessary documentation, planning and processing required for NEPA approval of field testing the rotating contactor will be conducted under this task.

Task 6. Fluid Dynamic Studies. This task includes both the experimental and analytical studies to develop an improved understanding of the flow phenomena occurring in a rotating contactor. Subtasks include, 1) the effects of packing type on residence time and entrainment within a rotating contactor, and 2) the effects of viscosity and surface tension of fluids in rotating contactors, specifically related to wetting effects and interfacial area, enhancement factors, and residence time in the packing.

Task 7. Mass-Transfer Coefficient Studies. The objective of this task is to obtain mass-transfer coefficients for scale-up of separations of interest for the gas industry. Available information on the relationships involving mass-transfer coefficients and operating parameters will be evaluated. This database will be expanded as needed for covering many potential applications of interest, including but not limited to, dehydration, bulk acid-gas removal, and selective acid removal.

This task will also concentrate on a model for dehydration. The purpose of the model is to deduce overall mass-transfer coefficients, provide feedback to the experimental program, evaluate the equipment design, and generate performance estimations, all with a modular program that can be easily interfaced with commercially available simulation packages.

Task 8. Field Experimental Studies. After a site selection, installation, and performance characterization experiments are complete, the unit will be placed in an operational mode for a period extending up to 6 months, after which the unit will be disassembled and the critical components will be inspected to determine if wear and/or degradation has occurred.

Task 9. Data Analysis and Reports. This task is to collect fundamental and process data, to assess the rotary contactor's performance, and to report findings and recommendations. Data collected from this project and from existing literature will be correlated and reported.

RESULTS

Accomplishments since October 1992 include the following:

- Successful completion of the National Environmental Policy Act (NEPA) for experimental work to be conducted at IGT.
- Generation of experimental test matrix and its submission to GRI, DOE, SMP, and Glitsch for approval.
- 95% completion of the low pressure "plastic" rotary contactor system to conduct fluid dynamic studies. Three key elements to be provide by Glitsch have not arrived yet: variable frequen-cy drive, blower, and computer data acquisition system. Shipping of this equipment is pending subcontract negotiations between IGT and Glitsch.
- Initiated design of gas processing system for operation of the high pres-sure Higee™ unit call the "China Unit." This system is to include a ten gpm amine plant, a gas recycle system capable of circulating 0.5 MMSCFD of subquality natural gas up to 1200 psia, a solvent drainage and multiple solvent storage system, and a skid mounted glycol dehydration system capable of processing 0.5 MMSCFD of saturated natural gas.
- Contacted Marathon, Texaco, NiGas, and Columbia Gas as potential site hosts.

FUTURE WORK

The work to be conducted during FY94 will be the continuation of the activities begun in FY93 on:

- Field Experiment Site Selection
- Field Experiment Skid Unit Design and Preliminary Economic Evaluation
- Fluid Dynamic Studies
- Mass Transfer Coefficient Studies
- Data Analysis and Reports

and initiation of the following items:

- Project Review
- Field Experimental Studies.

Over FY93 the following tasks should be completed:

- Field Experiment Site Selection
- Field Experiment Skid Unit Design and Preliminary Economic Evaluation
- Fluid Dynamic Studies
- Project Review.

Poster Session

P2 Site Selection and Evaluation of a Horizontal Well in the Clinton Sandstone

Thomas H. Mroz
Morgantown Energy Technology Center

William A. Schuller
EG&G WASC, Inc.

ABSTRACT

A integrated geologic and reservoir study was completed as part of the site evaluation to locate a horizontal well in the Clinton Sandstone in Mahoning County, Ohio. The effort is part of a study to evaluate site selection criteria, drilling and completion technologies and fracture diagnostics in low permeability reservoirs.

The information presently includes data from a number of sources; core and reservoir analysis data from a GRI sponsored vertical well, geologic and well data from Belden & Blake, Inc., and the integrated two dimensional and three dimensional geological model interpretation data. The integrated information is used as input for predicting vertical verses horizontal well production and economics.

The integrated methodologies show the criteria needed to design and drill a horizontal well effectively in the Clinton Sandstone of eastern Ohio.

P3 Natural Gas Product and Strategic Analysis

Abbie W. Layne
John R. Duda
Anthony M. Zammerilli
Morgantown Energy Technology Center

Product and strategic analysis at the Department of Energy (DOE)/Morgantown Energy Technology Center (METC) crosscuts all sectors of the natural gas industry. This includes the supply, transportation, and end-use sectors of the natural-gas market. Projects in the Natural Gas Resource and Extraction supply program have been integrated into a new product focus. Product development facilitates commercialization and technology transfer through DOE/industry cost-shared research, development, and demonstration (RD&D). Four products under the Resource and Extraction program include Resource and Reserves; Low Permeability Formations; Drilling, Completion, and Stimulation; and Natural Gas Upgrading.

Product and strategic analysis involves technical evaluation of engineering processes, economic assessment, risk/sensitivity analysis, and product plan development. Engineering analysis is conducted to evaluate the performance of natural-gas supply technologies and to identify design improvements. Economic evaluation and risk/sensitivity analysis measure the commercialization potential of the products and determine barriers to market entry. Product plan development (1) assists in integrating technologies into products, (2) coordinates METC strategic planning activities with the DOE Natural Gas Program, (3) guides program direction through resource allocation and product development implementation strategies, and (4) coordinates the planning activities of funding organizations such as the Gas Research Institute. Figure 1 depicts the relationship between product and strategic analysis, the budget development process, and program planning.

Engineering process analyses have been performed for the Slant Hole Completion Test project. These analyses focused on evaluation of horizontal-well recovery potential and applications of slant-hole technology. Figures 2 and 3 depict slant-well in situ stress conditions and hydraulic fracture configurations. Figure 4 presents Paludal Formation coal-gas production curves used to optimize the hydraulic fracture design for the slant well. Economic analyses have utilized data gathered from vertical test wells to evaluate the profitability of horizontal technology for low-permeability formations in Yuma County, Colorado, and Maverick County, Texas.

Figures 5 and 6 describe the methodologies used to evaluate horizontal well profitability and select horizontal well sites. Evaluations are based on a probabilistic approach, with distribution curves similar to Figure 7 used for input into the methodology. Figure 8 depicts the location of the Vernon field study site for the horizontal well in the Niobrara Formation. Figures 9 and 10 are net-present-value graphs used to evaluate the profitability of horizontal well technology for the Niobrara Formation. Figure 9 depicts the first evaluation case for the Niobrara Formation. Figure 10 depicts the second evaluation case, where the Niobrara Formation permeability is lower than that shown in Figure 9. The product planning process has provided guidelines for development of new supporting projects and integration of existing projects into products.

Future efforts will focus on evaluation of technology applications for naturally fractured reservoirs with stochastic-reservoir and natural/induced hydraulic-fracture simulators, economic assessments for existing and new products, and evaluation of a gas-systems-analysis model. Natural fractures play a significant role in determining the flow potential of low-permeability reservoirs. A stochastic reservoir model is currently being developed by DOE/METC to better understand the impact of natural fractures on the flow mechanisms in low-permeability reservoirs.

A user friendly and transportable version of FEFFLAP (Finite Element Fracture Flow Analysis Program) will be evaluated by industry and METC in-house personnel. A description of the physical situation simulated by FEFFLAP is given in Figure 11, and Figure 12 is the numerical representation of this situation as simulated by FEFFLAP.

A schematic of the Gas Systems Analysis Model (GSAM) is shown in Figure 13. This model is being developed to provide a tool for industry and government agencies to evaluate the resource-technology and economic interactions of a natural-gas system. Product plan development will continue to be an ongoing activity, providing annual updates for program RD&D, budgets, and direction.

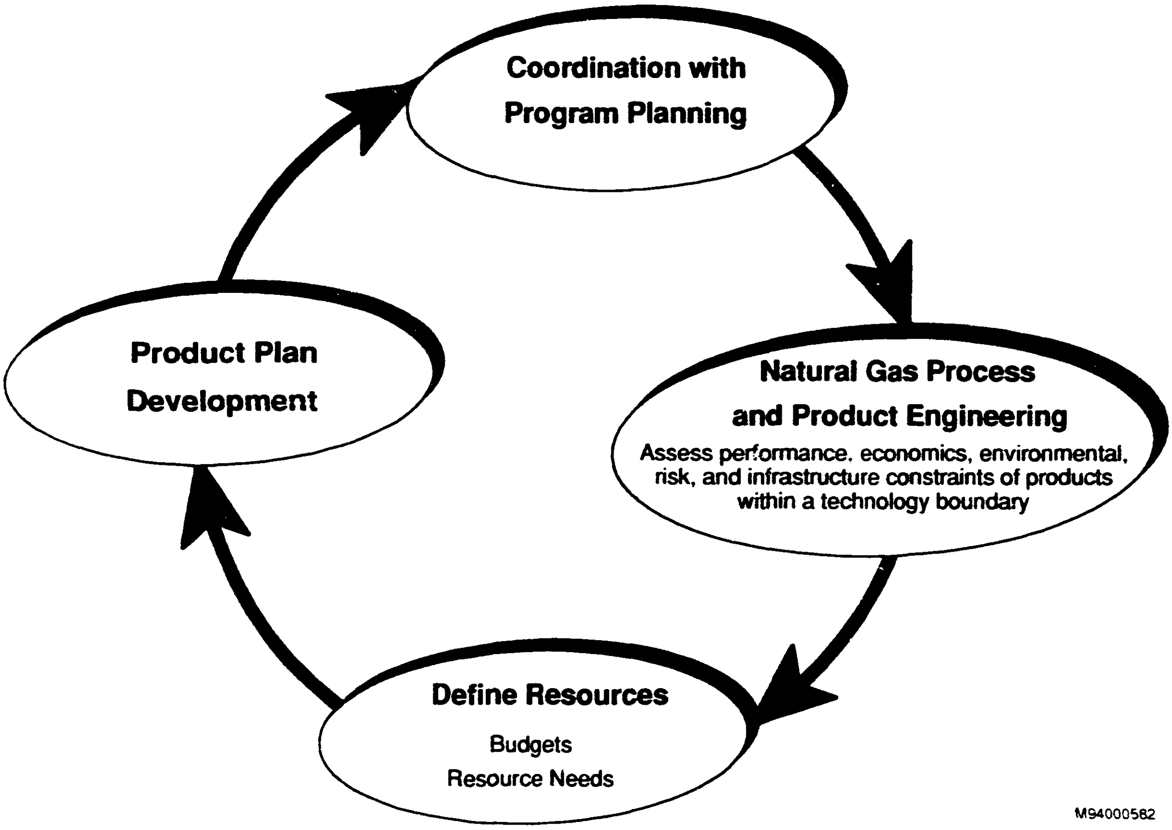

Figure 1. Product and Strategic Analysis Program Relationships

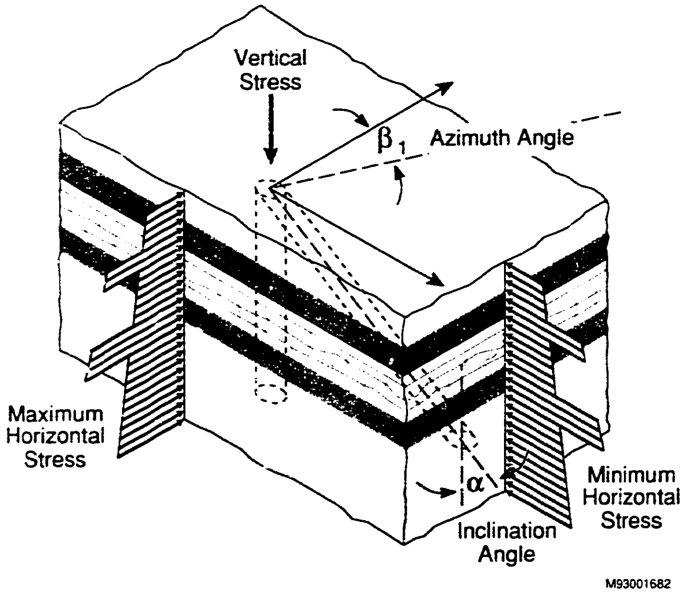

Figure 2. Schematic of Inclined and Vertical Wellbores

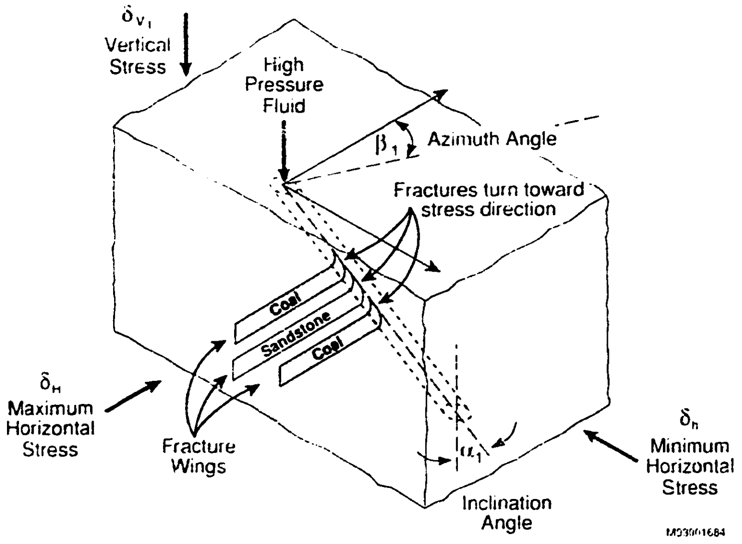

Figure 3. Hydraulic Fracture Propagation From an Inclined Wellbore

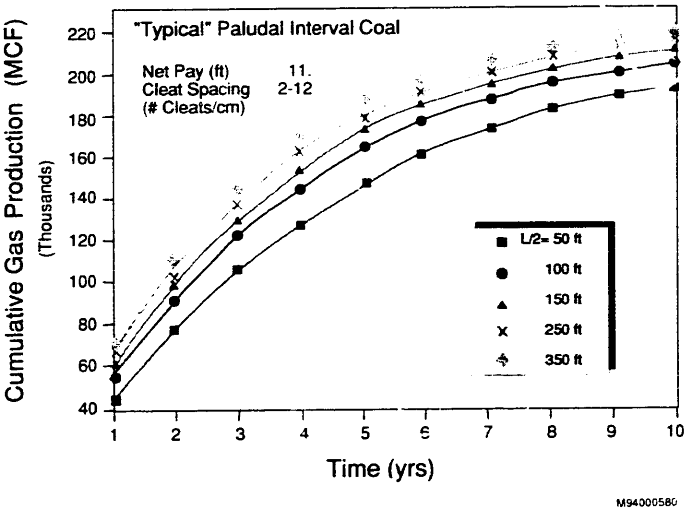

Figure 4. Stimulating Well Performance to Optimize Fracture Design

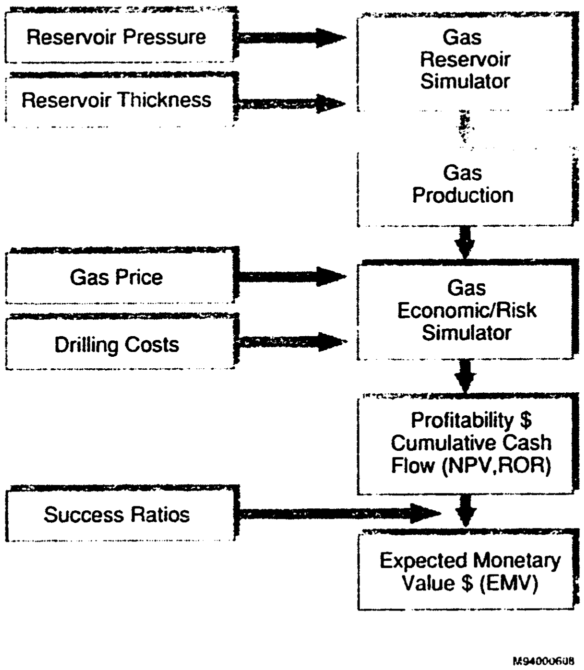

Figure 5. Methodology for Horizontal Well Site Selection

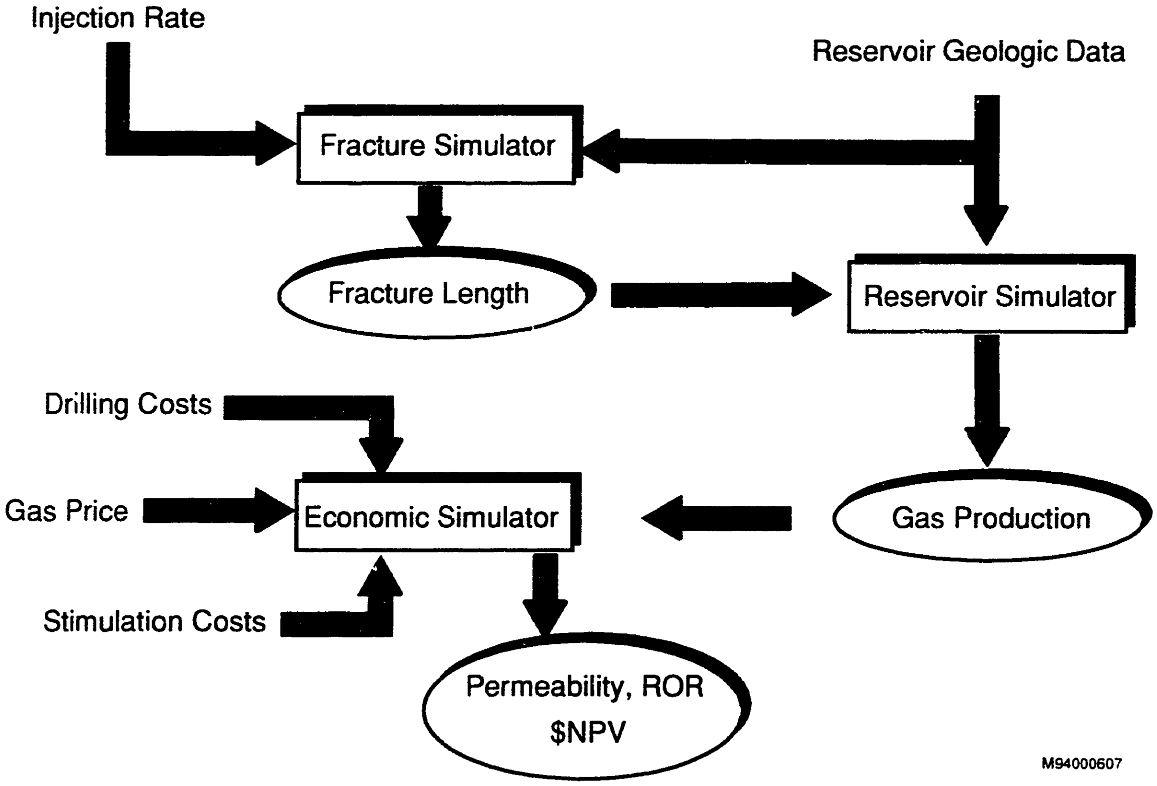

Figure 6. Horizontal Well Profitability Analysis Methodology

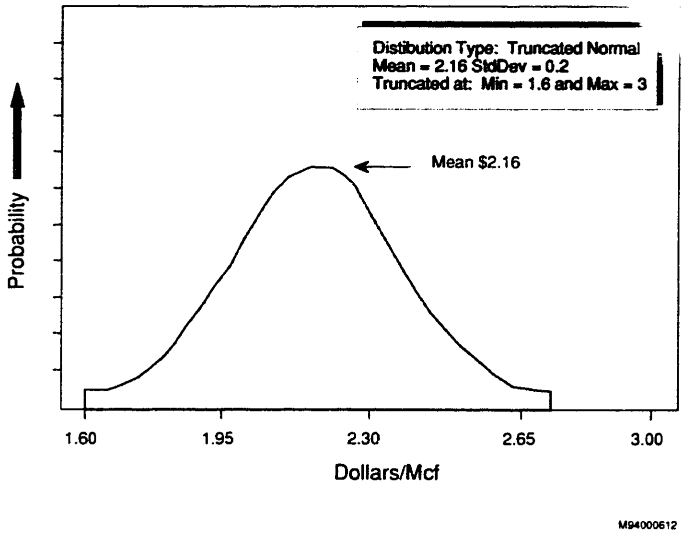

Figure 7. Gas Price Probability Distribution

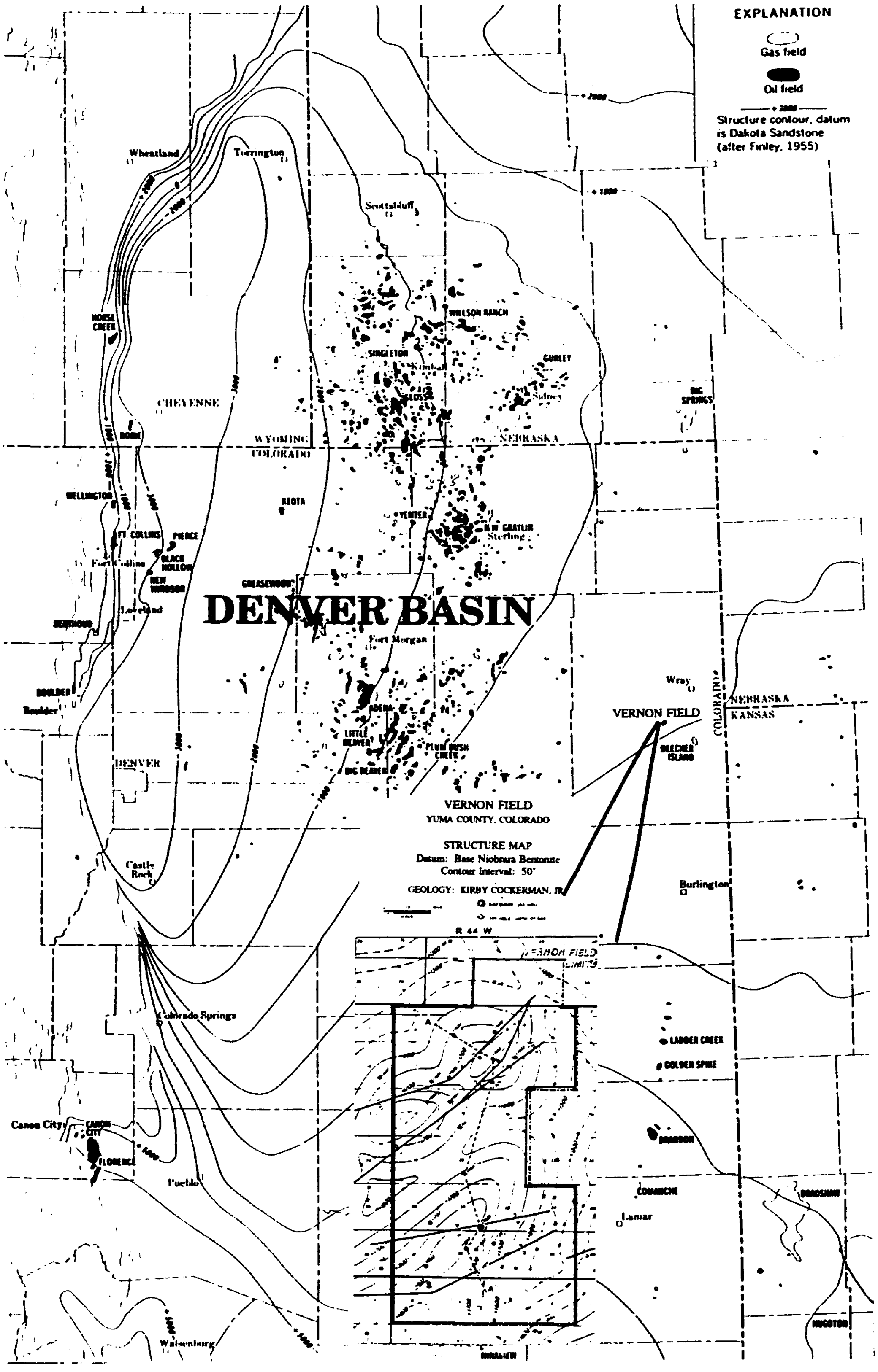

Figure 8. Yuma County, Colorado, Horizontal Well Site

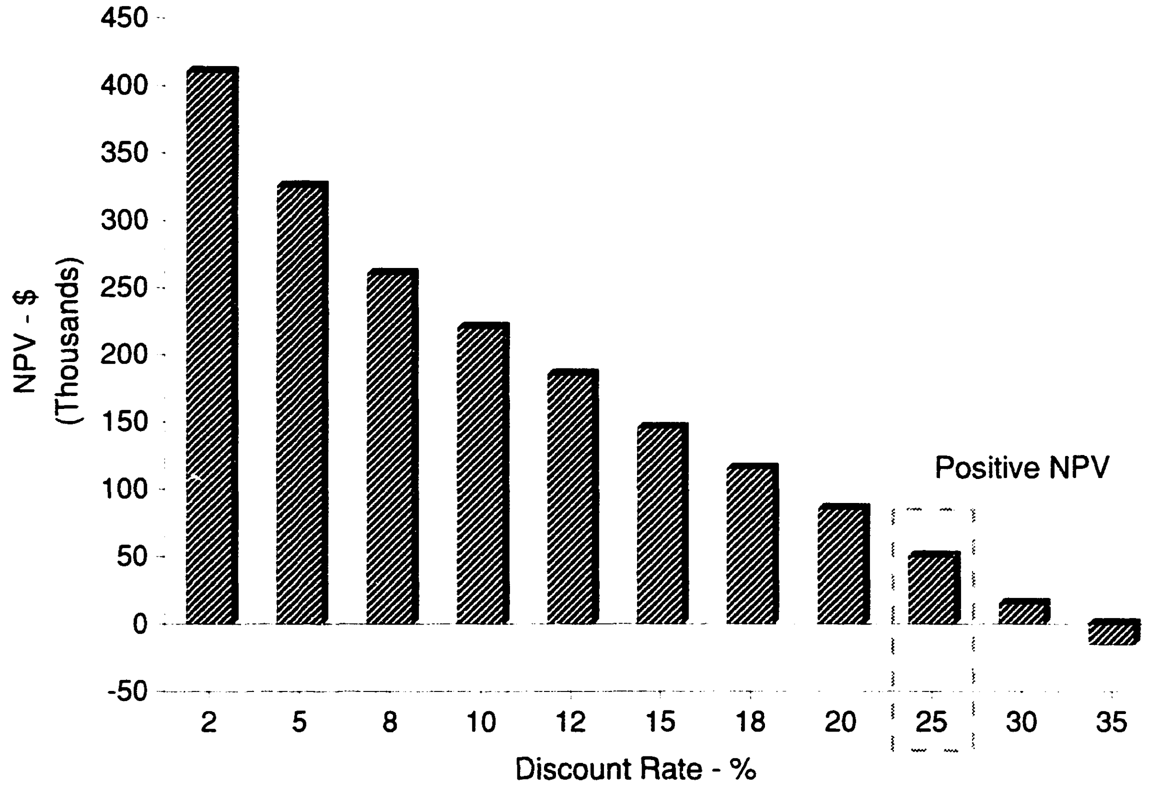

M94000609

Figure 9. Net Present Value (NPV), Niobrara Horizontal Well, Case I

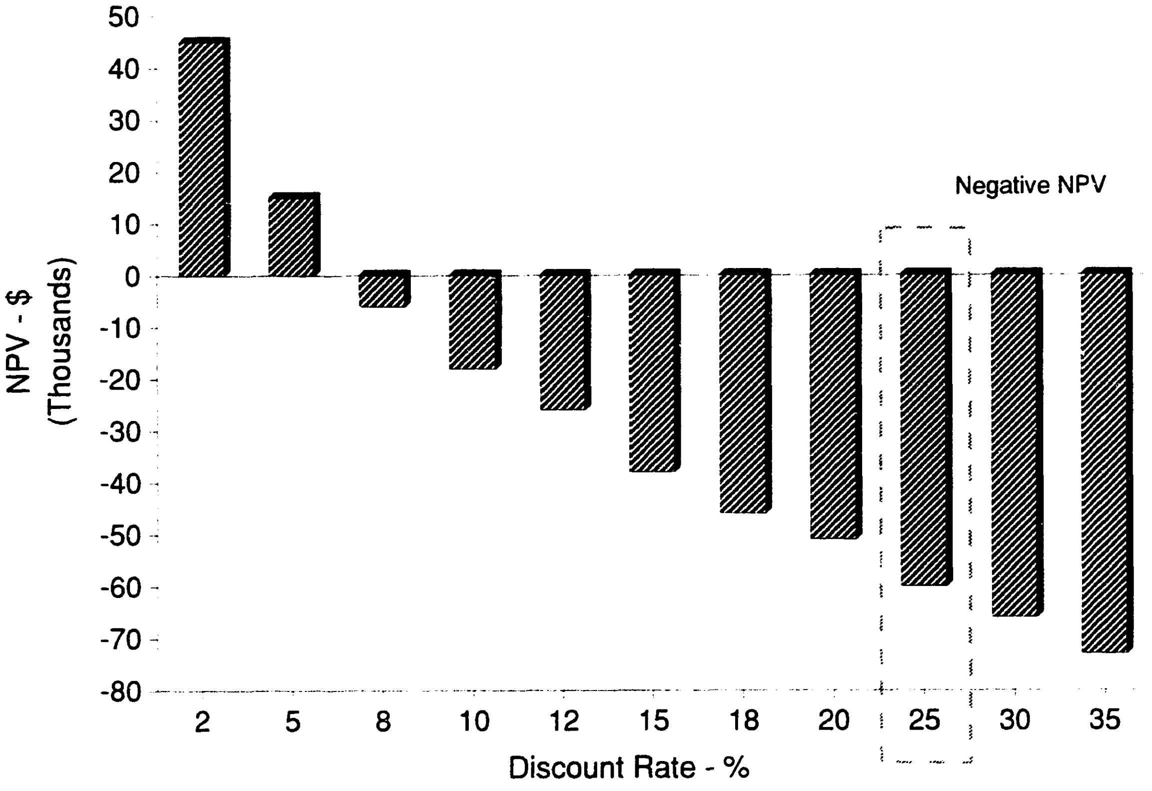

M94000610

Figure 10. Net Present Value (NPV), Niobrara Horizontal Well, Case II

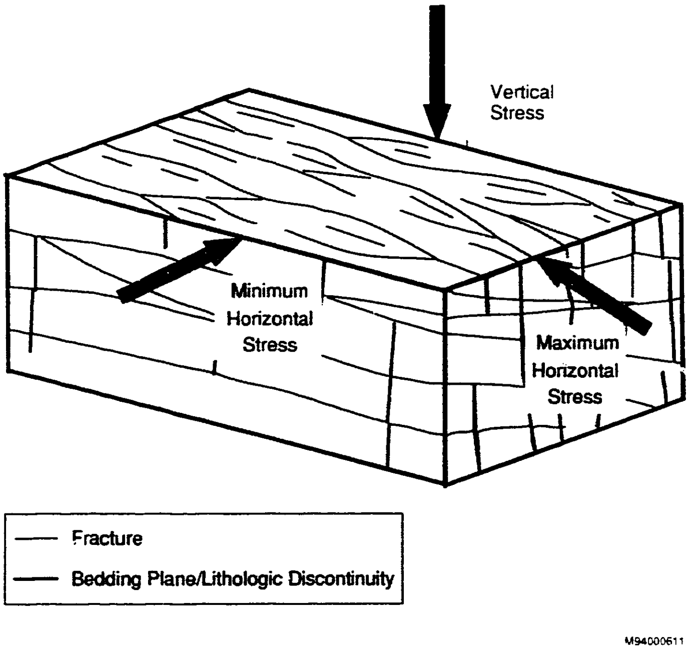

Figure 11. In-Situ Description of a Naturally Fractured Reservoir

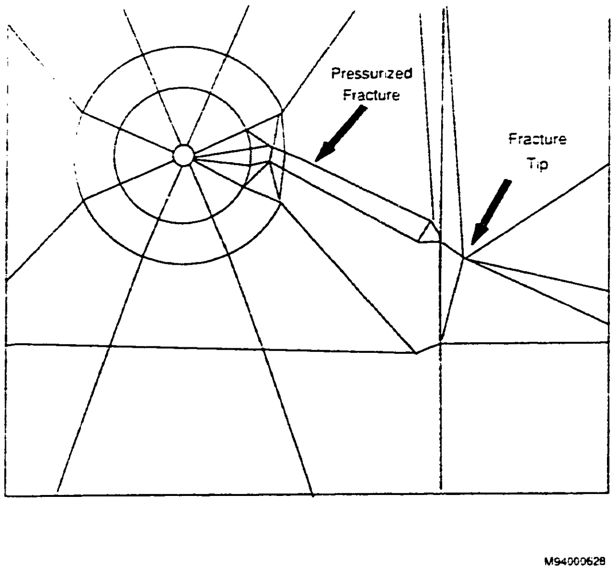

Figure 12. FEFFLAP Representation of a Hydraulic Fracture in a Naturally Fractured Reservoir

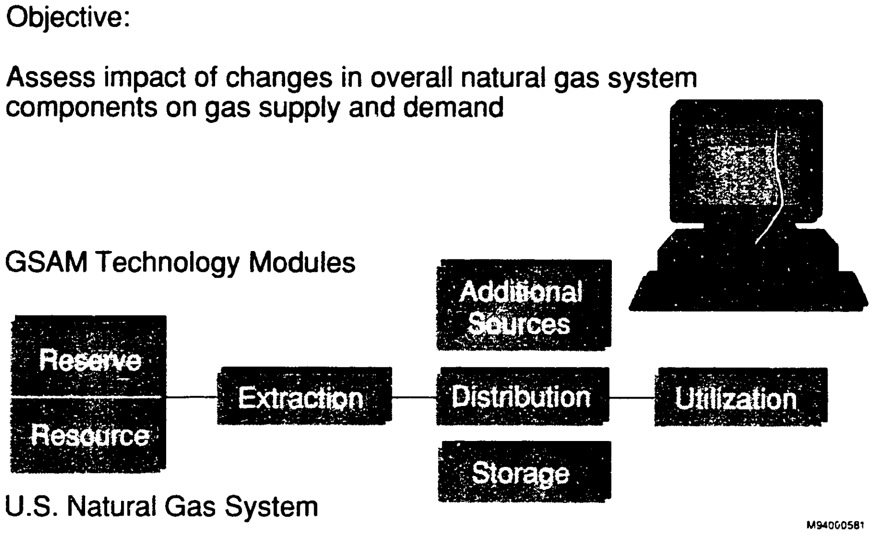
Objective:

Assess impact of changes in overall natural gas system components on gas supply and demand

Figure 13. Gas Systems Analysis Model (GSAM)

P4 Evaluation and Optimization of Vertical Gob Gas Ventilation Wells

CONTRACT INFORMATION

Contract Number	DE-FG03-92ER81442
Contractor	Resource Enterprises, Inc. 360 Wakara Way Salt Lake City, UT 84108
Contractor Project Manager	Matt J. Mavor
Principal Investigators	Matt J. Mavor John R. Robinson Rick B. Marshall
METC Project Manager	Charles W. Byrer
Period of Performance	October 92 - April 93

ABSTRACT

A gob well was completed and instrumented to independently monitor total gas and methane production and associated surface producing pressures from a mined out coal seam and the overlying strata. The purpose of the project was to collect sufficient data from which to estimate the properties and volume of the gob region contributing to flow. The test gob well was the 190 C located above B seam in the 9 Left D East Longwall panel of the Cambria 33 Mine. The Cambria 33 Mine is operated by BethEnergy Mines Inc. and is located in Cambria County, Pennsylvania. Data was collected prior to the mine face reaching the location of the test well, during the mine through, and for approximately two weeks after mine through.

The project was successfully completed as sufficient data was collected to evaluate the gob region properties and the drainage volume of the well. Evaluation of the vertical well performance with a coal gas reservoir simulator suggested that the 190 C well was draining gas from a thirteen foot thick, 7.5 acre drainage area. The mined coal volume is contained within a 700 by 4,200 foot area corresponding to 67.5 acres. This comparison suggests that 9 vertical wells may be sufficient to control gas emissions into the workings if the productivity of the vertical wells can be maintained. Gas emissions in this panel were controlled with fourteen vertical wells and six boreholes. A significant potential exists for reduction of the degasification cost.

The gob gas test well produced approximately 7.0 million standard cubic feet of methane gas from the upper coal seams during the 9 day test period of this project. The minimum drainage area of the test well was 7.5 acres which is equivalent to 45 million standard cubic feet of gas in place. The gas recovery of 15% of the gas in place suggests that the drainage efficiency of the vertical well was much lower than would be expected.

There are unresolved questions concerning the very short producing life of the vertical well. The test data collected during this project suggested that a two fold reduction in permeability occurred within approximately 10 days from the start of gas production. The degree of reduction is insufficient to explain the fact that the 190 C well will not produce gas at this time. Further decreases in permeability may have occurred after the data collection operations for this project ceased. The decrease in gas production is not due to depletion of the volume of gas in place. The lack of gas production could also be caused by other problems such as a liquid level increase in the well or increased resistance to flow near or in the wellbore. The increased resistance to flow could have been caused by collapse of coal or other rock into the annulus between the casing and the drilled hole diameter. This possibility was also suggested by interpretation of liquid level measurements collected during the research operations. Eventual optimization of the gob region drainage may require that the completion techniques for the vertical wells be altered to increase the wellbore integrity after mine through.

Horizontal boreholes producing gas from the same longwall panel have not experienced significant reductions in gas deliverability suggesting that the permeability of the induced fractures is maintained over time and that the horizontal boreholes retain a greater degree of connectivity to the induced fractures than is possible with a vertical well. The horizontal borehole integrity may be greater than that of the vertical holes due to the fact that the boreholes are drilled through competent formations between the mined seam and the coal seams located above the mined seam.

P5 Computer Modeling of Geologic Strata in the Multi-Strata Project Area (Beckley)

Thomas H. Mroz, Charles W. Byrer, and Donald M. Evans
Morgantown Energy Technology Center

Faleh Al Saadoon
Texas A&I University

ABSTRACT

The Multistrata Test is a contract effort with the College of West Virginia and BDM Corporation as a subcontractor on the technical aspects of the effort. The study was initiated to show independent coal operators and gas companies the potential to develop the total energy resources in a given area. This presentation covers the review of the geologic setting and well completions of the three wells drilled west of Beckley, West Virginia.

The geologic setting is presented by BDM Corporation in their final report. The well locations picked lie on the west limb of a north south structurally high block which is controlled by basement faults. The area immediately to the west is a structurally complex faulted low block and is mined at the Beckley coal horizon. The mine maps show a highly faulted area with some of the faulting controlling deposition of the coals. The wells are located on the limb and are completed in the Beckley and Pocahontas coals, the Ravencliff sandstone, and the Big Lime. A review of the geologic setting was done to determine if water and gas saturations could be explained by the location of the wells to the surrounding geologic structures. The structure does not explain the total gas and water distribution in the productive formations.

The well completions were also evaluated to determine if the production would be enhanced by limiting the water production. The three wells show that water is the main problem in limiting gas flow and the following suggestions were made to recomplete the wells.

A completion strategy was to evaluate present production from the individual reservoir formations and determine the combinations that would give the highest production by controlling the influx of water to the well bore. All wells were completed to separate the coalseam gas production from the lower sandstone and limestone production. Water production was evident in all wells and all formations. It was therefore decided to put the effort into pumping the water off of the coals and put them on suction to maximize production. The lower sandstone and limestone production was determined and low production zones were plugged to maximize flow and cut water influx that hampered gas flow.

Geologic analysis, completion and production data are presented to show the impact of multistrata wells in southwestern West Virginia.

P6 Inorganic Polymer-Derived Ceramic Membranes

CONTRACT INFORMATION

Contract Number	91MC-28074
Contractor	Sandia National Laboratories P.O.Box 5800 Albuquerque, NM 87185-5800 (505) 272-7627
Contract Project Manager	C. Jeffrey Brinker
Principal Investigator	C. Jeffrey Brinker R. Sehgal N. Raman P. R. Schunk T. J. Headley
METC Project Manager	Venkat K. Venkataraman
Period of Performance	July 1, 1991 to June 30, 1994

Schedule and Milestones

FY 94 Program Schedule

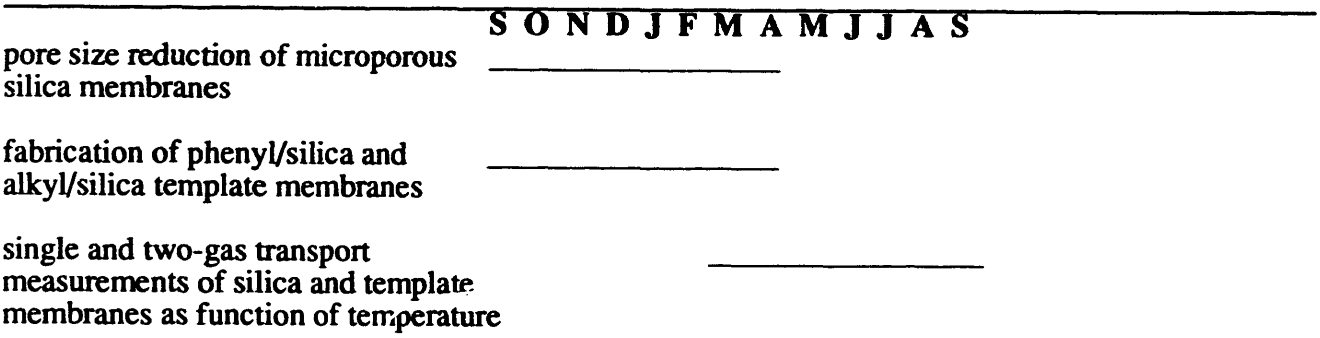

ABSTRACT

Polymeric silica sols were used to prepare membranes on commercial γ-Al_2O_3 supports. Aging of the silica sols was shown to be effective to form discrete membrane layers. He/N_2 selectivity factors exceeding ideal Knudsen values were observed when the sols were prepared under conditions in which the condensation rate was minimized. We propose that the average pore size of the membrane depends on the balance of capillary pressure and modulus during membrane deposition and that the breadth of the pore size distribution might be influenced by the extent of condensation accompanying membrane deposition. The use of organic templates may allow independent control of pore size, pore shape, and pore volume.

OBJECTIVES

The primary objective of this study is to prepare supported inorganic membranes suitable for gas separation/gas purification applications in the processing of natural gas. The design criteria for such membranes include: high selectivity and high flux combined with excellent chemical, thermal, and mechanical stability.

BACKGROUND INFORMATION

In the processing of natural gas, membranes have been proposed as replacements for more energy intensive purification processes for the removal of H_2O, CO_2, H_2S, and higher hydrocarbons from methane. Due to their inherent thermal, mechanical, and chemical stability, inorganic membranes are attractive for such applications. For practical gas separations, an inorganic membrane must combine high flux J with a high selectivity factor α. The membrane flux for Knudsen transport is proportional to the pore radius r_p divided by the film thickness h:

$$J_K(\mathrm{cm/s}) \propto \frac{\varepsilon r_p}{\tau^* h}\sqrt{\frac{1}{RT}}\,\Delta P \qquad (1)$$

where ε is the porosity, ΔP is the pressure drop across the membrane, and τ^* is the tortuosity. Membrane selectivity is related to pore size and pore size distribution. When the pore size is reduced below the mean free path of a gas molecule, gas transport occurs by Knudsen diffusion, and the separation factor for a binary gas mixture depends on the inverse ratio of the respective molecular weights. For example, the Knudsen selectivity factor α_K for a He/N_2 mixture is 2.65. Much greater separation factors (approaching ∞) are achieved when the pore size is reduced sufficiently and the pore size distribution is sufficiently narrow to admit and exclude molecules on the basis of size, a mechanism referred to as molecular sieving. Thus to combine high flux with high selectivity it is necessary to prepare extremely thin, porous films with a narrow distribution of extremely small pores ($r_p \sim$ molecule size) and no cracks or other imperfections that would serve as large pores and diminish selectivity.

The traditional approach to the preparation of thin inorganic membranes with controlled pore sizes is to deposit (slip-cast and/or dip-coat) particulate sols with narrow particle size distributions on porous supports [1-3]. If aggregation is avoided, the pore size of the membrane is controlled by the particle size of the sol - smaller particles yield smaller pores. An advantage of this approach is that the porosity of the membrane, which dictates its flux (Eq. 1) is independent of the particle size. So-called Knudsen membranes prepared from particulate sols have been successfully demonstrated by many research groups and are now commercially available [4]. However due to problems with cracking [5] and pore size coarsening at elevated temperatures [6], it has proven difficult to prepare molecular sieving membranes using this traditional approach.

This paper considers the use of polymeric silicate sols to prepare thin supported membranes, where the distinction between particles and polymers, made on the basis of nuclear magnetic resonance (NMR) and small angle x-ray scattering (SAXS) measurements [6], is that the polymeric sols contain no regions of fully condensed silica. The idea of this alternative approach is to utilize the fractal properties of polymeric sols to favor polymer interpenetration during membrane deposition. This concept is qualitatively understood on the basis of the following relationship describing the mean number of intersections $M_{1,2}$ of two mass fractal objects of size R placed in the same region of space [7]:

$$M_{1,2} \propto R^{D1+D2-d} \qquad (2)$$

where D1 and D2 are the respective mass fractal dimensions and d is the dimension of space, 3. From Eq. 2, we see that if D1 + D2 < 3, the probability of intersection decreases indefinitely with R. This suggests that as D is reduced polymers should more easily interpenetrate as they are concentrated during slip-casting/dip-coating. If compliant, such interpenetrating networks should collapse during drying to create pores of molecular dimensions appropriate for molecular sieving.

A practical advantage of this polymer approach with respect to the preparation of supported membranes is that the final pore size should be independent of the polymer size. Thus aging can be used to grow the polymers large enough to be trapped on the support surface during membrane deposition (avoiding the creation of thick often imperfect membranes by so-called "pore plugging" (see Figure 1)) without detrimentally increasing the pore size. Also a broadening of the polymer molecular weight distribution should not necessarily be manifested as a broadening of the pore size distribution.

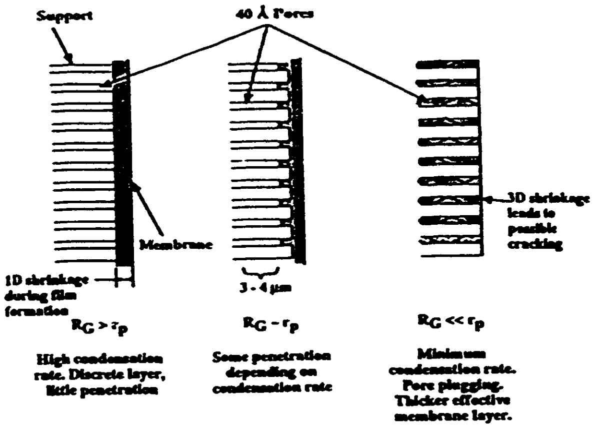

Fig.1 Schematic illustration of the effect of the relative sizes of polymers and support pores on membrane formation.

A second advantage of this approach is that polymeric sols generally lead to the formation of amorphous membranes that do not exhibit grain growth or phase transformations during heating (as is often observed for particulate sols). Thus compared to particulate membranes, the pore dimensions of polymeric membranes should exhibit improved thermal stability.

A possible disadvantage of this approach is that small pore sizes are achieved at the expense of pore volume. This limitation may be overcome by the use of organic molecules or ligands as pore templates.

This paper first reports on the effects of sol aging conditions and condensation rates on the microstructure and transport behavior of supported silica membranes. We then consider what factors govern the pore size of membranes prepared from polymeric sols and propose a means of independently controlling pore size and pore volume based on an organic template approach.

PROJECT DESCRIPTION/EXPERIMENTAL DETAILS

Sol Synthesis and Membrane Deposition

One series of silicate sols was prepared from tetraethoxysilane [$Si(OC_2H_5]$ (TEOS) dissolved in absolute ethanol using variations of a two-step hydrolysis process previously referred to as A2 [6]. In the first step TEOS, EtOH, and H_2O were combined with varying concentrations of HCl, producing stock solutions with TEOS:EtOH:H_2O:HCl molar ratios ranging from 1:3.8:1.1:2x10^{-3} to 1:3.8:1.1:7x10^{-6} These solutions were refluxed for 90 min at 60°C. After various times of aging at 0°C, additional water plus acid were added to the stock solutions at room temperature, resulting in final molar ratios (TEOS:EtOH:H_2O:HCl) ranging from 1.0:3.8:5.1:0.18 to 1.0:3.8:5.1:6 x 10^{-4}. These sols were aged at 50°C for various periods of time corresponding to t/t_{gel} values of 0.05 to 0.83 and then diluted 2:1 with EtOH (volume EtOH:volume sol = 2:1). The sol structures were characterized during aging using ^{29}Si NMR and SAXS as reported previously [8].

A second series of sols was prepared by co-condensation of tetraethoxysilane with a biphenyl bridged silsesquioxane [bis(triethoxysilyl)biphenyl] (BESB) under acid-catalyzed conditions with a H_2O:(TEOS + BESB) ratio of 1:5. The ratio of TEOS/BESB was varied to produce sols in which the condensed phase contained either 10 or 25 vol % of the biphenyl template ligand.

Table 1. Energy dispersive spectroscopic analyses of the Si/Al ratios measured in the γ-Al_2O_3 support layer for the same series of TEM cross-sections shown in figure 4.

	d[μm]	Si Count	Al Count	Si/Al Ratio
$t/t_{gel} = 0.05$	0.05	966	7151	0.135
	0.25	918	7148	0.128
	1.00	1032	7027	0.147
	2.75	1042	7258	0.144
	3.25	0	0	0
$t/t_{gel} = 0.24$	0.05	753	7289	0.103
	0.25	881	7285	0.121
	1.00	1087	7283	0.157
	2.75	964	7316	0.132
	3.25	0	0	0
$t/t_{gel} = 0.83$	0.05	768	7105	0.108
	0.25	606	7111	0.085
	1.00	554	6974	0.079
	2.75	516	7195	0.072
	3.25	0	0	0

Sols were deposited on 5 cm sections of asymmetric tubular alumina supports and supplied by U.S. Filter™. The tubes were composed of three layers of α-Al_2O_3 and one ~ 4 μm thick layer of γ-Al_2O_3. The pore size varied from about 10μm at the outside diameter to about 4.0 nm at the inside diameter, corresponding to the γ-Al_2O_3 layer. Prior to coating the support tubes were cleaned with CO_2 snow and outgassed in He at 150°C. Outgassed tubes were mounted vertically on a linear translation stage in a dry box and lowered into the sol at 20 cm/min. After an immersion period of 100 s, the supports were withdrawn at a rate of 20 cm/min and allowed to dry in a flowing N_2 ambient for 15 min. Companion samples were prepared on single crystal silicon <100> wafers or single crystal quartz surface acoustic wave (SAW) substrates [9]. The deposited membranes or films were calcined in air at a rate of 1°C/min up to 400°, maintained at 400°C for 10 min and cooled to room temperature.

The microstructure and chemical composition of the deposited membranes were characterized by cross-sectional TEM, energy dispersive spectroscopy, and x-ray fluorescence spectroscopy as reported previously [8]. The thickness and refractive index of companion films deposited on Si supports were determined by ellipsometry. Gas adsorption-desorption isotherms of films deposited on quartz substrates were acquired using a surface accoustic wave (SAW) technique [9]

Transport Measurements

He and N_2 permeabilities of both the bare and coated tubes were measured over the pressure range 0 - 100 psi. The tubular membrane was supported in a gas flow cell configured so that compression of VITON™ end gaskets prevented gas by-passing [8]. Prior to transport measurements the samples were outgassed for over eight hours at 150°C in flowing He (~10 cm^3/min).

RESULTS

Membrane Deposition

According to Darcy's law, the flux of liquid flowing in a porous medium is proportional to the stress gradient in the liquid ∇P:

$$J_D = (D/\eta)\nabla P. \qquad (3)$$

where J_D is the flux, D is the permeability, and η is the viscosity of the liquid. Thus, when the support is immersed in the sol, liquid flows into the support due to the pressure gradient in the liquid created by the formation of liquid-vapor menisci within the support pores. The pressure gradient $\nabla P = \Delta P/l$ where ΔP equals approximately the capillary pressure P_c:

$$P_c = -2\gamma_{LV}\cos(\theta)/r_s \qquad (4)$$

and γ_{LV} equals the liquid-vapor surface tension, θ equals the wetting angle, r_s equals the pore radius of the support, and l equals the length of the pore. From Eqs. 3 and 4, we see that for wetting pore fluids ($\cos\theta > 0$), liquid flows into the support with a flux proportional to D/r_s. Based on Poiseuille's law for flow of liquid through a straight circular pipe, the characteristic time t to fill a pore of length l and radius r_s is $t = 2l^2\eta/\gamma_{LV}r_s$ [10].

Based on the above considerations, we expect that when the assymetric support is immersed in the sol, the 4 nm pores will fill almost immediately (~ms) concentrating polymer on the inner support surface by a process analogous to slip-casting. The flux of liquid through the coarse (10µm), outer surface of the support is less and the time scale to fill these pores much longer. Assuming deposition of silica (with density = 2.0 g/cm^3) to occur only on top of the 4.0 nm support surface, slip-casting could account for up to 35 nm of the deposited film thickness in our case. (Whether polymer deposition actually occurs on the support surface or within the support pores depends on the relative sizes of the polymers and pores as discussed below).

When the support is withdrawn from the sol at a constant rate U, a fluid mechanical boundary layer is entrained on the support surface (see Figure 2). Assuming the 4-nm support surface to be completely filled with liquid, the entrained film thins by gravitational draining accompanied by evaporation, causing the fluid film to acquire a parobolic shape in the vicinity of the drying line (x = 0 in fig. 2) [11]. For a binary EtOH-water mixture, preferential evaporation of EtOH enriches the sol in water[§] + polymer [11,12], promoting further condensation reactions and leading to the formation of a physical or chemical gel. At the final stage of the deposition process, liquid-vapor menisci created at the free surface cause the liquid to be in tension there. We expect that the tension in the liquid (P_c, Eq. 4, where we replace r_s with the pore radius of the membrane r_m) will contribute to the collapse of the depositing film as well as drive flow of liquid from the support into the membrane, when $r_m < r_s$. As a consequence, the drying time of membranes deposited on porous supports will be protracted compared to conventional dip-coating of films on solid supports.

Effect of Sol Aging

For two-step hydrolysis processes, aging of the sol may be performed after the first step, after the second step, or both. From ^{29}Si NMR studies performed on several of the A2 series of sols, we have observed that sol aging after the first step (stock solution, $H_2O/Si = 1.1$) favors the formation of cyclotetrasiloxanes apparently through condensation of the dimer $(EtO)_4(HO)_2Si_2O$ [13]. ^{29}Si NMR and SAXS studies of aging after the second hydrolysis step ($H_2O/Si = 5$) show in general increased extents of condensation, increased Guinier radii, and increased values of the mass fractal dimension D with increasing t/t_{gel} for sols prepared from either aged or fresh stock solutions (see for

---

[§] Dip-coating experiments of $EtOH\text{-}H_2O$-based silica sols on dense, flat substrates indicate that for starting water concentrations ranging from 3 to 25 vol%, the composition of water at the drying line ranges from 50 to 82 vol% [12].

example Figure 3). However, the increased cyclic contents of the aged stock solutions contributed to comparatively much higher Q^2 concentrations at short aging times, and although the Q distributions became practically identical at long aging times, sols prepared from aged stock solutions consistently exhibited lower mass fractal dimensions and a much greater range of power law scattering behavior than their counterparts prepared from fresh stock solutions. This behavior is attributed to the hydrolytic stability of cyclic species and their ability to stiffen the evolving polysiloxane network, leading to more extended networks.

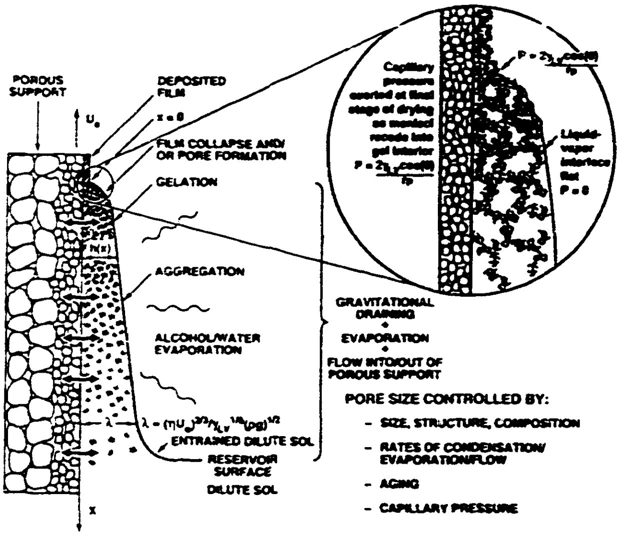

Fig. 2. Schematic illustration of membrane formation on a porous support.

For sols prepared from either fresh or aged stock solutions, we observe that it is possible to grow the polymers so that the Guinier radius R_G exceeds the pore radius of the support, $R_G > r_c = 2$ nm, while maintaining values of D below about 1.8. For these aging conditions, we expect that polymers should be captured on the support surface, forming a discrete layer, yet mutually interpenetrate leading to small pore sizes* Cross-sectional TEM images of membrane/substrate interfaces (e.g. Fig. 4) reveal that when $R_G \geq r_s$ a discrete membrane layer is formed on the support surface. There is no evidence of an external membrane layer when $R_G < r_s$

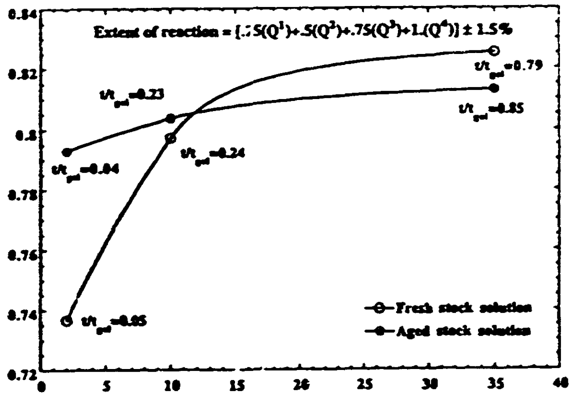

Fig. 3a. Extents of reaction versus relative gel times t/t_{gel} for two-step acid-catalyzed sols prepared from fresh aged or fresh stock solutions.

The formation of a discrete external membrane layer does not mean that there is no penetration of silica into the support, however. Kinetically limited aggregation processes, such as reaction-limited cluster aggregation, which account for growth of silica polymers, lead to highly polydisperse systems [6]. Corresponding energy dispersive spectroscopy (EDS) analyses of the cross-sections shown in Figure 4 indicate that silica penetrates the 4 nm γ-Al_2O_3 layer to a depth of about 3 µm (Table 1), which is the approximate thickness of this layer. Increased aging times reduce the concentration of silica, but do not eliminate it. It is unlikely that the silica contained within the support pores forms an effective membrane, since constrained three-dimensional shrinkage within the substrate pore channels could lead to cracking (see Figure 1).

Effect of Condensation Rate

Refractive index measurements verify the qualitative picture that, for low values of D, polymer interpenetration is promoted

---

* Equation 2 assumes that the sticking probability at each point of intersection is unity, lower probabilities should promote polymer interpenetration at higher values of D. In general, based on ellipsometry measurements, we find that for acid-catalyzed silicates, D < 2 is sufficient to achieve interpenetrating polymers.

leading to featureless (Fig. 4), dense films (volume fraction solids $\phi_S \rightarrow 0.9$), exhibiting practically no dependence of the refractive index ($\propto \phi_S$) on the measured polymer size of the sol (see Table 2). Corresponding SAW N_2 sorption measurments performed at 77K on A2 films deposited on solid supports consistently produced Type 2 isotherms indicating no adsorption of N_2 within the pore channel system over the time scale of the measurement [13]. Transport measurements of the corresponding membranes deposited on porous supports showed significant reductions in permeance, consistent with pore radii ≤ 0.5 nm [8]. However, despite these indications of very small pore sizes, He/N_2 separation factors did not exceed the ideal Knudsen value [8]. Based on models of gas transport in micropores, we concluded that the pore radii were in the range 0.35 nm $< r_p <$ 0.5 nm [14].

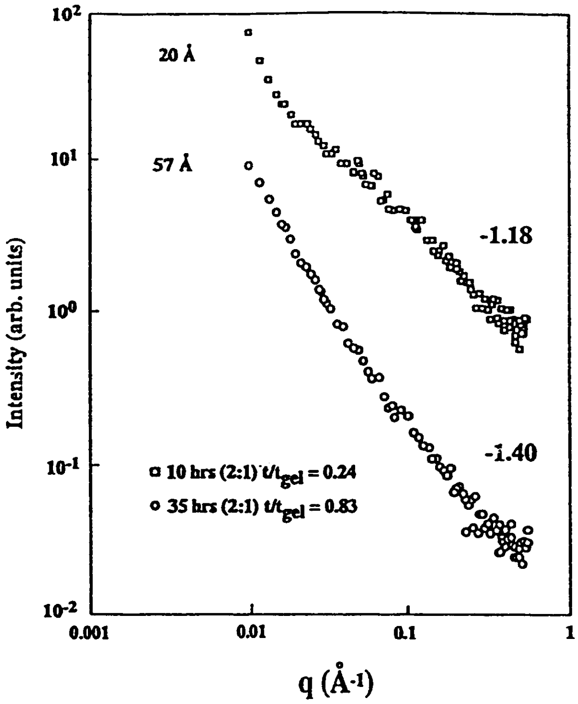

Fig. 3b. Porod plots of log scattered intensity versus log scattering wave vector for two-step acid-catalyzed silica sols prepared from an aged stock solution. Listed are corresponding values of the Guinier radius (Å) and Porod slope.

To further reduce the pore size into the molecular sieving regime, we can consider the classical drying theory developed by Scherer [6]: the final pore size is established by the extent of collapse of the gel network in response to the maximum capillary pressure developed at the critical point. To obtain smaller pores it is necessary to promote further collapse of the gel network in response to the capillary pressure. Considering the network to be elastic, the deformation or strain is increased for a particular P_c as the modulus is decreased.

Through minimization of the condensation rate, it is expected that, during membrane deposition and drying, the polymers should readily interpenetrate (very few points of intersection $M_{1,2}$ result in "sticking", Eq. 2) and the network should exhibit the greatest strain in response to the capillary pressure. Figure 5 shows the effect of the final pH[#] on the condensation rate as estimated from reciprocal gel times $1/t_{gel}$ for the series of two-step acid-catalyzed sols along with several values of the He/N_2 separation factors calculated from single gas permeability measurements of supported membranes. We observe separation factors exceeding ideal Knudsen values only for membranes prepared from two coatings of sol A2** corresponding to the sol composition exhibiting the minimum condensation rate. Based on the model of gas transport in micropores developed by Fain [14], we estimate that the membrane pore size has been reduced to $r_m \leq 0.35$ nm.

This result at first seems consistent with the classical picture. However to achieve even a 10% reduction in pore size, it would be necessary to reduce the pore volume by over 25%. Corresponding refractive index measurments of films prepared on dense supports show little difference between the A2, A2*, and A2** compositions (they all correspond to about $\phi_S \approx 0.9$). This may indicate that the effect of minimization of the condensation rate is instead to significantly narrow the pore size distribution without so much affecting the average pore size. This idea may be rationalized by consideration of

---

[#] pH for this mixed solvent system calculated as $-\log[H^+]$

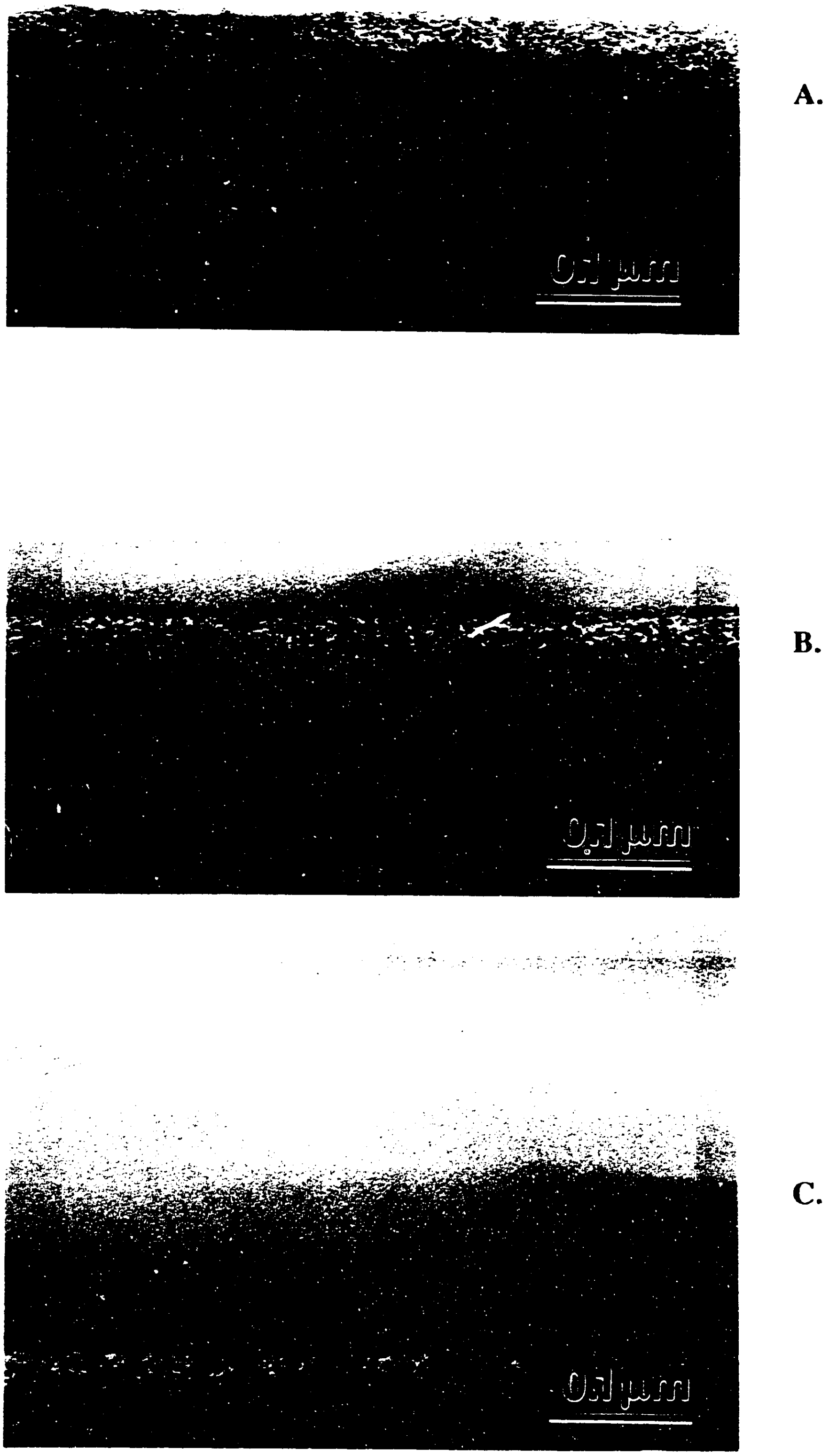

Figs. 4a, 4b, and 4c. Cross-sectional TEM images of membrane/support interfaces. Membrane layers were deposited from two-step acid-catalyzed sols prepared from aged stock solutions and deposited at $t/t_{gel} = 0.05$ (4a), 0.24 (4b), or 0.83 (4c).

the equivalent phase diagram for a polymer gel in semi-dilute solution with good solvent (see Fig. 6) [15]. If the original sol is prepared in the one phase region, minimizatioin of the condensation (reaction) rate might allow the formation of a single phase gel as the polymer phase is concentrated during membrane deposition (path A in Fig). The effect of increasing extents of reaction is to reduce the equivalent temperature so, for sol compositions corresponding to greater condensation rates, concentration causes the reaction path to cross the coexistence line (path B in Fig. 6). Although crosslinking of the gel prevents a macroscopic segregation, the gel probably experiences at this point a "microphase separation" that would serve to increase the pore size distribution.

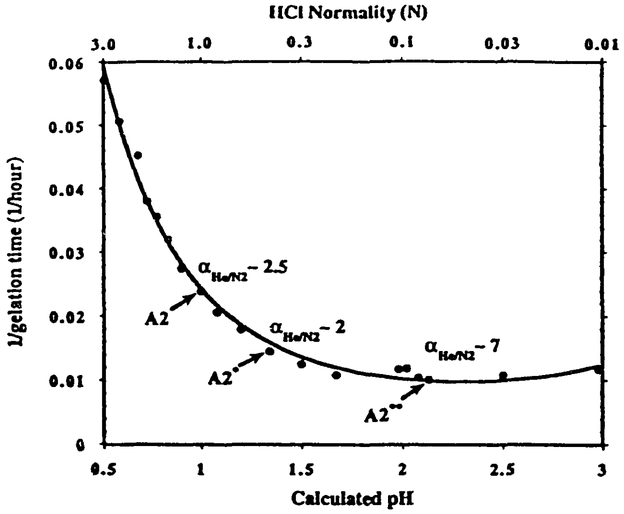

Fig. 5. Reciprocal gel times (proportional to average condensation rates) versus calculated pH for a series of two-step acid catalyzed silica sols. Alpha values represent the He/Ne$_2$ seperation factors for the corresponding membranes prepared from the A2 A2* and A2 sols.**

Control of Pore Size

From the above discussion we may suppose that the collapse of the gel in response to the capillary forces establishes the pore volume and average pore size, while factors such as the condensation rate influence the pore size distribution. To achieve smaller average pore sizes, it is necessary to reduce the pore volume. However, the bulk moduli K_p of a wide variety of wet and dry silica gels has been shown to scale as approximately $K_p = K_0(V_0/V)^{3.8}$, where V_0 is the volume of the gel at the gel point and V is the volume after varying extents of drying. [16]. Thus the extent of collapse of the gel and correspondingly the minimum attainable average pore size may be ultimately limited by the increasing modulus. For the dip-coating process, we can attempt to approximate the volume fraction (V/V_0) at which point shrinkage stops, thus establishing the pore size, by evaluating the capillary pressure and modulus as a function of position x for the depositing film (see Fig. 2). Shrinkage will stop at the point where the resistance stress of the network is balanced by the capillary pressure [16]. Previous experimental and computational analyses of the steady state dip-coating process have established both the volume fraction solids ϕ_s and mean interparticle spacing $<r_m>$ as a function of position x (see Figure 2) [11]:

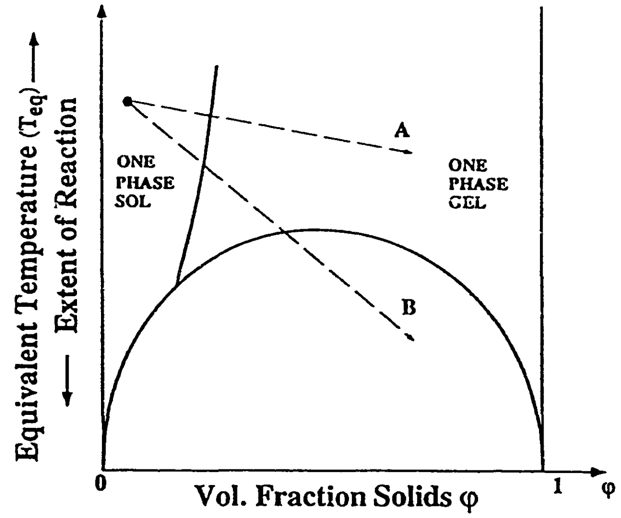

Fig. 6. Schematic phase diagram for a polymeric gel system in semi-dilute solutions with good solvent. Two reactions pathways are represented corresponding to film formation when the condensation rate is low (Pathway A) or high (Pathway B). From de Gennes [15].

$$\phi_s \sim x^{-1/2}, \quad <r_m> \sim x^{1/6} \quad (5)$$

By taking the gel network to be perfectly elastic and compressible and the film thickness to be much less than the film width and breadth, we can arrive at the following force balance:

$$P_c = 2\gamma_{LV}\cos(\theta)/<r_m> = G_o(\phi_s/\phi_s^o)^{3.8}(\phi_s/\phi_s^o)^{-2} \quad (6)$$

where G_o is the shear modulus and ϕ_s^o is the volume fraction solids at the gel point. Although the assumption of perfect compressability is not strictly true, i.e., a Poisson's ratio of zero, we use it here for the sake of illustration. The effect of a nonzero Poisson's ratio would show up in Eq. 6 as a factor larger than unity multiplying G_o.

Figure 7 shows the results of finite element based calculations of how the resistance stress of the network (right hand side of Eq. 6), mass fraction solids, and capillary pressure vary with position in the depositing film for the case of G_o = 0.5 MPa and $\phi_s^o = 0.4$. Noteworthy is that the ratio of capillary stress to network stress decreases with distance up the substrate, with the network stress equalling the capillary pressure at a mass fraction solid in the range ϕ_s = 0.72 to 0.8, values reasonably consistent with the experimentally measured value ϕ_s = 0.9 (see Table 2). It is important to keep in mind that these results are highly dependent on the gel point volume fraction solids $\phi_s{}^o$ and the corresponding shear modulus. Future work will be aimed at directly measuring these values using optical techniques [see, e.g.12] and considering the viscous and visco-elastic cases.

Table 2. Refractive index and thickness measurements for films deposited on silicon supports after aging to various values of t/t_{gel}.

Aging at 50°C (t/t_{gel})	A2 sols from Fresh stock solution			A2 sols from Aged stock solution		
	Thickness (Å)	Refractive Index	Vol. Frac. Porosity	Thickness (Å)	Refractive Index	Vol. Frac. Porosity
0.05	1580	1.403	0.1	1376	1.398	0.1
0.24	1590	1.398	0.1	1359	1.415	0.08
0.82	2245	1.401	0.1	1369	1.409	0.09

Use of Templates

As described in the previous discussion, using the polymeric silica approach, small pore sizes are created by promoting collapse of the gel structure. This causes a reduction in both the pore size and the pore volume, so selectivity improvements are achieved at the expense of flux. One means of de-coupling pore size and pore volume is to create pores within a dense matrix by the removal of a *pore template* [17]. Our idea (see Figure 8) is to embed the organic template (e.g. biphenyl) in a dense silica matrix. Conceivably the template could be designed to mimic the size and shape of a specific target molecule to achieve molecular recognition capabilities or it might be designed to mimic a transition state of a desired reaction to achieve a catalytic function. Removal of the template, by oxidation or ozonolysis, then creates a pore the size and shape of the biphenyl spacer. With this strategy the pore size and shape depend on that of the template, while the pore volume and connectivity depend on the volume fraction of the template phase. (In order to achieve connectivity of the pores, we must exceed the percolation threshold of the templates or perhaps rely on phase separation).

In order to demonstrate this strategy in the fabrication of thin films useful for membranes we have co-condensed tetraethoxysilane [$Si(OC_2H_5]$ with a biphenyl bridged silsesquioxane [bis(triethoxysilyl)biphenyl] and have prepared thin films from the resulting sols.

Table 3 lists values of the refractive index measured by ellipsometry for silica films containing either 0, 10, or 25 vol % biphenyl after deposition at room temperature and after heating to either 400 or 500°C. We observe that for samples containing biphenyl, the refractive index is reduced upon heating to 500°C by which temperature corresponding TGA shows the biphenyl to be removed. Using the Lornetz-Lorenz model and assuming the refractive index of dense vitreous silica to be 1.45, values of the refractive index were used to calculate the vol % porosities of the films created by removal of the templates. From Table 3 we see that the vol % porosities correspond approximately to the vol % of the added templates. From this observation we can conclude that template removal is not accompanied by collapse of the surrounding matrix, suggesting that the created pores might faithfully reproduce the size and shape of the templates.

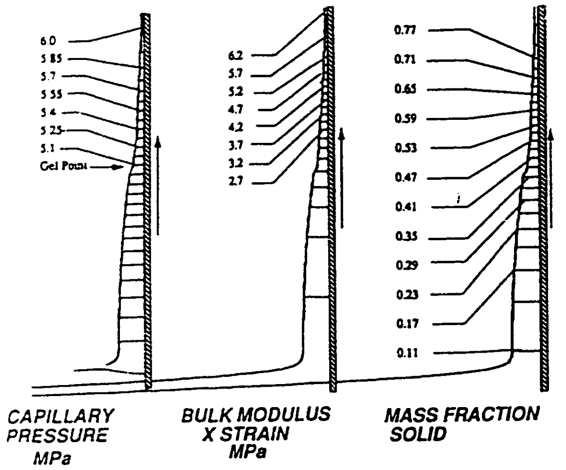

Fig. 7. Capillary pressure, network stress, and mass fraction solids in the deposition region of the dip-coating process. The liquid starts as 70%/20%/10% ethanol/water/silica by weight and is coated at a speed of 0.4 cm/s. The capillary stress is computed as $2\gamma_{LV}/<r>$ and the network stess is computed from Eq. 6. G_0 is taken as 0.5 MPa and the mass fraction solids at the gel point is taken as 0.4.

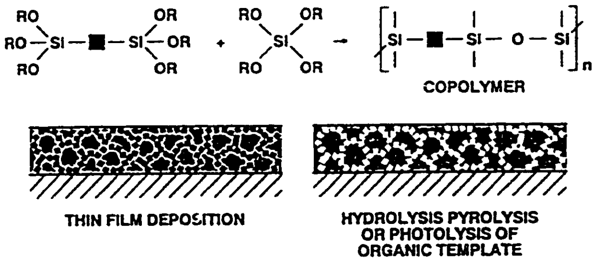

Fig. 8. Schematic illustration of molecular engineering of porosity in silica films using organic templates. Removal of the template creates a pore that mimics the size and shape of the organic ligand.

To evaluate the corresponding pore size and connectivity, companion thin film samples were prepared on surface acoustic wave (SAW) substrates. Figure 9 a and b plot the N_2 and partial CO_2 isotherms acquired at 77K and 0°C, respectively. The N_2 isotherm is of Type 2 characteristic of adsorption on a non-porous solid, while the limited CO_2 isotherm is clearly of Type 1 indicative of the presence of microporosity. Since the kinetic diameters of N_2 and CO_2 are quite similar, this apparent discrepancy suggests that at 77K transport into the micropores is kinetically unfavorable.

Based on the combined ellipsometry and adsorption results, several important conclusions can be drawn: 1) heat treatments that pyrolyze the biphenyl template create porosity in the film; 2) the volume fraction porosity corresponds approximately to the volume fraction of the template phase; 3) a continuous microporous network is created by template removal (isolated pores would not give rise to a Type 1 isotherm); 4) from the complete N_2 isotherm we see no evidence of the creation of mesoporosity; and 5) the steepness of the CO_2 isotherm and the absence limited adsorption of N_2 at 77K are both suggestive of very small pores consistent with the removal of the biphenyl template ($r_p < 0.5$ nm). Unfortunately there is not yet appropriate theory to allow us to calculate the surface area and pore size of the film based on the CO_2 sorption data.

Table 3. Effects of template concentration and calcination temperature on the refractive indices of composite silica/4,4'bis(triethoxysilyl)biphenyl films prepared on silicon wafers. Corresponding TGA shows that the biphenyl ligands are largely removed between 400 and 500°C. Percent porosities of the films heated to 500°C were calculated from the refractive index values (see text). Heating rates were 1°C/min.

Temperature (1°C)	Volume % Biphenyl Spacers in Silica Film Matrix		
	0%	10%	25%
As deposited	1.437	1.485	-
400°C	1.419	1.615	2.115
500°C	1.421	1.388	1.313
		(~9% Porosity)	(~28% Porosity)

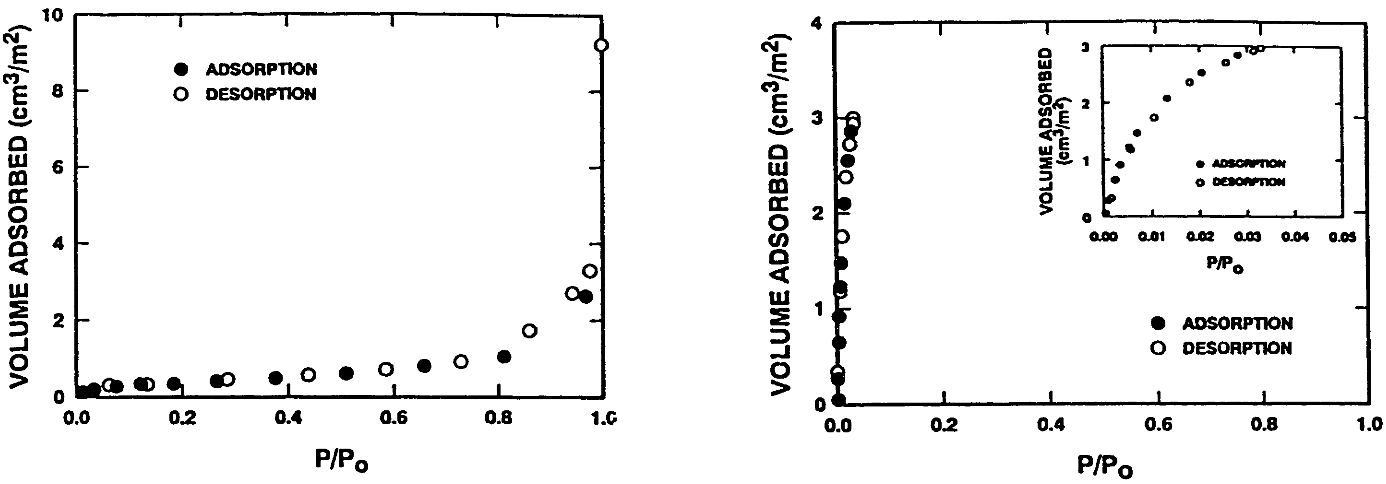

Figs. 9a and 9b. Sorption isotherms, obtained using Saw techniques, of composite silica (A2)/4,4'bis(triethoxylsilyl)biphenyl films containing 25 vol% of the biphenyl spacer ligand and calcined to 500°C. Nitrogen sorption at 77 K (a) shows a Type 2 isotherm indicative of a non-porous film. The partial carbon dioxide isotherm at 273 K of the same film (b) shows a Type 1 isotherm indicative of microporosity, seen more clearly in the expanded scale of the inset figure. The y-axis represents the volume of gas adsorption per area of the coated substrate.

SUMMARY/FUTURE WORK

For silica membranes prepared from two-step acid-catalyzed sols, we have shown that sol aging times can be used to grow the polymers large enough to form a discrete membrane layer on a commercial alumina support with $r_s = 2$ nm. Quite dense films ($\phi_s \equiv 0.9$) were formed for the complete range of acid-catalyzed conditions studied, consistent with the idea of mutually interpenetrating polymer networks. However the corresponding He/N_2 selectivity factors did not exceed the ideal Knudsen value except for the system in which the condensation rate was minimized. Since the average pore size is established by the balance of the increasing capillary pressure and the increasing network modulus during drying, one effect of minimization of the condensation rate may be to reduce the modulus to foster more complete collapse of the gel network, resulting in smaller pore size. We are currently testing this idea by determining the effects of condensation rate on the scaling relationship of modulus and gel volume. A second effect of minimization of the condensation rate may be suppression of phase separation which could serve to narrow the pore size distribution. Organic templates appear to be a promising strategy to control both the pore size and pore volume of microporous membranes.

Future work will concentrate on modification of pre-formed molecular sieving membranes, using small monomeric or oligomeric species, to further reduce pore sizes. We will also study the use of bis(triethoxysilyl)phenyl precursors (single phenyl templates) that should allow the formation of pores of radius 0.33 nm suitable for molecular sieving characteristics.

ACKNOWLEDGMENTS

National Science Foundation, the Electric Power Research Institute, the Gas Research Institute, Morgantown Energy Technology Center, and the Department of Energy Basic Energy Sciences Program. We are grateful to Roger A. Assink for the NMR results and D. W. Hua for the SAXS measurements. Sandia National Laboratories is a U. S. Department of Energy facility supported by Contract Number DE-AC04-76-DP00789.

REFERENCES

1 A.F.M. Leenars, K. Keizer and A.J. Burggraaf, J. Mat. Sci., 10, 1077-1088 (1984).
2. A. Larbot, J.A. Alary, J.P. Babre, C. Guizard and L. Cot, "Better Ceramics Through Chemistry II", Eds. C.J. Brinker, D.E. Clark and D.R. Ulrich, Mat. Res. Soc. Symp. Proc., Vol. 73, Mat. Res. Soc., Pittsburgh, PA (1986), 659.
3. M.A. Anderson, M.J. Gieselman and Q. Xu, J. Membrane Sci., 39, 243-258 (1988).
4. J. Guibaud in ICIM-89, "The First International Conference on Inorganic Membranes, eds. L. Cot and J. Charpin, Montpellier, France, 1989.
5. T.J. Garino, Ph.D. Dissertation, MIT., Cambridge, MA, 1986.
6. C.J. Brinker and G.W. Scherer, "Sol-Gel Science", Academic Press, San Diego (1990)
7. B.B. Mandelbrot, "The Fractal Geometry of Nature", Freeman, San Francisco (1982).
8. C. J. Brinker, T. L. Ward, R. Sehgal, N. K. Raman, S. L. Hietala, and D. M. Smith, D. W. Hua, and T. J. Headley, J. Membr. Sci, 77 [2-3] 165-179 (1993).
9. G. C. Frye, A. J. Ricco, S. J. Martin, and C. J. Brinker, "Better Ceramics Through Chemistry III", Eds. C.J. Brinker, D.E. Clark and D.R. Ulrich, Mat. Res. Soc. Symp. Proc., Vol. 121, Mat. Res. Soc., Pittsburgh, PA (1988) p. 349-354.
10. T. W. Kueper, S. J. Visco, and L. C. DeJonghe, J. Am. Ceram. Soc., to be published.
11. C. J. Brinker, A. J. Hurd, P. R. Schunk, G. C. Frye, and C. S. Ashley, J. Non-Cryst. Solids, 147&148, 424-436 (1992).
12. F. Nishida, B. Dunn, J. M. McKiernan, J. I. Zink, A. J. Hurd, and C. J. Brinker, "Proceedings of the VIIth Intl. Workshop on Glasses and Ceramics from Gels", to be published, J. Sol-Gel Sci. and Tech., 1993.
13. C. J. Brinker, N. K. Raman, R. Sehgal, M. N. Logan, T,. L. Ward, R. A. Assink, and D. W. Hua, submitted to J. Sol-Gel Sci. & Tech.
14. D.E. Fain, Key Engineering Materials, 61&62, 327-336 (1991).
15. P-G de Gennes, "Scaling Concepts in Polymer Physics", Cornell University Press, Ithaca, (1979) p. 151.
16. G. W. Scherer, J. Non-Cryst. Solids, 142, 18 (1992).
17. K. J. Shea, and D. Y. Sasaki, J. Am. Chem. Soc., 111, 3442, (1989).

P7

Examples from the Atlas of Major Appalachian Basin Gas Plays

CONTRACT INFORMATION

Contract Number	DE-FC21-91MC28176
Contractor	Appalachian Oil and Natural Gas Research Consortium P.O. Box 6064 Morgantown, WV 26506-6064 (304) 293-2867
Contractor Project Manager	Douglas G. Patchen
Principal Investigators	Khashayar Aminian Katharine Lee Avary Mark T. Baranoski Kathy Flaherty Brandon C. Nuttall Richard A. Smosna
METC Project Manager	Harold D. Shoemaker
Period of Performance	October 1, 1991 to September 30, 1994

Schedule and Milestones

FY94 Program Schedule

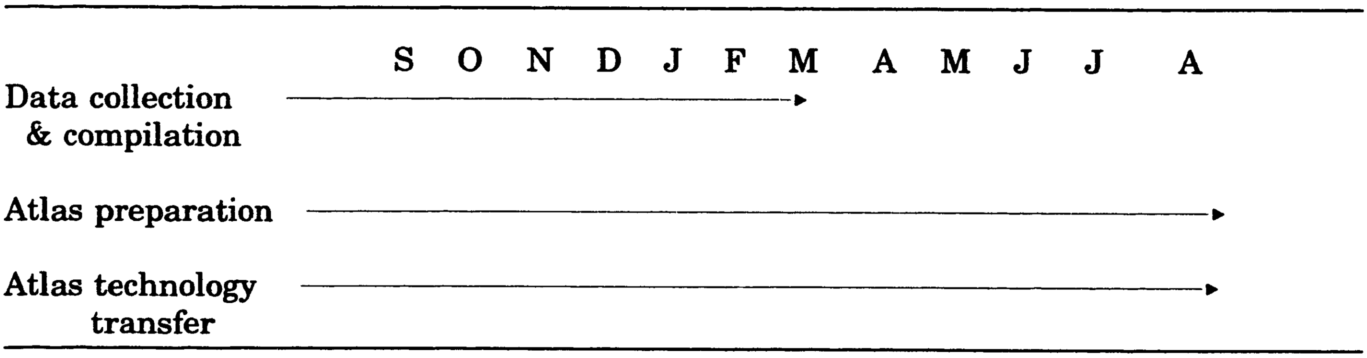

OBJECTIVES

The objectives of this contract are to produce a printed atlas of major Appalachian basin gas plays and to compile a machine-readable database of reservoir data.

BACKGROUND INFORMATION

In their "Gas Research Program Implementation Plan" issued in April 1990, the U.S. Department of Energy identified and discussed research activities for natural gas resource assessment and recovery with near-, mid-, and long-term objectives and described how to implement these activities. In the near-term, five research topics were identified, including "Gas Atlases Compilation/Reservoir Classification," and "Database Consolidation and Maintenance." DOE envisioned a close linkage between these two activities with data flowing between both as they were performed concurrently. However, DOE noted that it may be essential to develop an appropriate reservoir classification scheme that divides reservoirs in a region into groups with common geological and engineering characteristics before consolidating databases or producing the gas atlases. They further stated that this combination of activities (classification scheme, database consolidation, gas atlases) "... clearly represents a major effort...", one that will require the assistance of "... universities, industry, and state and federal geological surveys." The report goes on to state that the three activities are " an essential starting point for the entire gas program..." to guide further research and industry development and to expose gaps in data currently available for those pursuits.

The Appalachian Oil and Natural Gas Research Consortium (AONGRC or the Consortium), a partnership of the state geological surveys in Kentucky, Ohio, Pennsylvania, and West Virginia, and the departments of Geology and Petroleum and Natural Gas Engineering at West Virginia University (WVU), agrees with the need to classify gas reservoirs by geologic plays. During meetings with industry representatives, the small independents in the basin emphasized that one of their prime needs was to place each producing reservoir within a stratigraphic framework subdivided by environment of deposition to enable them to develop exploration and development strategies.

The Appalachian basin is a broad geologic province that spans several states. There is no central regulatory authority, similar to the Texas Railroad Commission, acting as a source of detailed reservoir data. The general absence of major oil and gas companies in the exploration and development of the basin has resulted in many small independent operators with limited geologic staffs generating internal reports on prospective areas for drilling; these reports are often not published. Most private vendors of oil and gas well and reservoir information are generally lacking in historical data typical of mature provinces. Finally, significant exploration and development occurred prior to the establishment of statewide regulatory agencies.

PROJECT DESCRIPTION

Six tasks were identified to accomplish the objectives. Task 1, Defining Gas Plays, resulted in the identification of 31 plays. Task 2, Data Collection and Compilation, is on going, as play descriptions are being written, tables and illustrations constructed, and the atlas database designed. Task 3, Atlas Preparation, is in progress at present. Task 4, Atlas Review, is following Task 3 closely, as an essential part of the play description preparation. Task 5, printing the atlas, will occur during the final months of the contract. Task 6, Technology Transfer, has been on-going throughout the contract, with presentations by project personnel at the 24th Annual Appalachian Petroleum Geology Symposium, the 1993 Eastern Section, American Association of Petroleum Geologists Annual Meeting, METC Contractors Review Meetings, and the Kentucky Oil and Gas Association 1993 Summer Meeting. The 25th Annual Appalachian Petroleum Geology Symposium, to be held in March, 1994 in Morgantown, WV, will be devoted to presentations on all of the Appalachian basin gas plays being included in the Gas Atlas.

RESULTS

The text for eight of the 31 play descriptions has been completed, drafting of illustrations for these plays is underway (or complete for some plays), and the review process is ongoing. The review process has been set up to ensure consistency, accuracy, and completeness for all play descriptions included in the atlas. Following internal reviews by three project members, the text and illustrations are sent to three external reviewers and to the METC project manager. After all external and METC reviewer comments have been examined by the author(s), the text and illustrations are reviewed by the technical editor. Upon approval of the text and illustrations by the technical editor, the production editor then prepares the text and illustrations for publication.

Eleven additional plays are scheduled to be completed by the end of November, 1993. The remaining 12 will be completed in early February, 1994.

Table 1 is the standard outline being used by all authors for the play descriptions. The use of the outline will enable the reader to quickly and easily find the same information for comparison of different plays. Table 2 lists the typical required and optional illustrations for each play. Table 3 is an example of the "Reservoir and Production Data of Major Pools Included in Play XX" table which will be included with each play description. A maximum of 24 fields or pools in each play will be published in the atlas. Data on all the fields and pools included in each play will be contained in the database.

Figure 1 is an example (the Lower Silurian Tuscarora Sandstone Fractured Anticline play) of the map showing the location of the fields and pools included in a play. This figure is designed to show the relative extent of each play within the basin. A correlation chart (Figure 2, for the Cambrian-Ordovician Knox Group unconformity play) serves to locate the play stratigraphically. Correlation charts may show both formal stratigraphic and informal drillers' terms. Isopach (Figure 3) and structural contour (Figure 4) maps of a key field (Oneida Consolidated field, Clay County, Kentucky, Lower Devonian- Upper Silurian unconformity play) are used to illustrate the relationship of structure and thickness to gas production. Type logs for key fields (Figure 5, east central Kentucky, Lower Devonian-Upper Silurian unconformity play) show log characteristics of the reservoir and surrounding units. Stratigraphic cross sections (Figure 6, the Cambrian-Ordovician Knox Group unconformity play) are used to illustrate regional stratigraphic relationships of the productive zones and overlying and underlying units.

FUTURE WORK

In the remaining year of the contract, all play descriptions and illustrations will be finalized and prepared for printing. The database will be compiled and formatted for delivery.

REFERENCES

Dolly, E.D., and Busch, D.A., 1972, Stratigraphic,structural, and geomorphic factors controlling oil accumulation in Upper Cambrian strata of central Ohio: American Association of Petroleum Geologists Bulletin, v. 56, no. 12, p. 2335-2369.

Janssens, A., 1973, Stratigraphy of the Cambrian and Lower Ordovician rocks in Ohio: Ohio Division of Geological Survey Bulletin 64, 197 p.

Milici, R.C., and de Witt, Wallace, Jr., 1988, The Appalachian Basin, *in* Sloss, L. D., ed., Sedimentary cover--North American Craton:U.S.: Geological Society of America,The Geology of North America, v. D-2, p. 427-469.

Patchen, D.G., Avary, K.L., and Erwin, R.B., 1985, Correlation of Stratigraphic Units of North America (COSUNA) project-Northern Appalachian Region: American Association of Petroleum Geologists, chart, 1 sheet.

Riley, R.A., Baranoski, M.T., Carlton, R.W., Harper,J.A., and Laughrey, C.D., 1993, Measuring and predicting reservoir heterogeneity in complex deposystems: the Late Cambrian Rose Run sandstone of eastern Ohio and western Pennsylvania: Final report, U.S. Department of Energy, contract no. DE-AC22-90BC14657, 220 p.

Table 1. Outline for play description

TITLE (play number, name, and author[s])

Location
Include a brief description of identifying features of the play if appropriate

Production History
Discovery, development, cumulative production

Stratigraphy
Producing formation(s), member(s), sand(s), zone(s), etc.
Age of producing unit(s)
Lateral equivalents of producing unit(s)
Environment(s) of deposition of producing unit(s)

Structure

Reservoir
Type of trap(s)
Source rock (age, lithology, maturity)
Migration of fluids
Depth to pay--range and average
Thickness--range and average
Rock pressure--range and average
Initial open flow--range and average
Final open flow--range and average
Heterogeneity (porosity types, porosity--range and average, permeability--range and average, type of reservoir [single layer, multi-layer], drive mechanism, completion strategies, production [per well--range and average, per acre--range and average], decline curves [typical well(s), typical pool(s)])

Description of Key Fields
(use field name to begin each description)

Resources and Reserves

Future Trends

References Cited

Table 2. List of play illustrations and tables

Illustrations

Typical field illustrations required for each play:
- Isopach or structure map
- Cross section (either structural or stratigraphic)
- Type log
- Pay or porosity map

Other illustrations:
- Pool map on basin base map
- Stratigraphic column (both formal and drillers' terms)
- Correlation chart

Plays defined by depositional systems or environments may include sketches or models of these systems. Other possible illustrations include types of traps, thermal maturity, and decline curve.

Tables

"Reservoir and Production Data of Major Pools Included in Play XX" will be included with each play description. For some plays, other tables may be appropriate.

Other tables which may have to be included:
- One table for one field per play with DOE's 41 data elements
- A table for the bigger plays with field names keyed to numbers on the pool map of the basin

Table 3. Reservoir and production data of major fields and pools in Cambrian-Ordovician Knox unconformity play

	Field/Pool PLAY 3	Lee Chapel Cons.	Burning Springs Cons.	Oneida Cons.	Pine Rock	Raccoon Mountain	Trixie Cons.	Buffalo	[illegible]	Lakeshore	Morrow Cons.
BASIC RESERVOIR DATA	POOL NUMBER	1601142368	1600320368	1601461368	1601319368	1601600368	1601702368	30029	30121	30013	30117082
	DISCOVERED	1975	1984	1985	1984	1955	1983			1949	1959
	DEPTH TO TOP RESERVOIR	1750	3450	3720	4600	3360	3720				3500
	AGE OF RESERVOIR	L.Ord.	L.Ord.	L.Ord.	L.Ord.	L.Ord.	L.Ord.	U.Camb.	U.Camb.	U.Camb.	U.Camb.
	FORMATION	Knox	Knox	Knox	BKMN	Knox	BKMN	THRA	THRA	THRA	Knox
	PRODUCING RESERVOIR	Knox	BKMN	BKMN	BKMN	Knox	BKMN	THRA	THRA	THRA	CPRG
	LITHOLOGY	dol.	dol.	dol.	dol.	dol.	dol.	ss.	ss.	ss.	dol.
	TRAP TYPE	Strat., Struc.	Strat., Struc.	Strat., Struc.	Struc.	Struc.	Struc.				Strat.
	DEPOSITIONAL ENVIRONMENT	Sh.mar.	Sh.mar.	Sh.mar.	Sh.mar.	Sh.mar.	Sh.mar.				Sh.mar.
	DISCOVERY WELL IP (gas)	150	20	700	146	488	90			2200	265
	DRIVE MECHANISM	g.e.	g.e.	g.e.	g.e.	g.e.	g.e.				s.g.,w.
	NO. PRODUCING WELLS	36	24	11	4	10	43	0	6	0	340
	NO. ABANDONED WELLS	5	3	0	0	0	2	2	0	1	241
	AREA (acres)	3369	1873	725	350	2100	700				9800
	OLDEST FORMATION PENETRATED	Knox	Knox	Knox	Rome	Knox	Knox				MTSN
	EXPECTED HETEROGENEITY DUE TO	fra.,dia.	fra.	fra.	fra.	dia.,fra.	fra.,dia.				dia.
RESERVOIR PARAMETERS	AVERAGE PAY THICKNESS (ft)	6	33	42	32	17	37				14
	AVERAGE COMPLETION THICKNESS (ft)										18
	AVERAGE POROSITY-LOG (%)	9	8	9	7	9	9				9
	MINIMUM POROSITY-LOG (%)	4	4	4	1	4	4				4
	MAXIMUM POROSITY-LOG (%)	12	16	15	16	15	17				18
	NO. DATA POINTS	4	10	9	4	6	11				30
	AVERAGE POROSITY-CORE (%)					8					8
	MINIMUM POROSITY-CORE (%)					5					3
	MAXIMUM POROSITY-CORE (%)					13					16
	NO. DATA POINTS					2					6
	POROSITY FEET	54	264	378	224	1 53	330				126
	AVERAGE PERMEABILITY (md)					5.8					7
	RELATIVE PERMEABILITY (md/ft)										
	RESERVOIR TEMPERATURE (°F)		85	93	92	83	82				98
	INITIAL RESERVOIR PRESSURE (psi)			1100	1450	800					1280
	PRODUCING INTERVAL DEPTHS (ft)	1400-1920	3170-3820	3540-3880	4520-4640	2990-3560	3540-3860				3000-4200
	PRESENT RESERVOIR PRESSURE (psi/date)		350/1987		235/1986	245/1991	420/1989				800/1992
FLUID & GAS PROPERTIES	Rw (ohm)		.06	.06	.06	.06	.06				.04
	GAS GRAVITY (g/cc)					.698					.62
	GAS SATURATION (%)		59	33	56	74	47				63
	WATER SATURATION (%)		41	67	44	26	53				25
	COMMINGLING										Y
	ASSOCIATED OR NONASSOCIATED	N.	A.	A.	N.	A.	A.				A.
	BTU					1076	1095				1062
VOLUMETRIC DATA	STATUS (producing, abandoned, storage)	P.	P.	P.	P.	P.	P.				P.
	PRODUCTION YEARS										1959-1992
	CUMULATIVE PRODUCTION (mcf) *										35,000,000
	ORIGINAL GAS IN PLACE (mcf)		12,600,000	4,200,000	2,500,000	10,000,000	4,700,000				52,000,000
	ORIGINAL GAS RESERVES (mcf)										42,000,000
	REMAINING GAS IN PLACE (mcf)										17,000,000
	REMAINING GAS RESERVES (mcf)										7,000,000
	INITIAL OPEN FLOW (mcf/d)						100			2200	390
	FINAL OPEN FLOW (mcf/d)	131	202	879	346	207	693			80	355
	RECOVERY FACTOR (%)										80

* ~~DOES~~ MAY NOT CORRESPOND TO NUMBER OF WELLS IN BASIC RESERVOIR DATA

ABBREVIATION KEY

AUGUST 25, 1993

U Camb - Upper Cambrian	GTBG - Gatesburg	ls. - limestone	struc. - structural	A. - Associated
L Ord - Lower Ordovician	UPSY - Upper Sandy	dol. - dolomite	s.g. - solution gas	N. - Non-Associated
BKMN - Beekmantown	CPRG - Copper Ridge	slst. - siltstone	w. - water	P. - Producing
RSRN - Rose Run	MTSN - Mount Simon	ss. - sandstone	g.e. - gas expansion	A. - Abandoned
LTFL - Little Falls	PC - Precambrian	sh mar - shallow marine	fra. - fractures	S. - Storage
THRA - Theresa		strat - stratigraphic	dia. - diagenesis	E. - Enhanced recovery
			depo. - deposition	Cons. - Consolidated

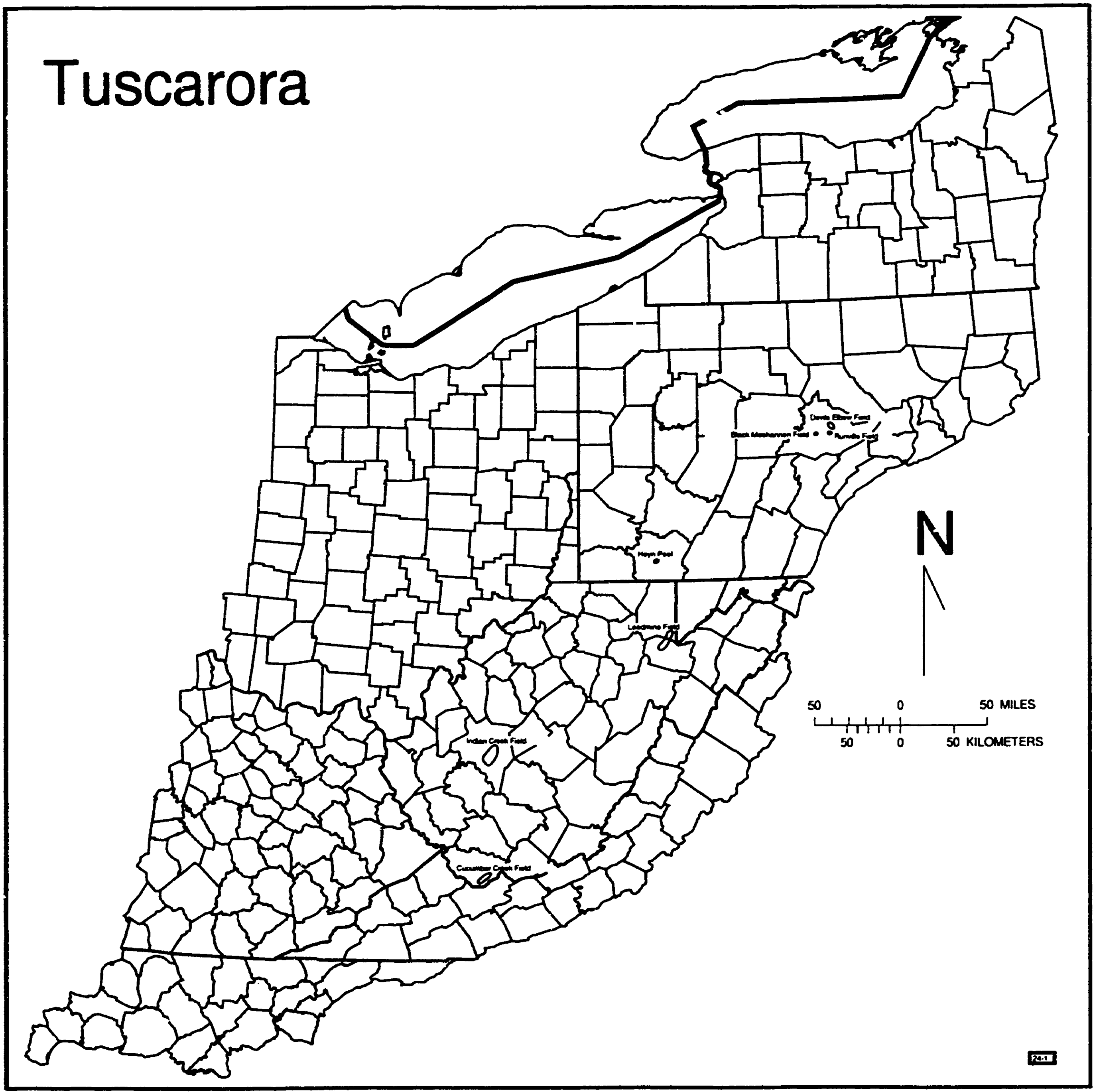

Figure 1. Map of the Appalachian Basin showing the location and extent of the Lower Silurian Tuscarora Sandstone fractured anticline fields and pools.

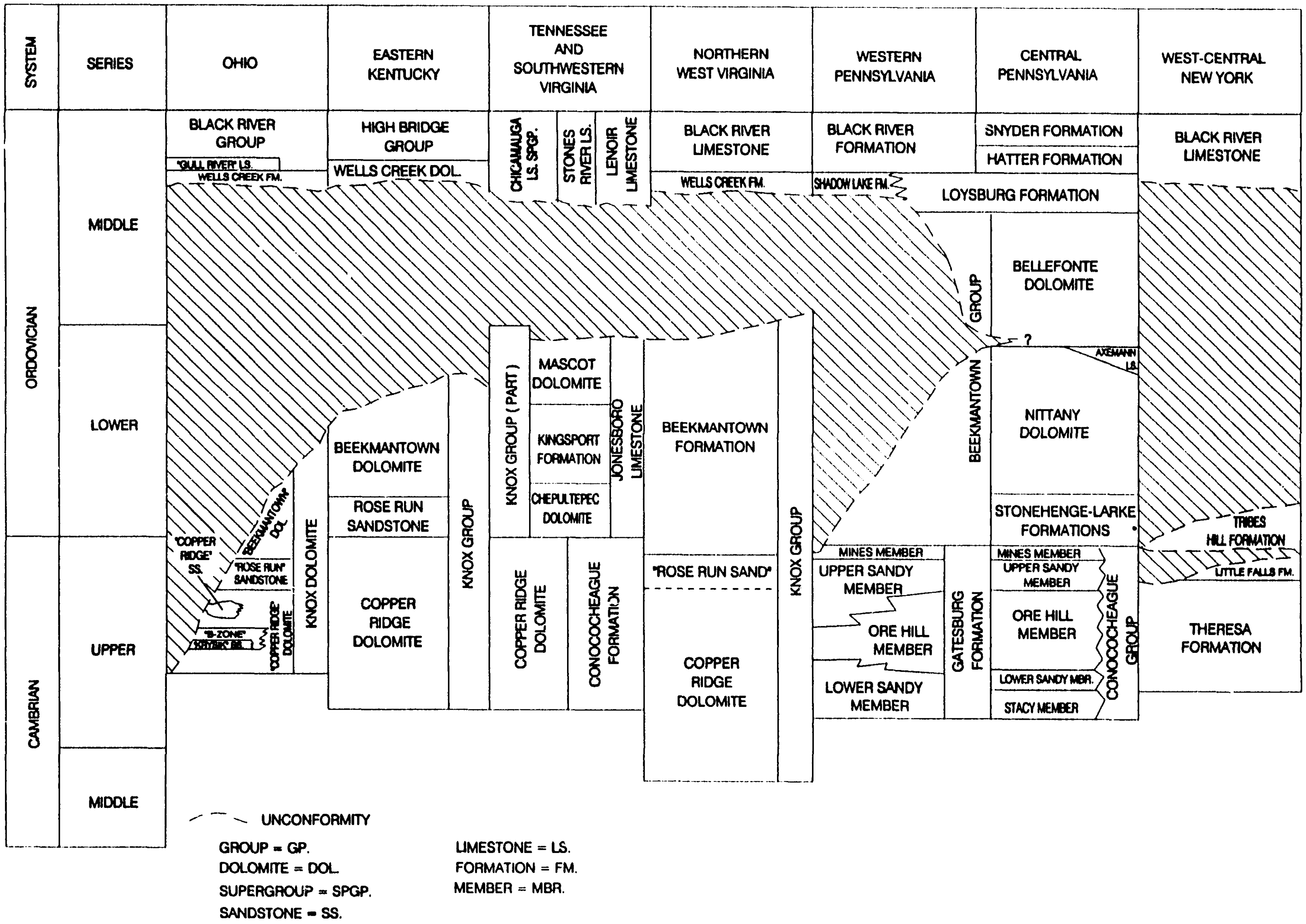

Figure 2. Correlation chart for part of the Ordovician and Cambrian of the Appalachian basin (modified from Janssens, 1973; Patchen and others, 1985; Milici and de Witt, 1988; and Riley and others, 1993), Cambrian-Ordovician Knox Group unconformity play

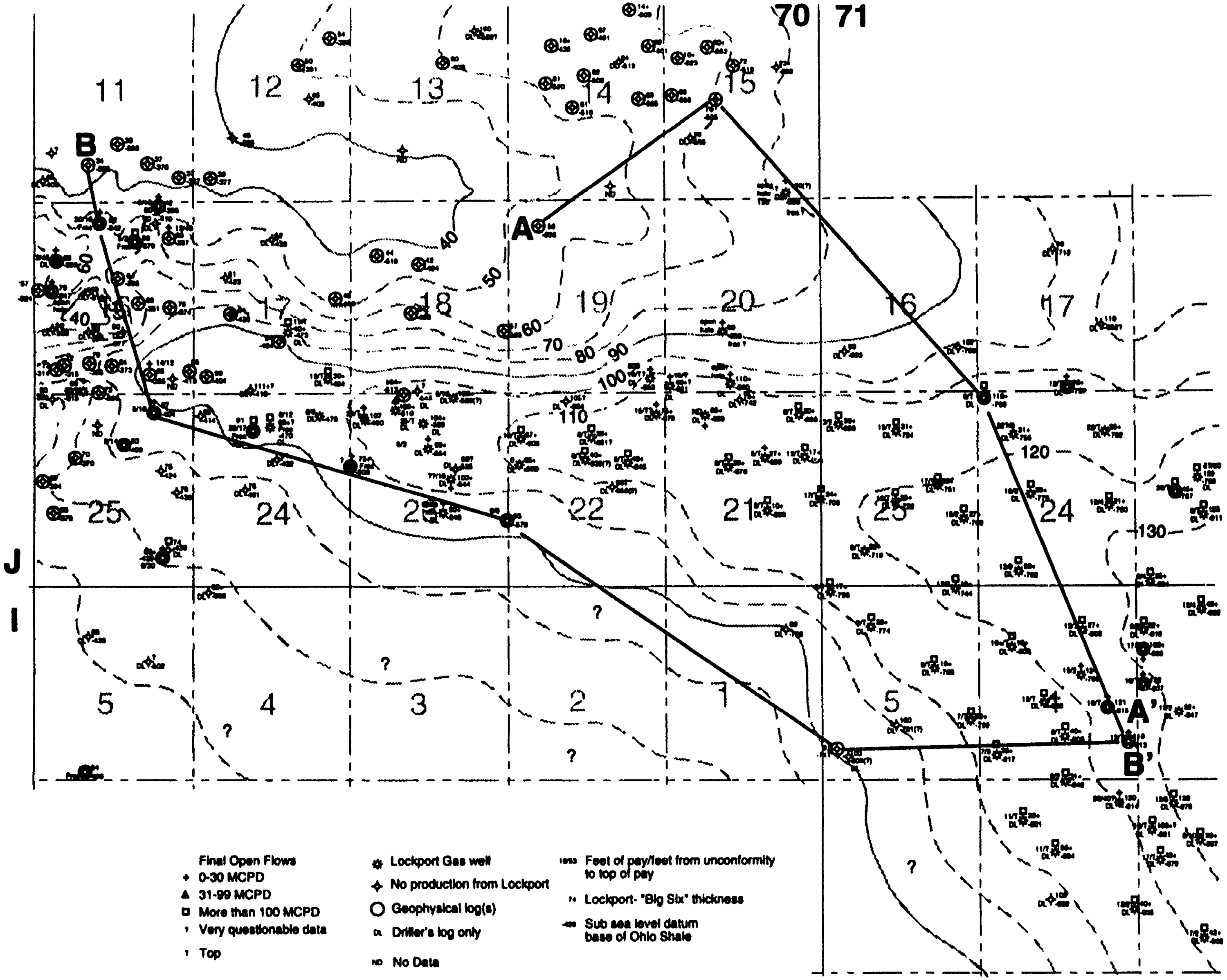

Figure 3. Isopach map of the Lockport Dolomite/"Big Six", Oneida Consolidated field, Clay County, Kentucky, Lower Devonian-Upper Silurian unconformity play

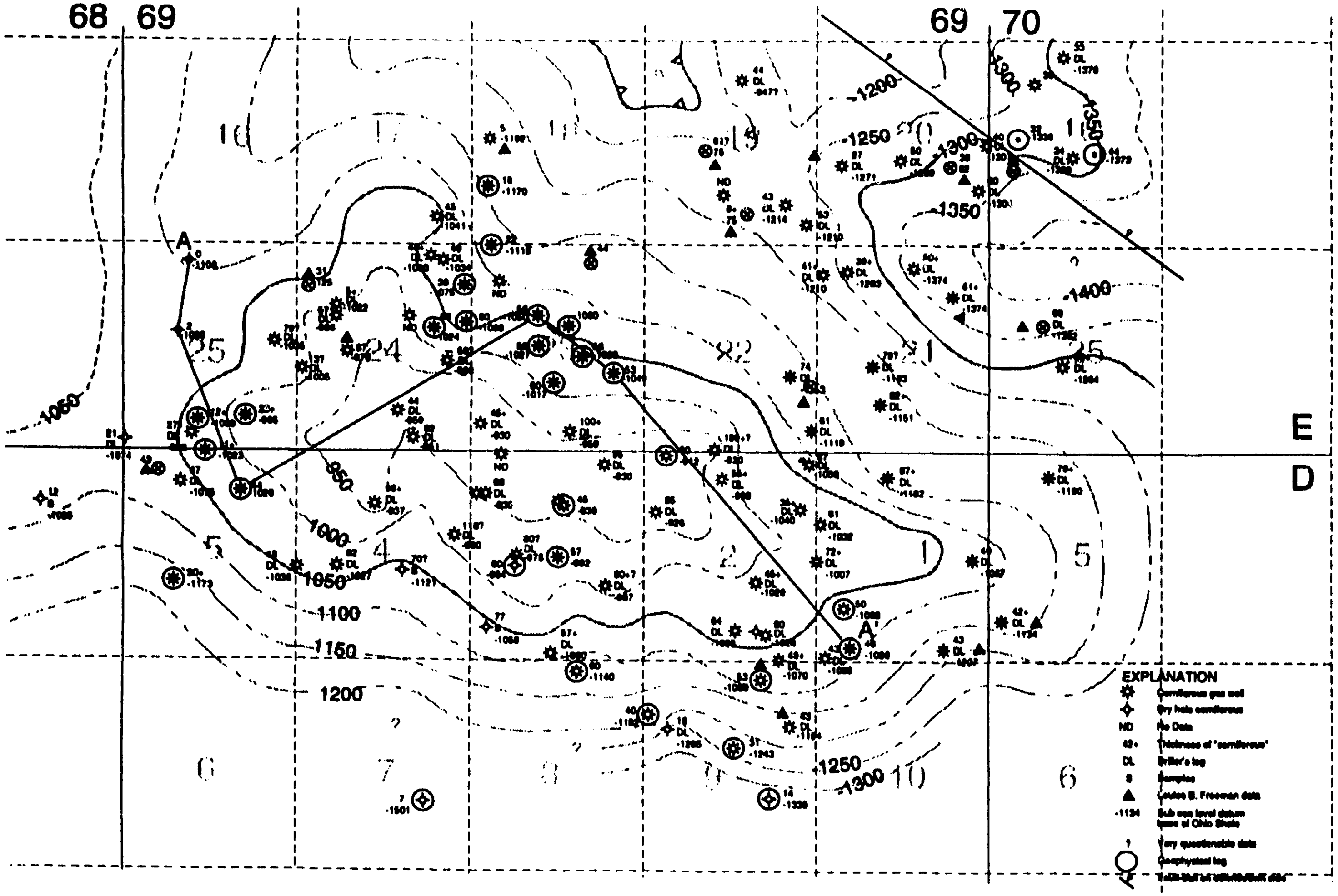

Figure 4. Structure contour map on the base of the Devonian Ohio Shale, Oneida Consolidated field, Clay County, Kentucky, Lower Devonian-Upper Silurian unconformity play

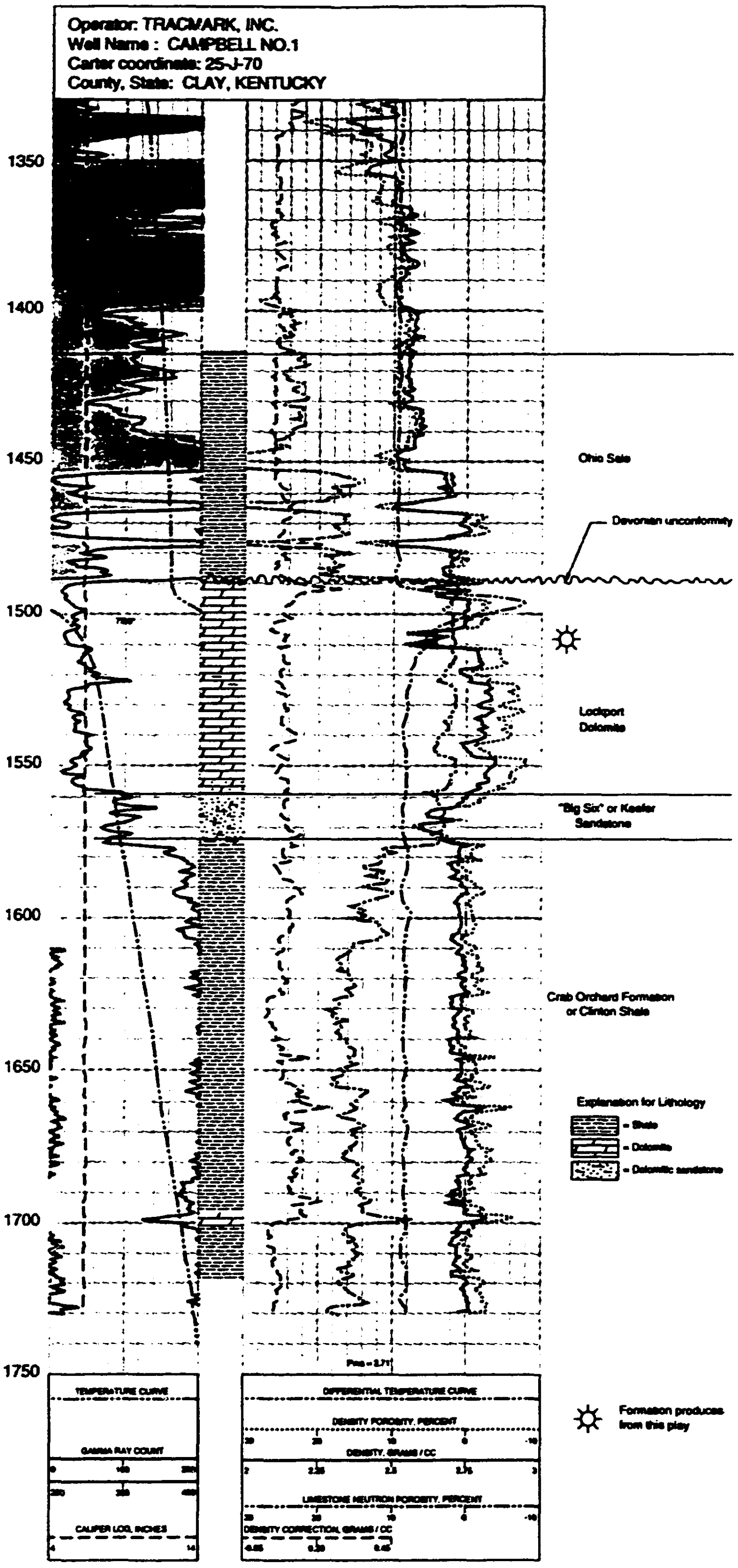

Figure 5. Type log for east central Kentucky (Clay County), Lower Devonian-Upper Silurian unconformity play

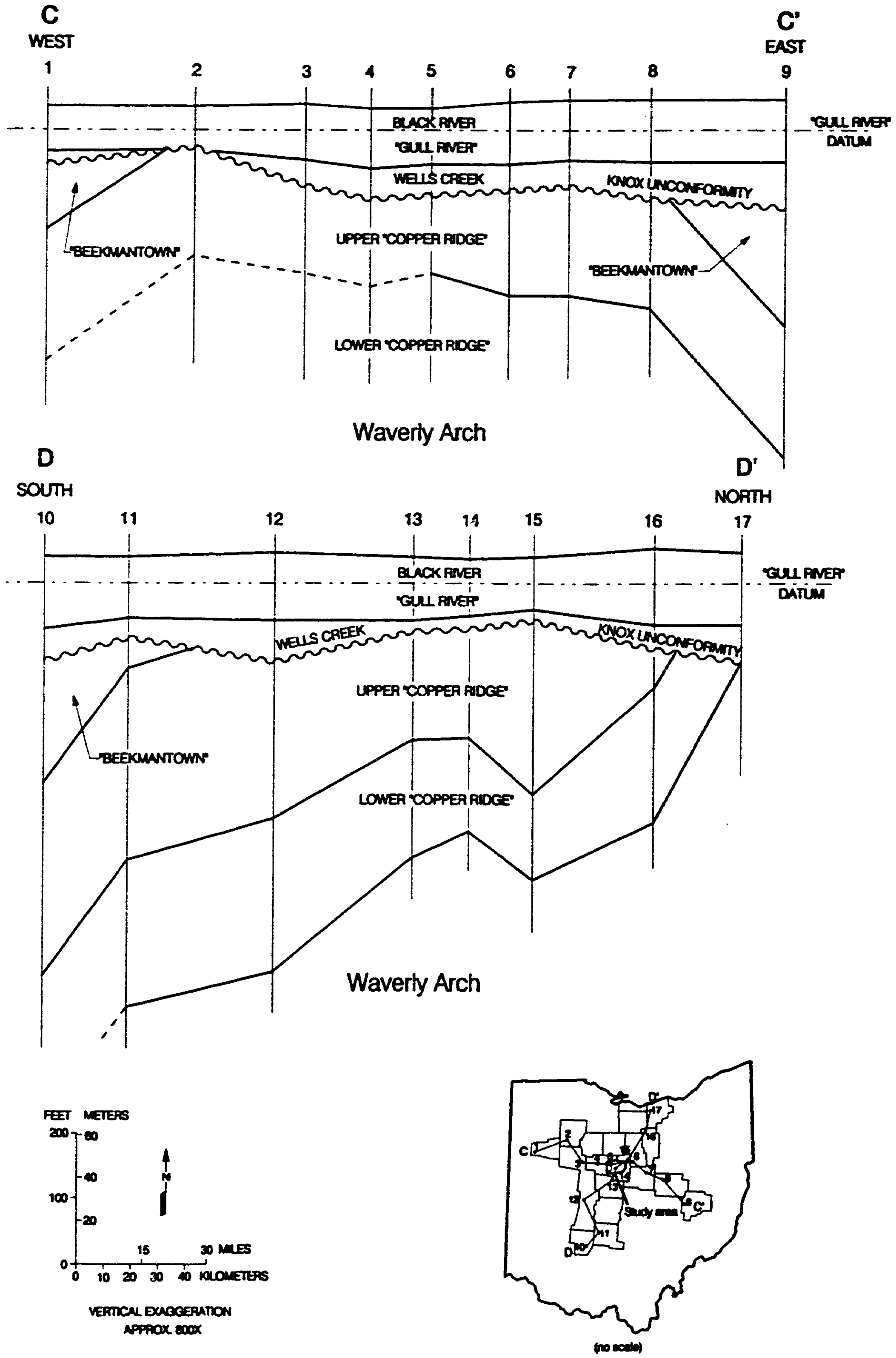

Figure 6. Regional cross sections of the Middle Ordovician and Upper Cambrian in central Ohio demonstrating the Knox unconformity and Waverly Arch (modified from Dolly and Busch, 1972), Cambrian-Ordovician Knox unconformity play

P8 Gulf of Mexico Oil and Gas Atlas Series: Play Analysis of Oligocene and Miocene Reservoirs from Texas State Offshore Waters

CONTRACT INFORMATION

Contract Number	14-35-0001-30683
Contractor	Bureau of Economic Geology The University of Texas at Austin University Station, Box X Austin, Texas 78713-7508 (512) 471-1534
Contractor Project Manager	Steven J. Seni
Principal Investigator	Robert J. Finley
METC Project Manager	Harold Shoemaker
Period of Performance	September 30, 1992 to September 29, 1996

Schedule and Milestones

FY93 Program Schedule

	O	N	D	J	F	M	A	M	J	J	A	S
Task 1. Program Coordination	—	—	—	—	—	—	—	—	—	—	—	—
Task 2. Atlas 1: Miocene and older plays												
Compile data, classify reservoirs, define plays.	—	—	—	—	—	—	—	—	—	—	—	—
Summarize statistics, prepare text and figures.										—	—	—
Cartography, computer mapping, editing, and production.										—	—	—
Task 3. Atlas 2: Plio-Pleistocene plays	No activity scheduled											

OBJECTIVES

The objective of the Offshore Northern Gulf of Mexico Oil and Gas Resource Atlas Series is to define hydrocarbon plays by integrating geologic and engineering data for oil and gas reservoirs with large-scale patterns of depositional basin fill and geologic age. The primary product of the program will be an oil and gas atlas set for the offshore northern Gulf of Mexico and a computerized geographical information system of geologic and engineering data linked to reservoir location. The oil and gas atlas for the Gulf of Mexico will provide a critically compiled, comprehensive reference that is needed to more efficiently develop reservoirs, to extend field limits, and to better assess the opportunities for intrafield exploration. The play atlas will provide an organizational framework to aid development in mature areas and to extend exploration paradigms from mature areas into frontier areas deep below the shelf and into deep waters of the continental slope. In addition to serving as a model for exploration and education, the offshore atlas will aid resource assessment efforts of State, Federal, and private agencies by allowing for greater precision in the extrapolation of variables within and between plays. Classification and organization of reservoirs into plays have proved to be effective in previous atlases produced by the Bureau, including the Texas oil and gas atlases, the Midcontinent gas atlas, and Central and Eastern Gulf Coast gas atlas.

BACKGROUND STATEMENT

The Offshore Northern Gulf of Mexico Oil and Gas Resource Atlas Series is a cooperative research effort managed by the Bureau of Economic Geology as lead technical contractor. Funding for the program is supplied by the Department of Energy (DOE) through Morgantown Energy Technology Center (METC) and Bartlesville Program Office (BPO), the Gas Research Institute (GRI), and the Minerals Management Service (MMS). The State of Louisiana Center for Coastal, Energy, and Environmental Resources and the Geological Survey of Alabama are subcontractors for research in their respective State waters.

PROJECT DESCRIPTION

The four-year program ended its first year in October 1993. The program is divided into three primary tasks: task 1—program management, task 2—Atlas 1, and task 3—Atlas 2. Task 2 represents the work required to complete Atlas 1: Miocene and older plays. Task 3 represents the work required to complete Atlas 1: Plio-Pleistocene plays. During the first year, both tasks 1 and 2 were initiated. Task 3 work is scheduled to begin in 1994.

RESULTS

Task 1

Program management efforts include completion of quarterly reports for DOE and monthly milestone reports for GRI as required by the contracts. The process for granting subcontracts to Louisiana and Alabama for work in their respective State waters was implemented. An important milestone under task 1 was establishing an Industrial Technical Advisors Committee (ITAC) that consists of major oil and gas operators active in hydrocarbon exploration and production in the Gulf of Mexico. The following companies agreed to support the Gulf of Mexico atlas through their participation in the ITAC: ARCO Oil and Gas Company; CNG Producing Company; Conoco Inc.; Marathon Oil Company; Oryx Energy Company; Shell Offshore

Inc., Exploration Assets; Texaco USA; and Unocal Corporation. On October 12, 1993, the first ITAC meeting was held in Austin, Texas. That meeting was hosted by the Bureau and attended by the funding agencies and the ITAC membership. During that meeting, Bureau representatives gave progress reports on the status of the atlas program, the framework and purpose of the ITAC was finalized, and a procedure for review of plays by the ITAC company staff members was determined.

Task 2

The primary goal of the atlas program is the integration of critically compiled reservoir data within a reservoir play framework. Compilation of data was the primary research effort during the first year of the contract. Collection of geologic and engineering reservoir data was concluded in the offshore Texas State Lands area. Quality control parameters of collected data, derivation of calculated reservoir volumetrics, and transfer of data into digital computer format are still being performed. Prior to this study, the MMS had previously compiled geologic and reservoir data for the Federal OCS in the FRRE database. During the first year, MMS staff rechecked and reorganized reservoir data in this database to integrate it with the atlas program.

A generalized play analysis procedure was implemented that is tailored specifically to the requirements of the atlas program. The procedure is as follows: (1) define chronozone map unit, (2) outline area of production, (3) collect reservoir engineering and geologic data, (4) identify reservoirs on field type log, (5) correlate productive intervals, biozones, structural style, and depositional facies on strike- and dip-oriented cross sections with type logs for fields, (6) identify and describe type reservoir/field within chronozone map unit, (7) tabulate reservoir engineering data for each reservoir, (8) synthesize defining attributes of each play, (9) outline area of play, and (10) write play description. Defining attributes that characterize specific plays include: (1) chronozone age, (2) depositional system, (3) structural style, (4) hydrocarbon type, (5) trapping mechanism, (6) hydrocarbon source, (7) exploration maturity, (8) frontiers, and (9) limitations.

Play Analysis. Preliminary play analysis of reservoirs in the offshore Texas State Lands and adjacent Federal OCS has identified 34 plays of Miocene and older reservoirs. This identification has concentrated on lower Miocene and Oligocene reservoirs because these plays are located predominantly in State waters. The distribution of Oligocene and lower Miocene plays is illustrated in figure 1. Plays associated with younger middle and upper Miocene reservoirs extend into the Federal OCS and are not shown in figure 1. The following discussion will provide examples of gas-prone plays from the Oligocene Frio–Anahuac and the lower Miocene.

Oligocene Frio–Anahuac Plays. Play analysis of Oligocene Frio–Anahuac reservoirs has almost been completed in the Texas offshore area. All geologic and engineering data have been compiled for Frio–Anahuac fields and reservoirs. In addition, Frio–Anahuac-type fields have been identified, and their geologic and engineering data have been synthesized. Aggregation of data from reservoirs to atlas sand-body reservoirs has also been completed. All Oligocene reservoirs have been located on the type logs, and type logs have been identified for all fields. A typical log shows the productive interval and the relationship of production to depositional facies and biozones. Data on cumulative production, cumulative probability, and total production by play have been tabulated and graphed. Oligocene production is predominantly gas with subordinate oil in updip plays (fig. 2).

Oligocene production is restricted to four plays in two regions of the Texas offshore, a southern region consisting of the Mustang and Matagorda Areas and a northern region including the Galveston Area. Both of these regions represent the downdip extension of distal facies that are productive onshore.

One of the key elements of play analysis is to display geologic data for type fields that represent the defining attributes characterizing a given play. Mustang Island Block 889 is an example of a type field characterizing Play 2b, as illustrated by a type log and location and structure-contour maps (fig. 3). Frio–Anahuac Play 2b is a gas play located predominantly in the Mustang Island Area that extends into the Matagorda Island Area. The most distal Frio–Anahuac fields in Play 2b do not extend into Federal OCS. Simple and faulted anticlines comprise the primary trapping mechanism of Play 2b. The depositional style of productive sandstones is characterized by progradational and aggradational distal shoreface and inner shelf sandstones ranging in age from *Marginulina howei* (lower Anahuac) to *Cibicides hazzardi* (upper Frio). Table 1 lists the defining attributes of Play 2b.

Lower Miocene Plays. The principal hydrocarbon producing zone in the Texas offshore area is the lower Miocene chronozone; production is primarily gas. Play analysis of lower Miocene reservoirs is almost finished in the Texas offshore area; eleven plays have been defined. In addition, most geologic and engineering data have been compiled and synthesized for lower Miocene fields and reservoirs. Aggregation of data from reservoirs to atlas sand-body reservoirs is ongoing. Type logs have been identified for all fields, and all reservoirs have been located on the type logs. Data on cumulative production, cumulative probability, and total production have been tabulated and graphed for three plays. Integrated play analysis has been finalized in a pilot area extending from Texas State Lands offshore waters into Federal waters from Galveston Area east to Vermilion Area.

One of the initial procedures in play analysis is to locate all reservoirs on field type logs. Strike- and dip-oriented cross sections based on the type logs then become a powerful tool for identifying plays on the basis of lateral and vertical association of productive reservoirs within consistent depositional systems. A cross section linking type logs along the offshore Texas State Lands shows the distribution of lower Miocene plays (fig. 4).

Lower Miocene production is predominantly gas with subordinate oil in updip plays and in association with salt domes. Lower Miocene Play 3b is a gas play in the High Island Area that is typical of the larger lower Miocene gas-prone plays. The depositional style of productive sandstones is characterized by progradational and aggradational deltaic facies of *Siphonia davisi* sandstones. In High Island 24-L, a type field, most production is from *Siphonia davisi* reservoirs in lower Miocene Play 4b (fig. 5), but substantial production also comes from Plays 4a and 3c. *Siphonia davisi* sandstones form laterally continuous sandbodies that are segmented by normal faulting into a series of fault-block reservoirs (fig. 5). The structural style and primary trapping mechanism are rollover anticlines associated with major extension of the lower Miocene shelf margin. A similar structural style extends down the coastline to the southwest in association with the large, continuous growth faults.

FUTURE WORK

Future work on task 2—Atlas 1: Miocene and older plays—will concentrate on compiling data needed to classify reservoirs and define plays for Miocene and older reservoirs; such compilation should be completed in calendar 1994. Preparation of text and figures will continue and should also be completed next year. Cartographic production and editing of text will be initiated in calendar 1994. Task 3—Atlas 2: Plio-Pleistocene plays—will begin in calendar 1994 with data compilation, statistical analysis, and reservoir classification.

Table 1. Texas State Lands Distal Frio–Anahauc Play 2b

Hydrocarbon Type—Gas prone.

Defining Attribute(s)—Downdip of Play 2a located entirely offshore near the northern margin of the Norias delta system. Growth-faulted rollover anticlines and shale ridges of Greta–Carancahua barrier/strandplain system in lower Anahuac to lower Frio.

Reservoir Facies—Production is from both thin progradational and aggradational distal shoreface and inner shelf sandstones *Marginulina howei* (lower Anahuac) to *Cibicides hazzardi* (upper Frio) in age. Reservoir sandstones are downdip of the Greta–Carancahua barrier/strandplain system and adjacent to the Norias delta system, where a broad sandy shelf interfingers with marine mudstones. Reservoir facies also include thicker sandstones *Marginulina texana* (middle Frio) in age that were probably transported along strike from the Norias delta system and deposited in structurally active basins (Mstg. Isl. Blk. 883–889-S fields).

Structural Style—Simple anticlines, faulted anticlines, growth faults, and shale ridges associated with extension of continental margin.

Trapping Mechanism—Rollover anticlines associated with the downthrown sides of major growth faults and diapiric shale, some production from upthrown side of growth faults and antithetic faults.

Possible Hydrocarbon Sources—Subjacent shelf and upper slope mudrocks.

Exploration Maturity—Immature to mature.

Frontiers—Distal shoreface and barrier/strandplain and slope sandstones in the southern Matagorda Island and Mustang Island offshore areas. Downdip limit of sand is undetermined.

Limitations—Relatively thin reservoir sandstones, porosity and permeability within the play decreases downdip and to the northeast away from the delta source, and gas fields are small.

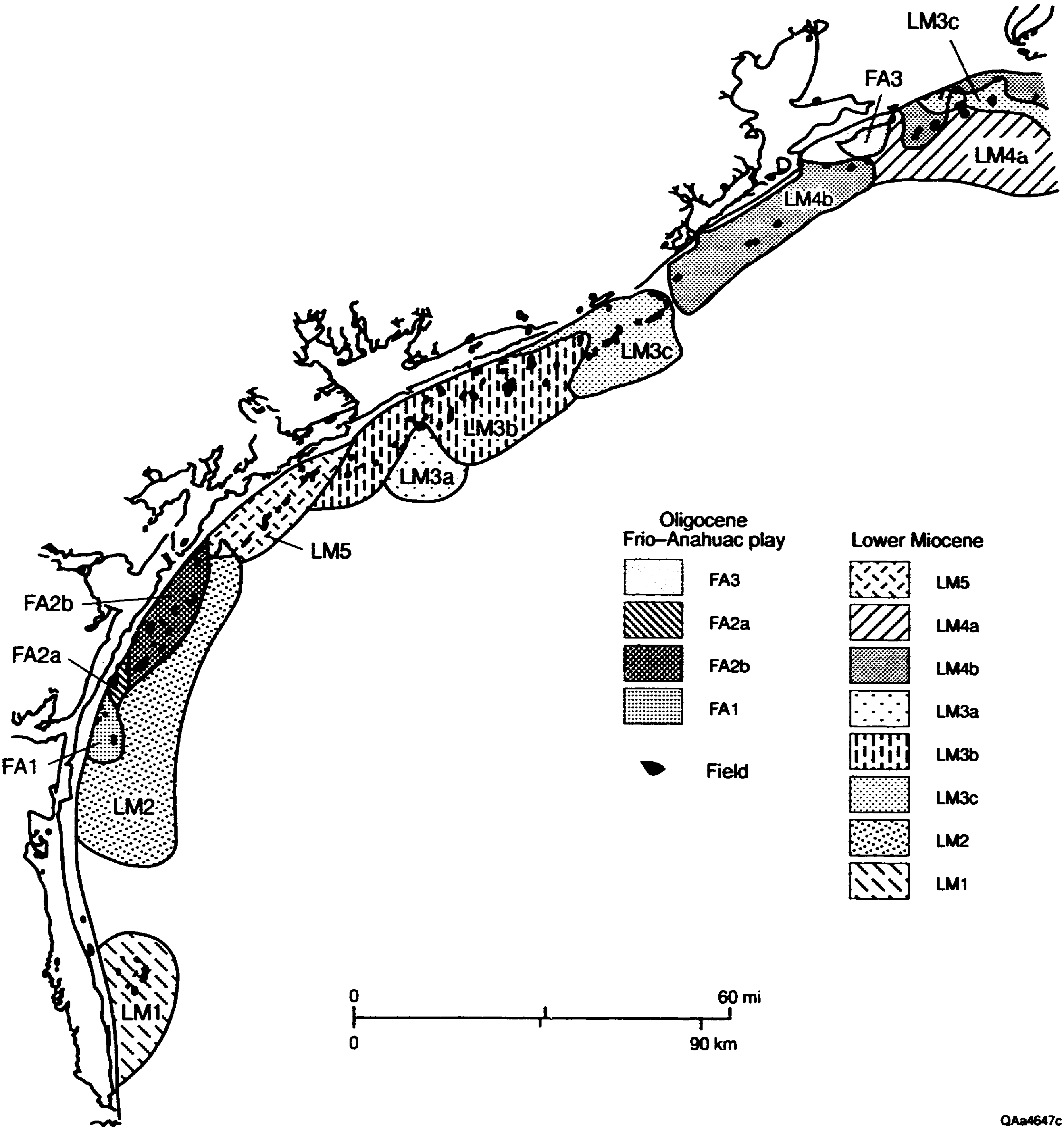

Figure 1. Map Outlining Distribution of Lower Miocene and Oligocene Plays in Offshore Texas State Lands

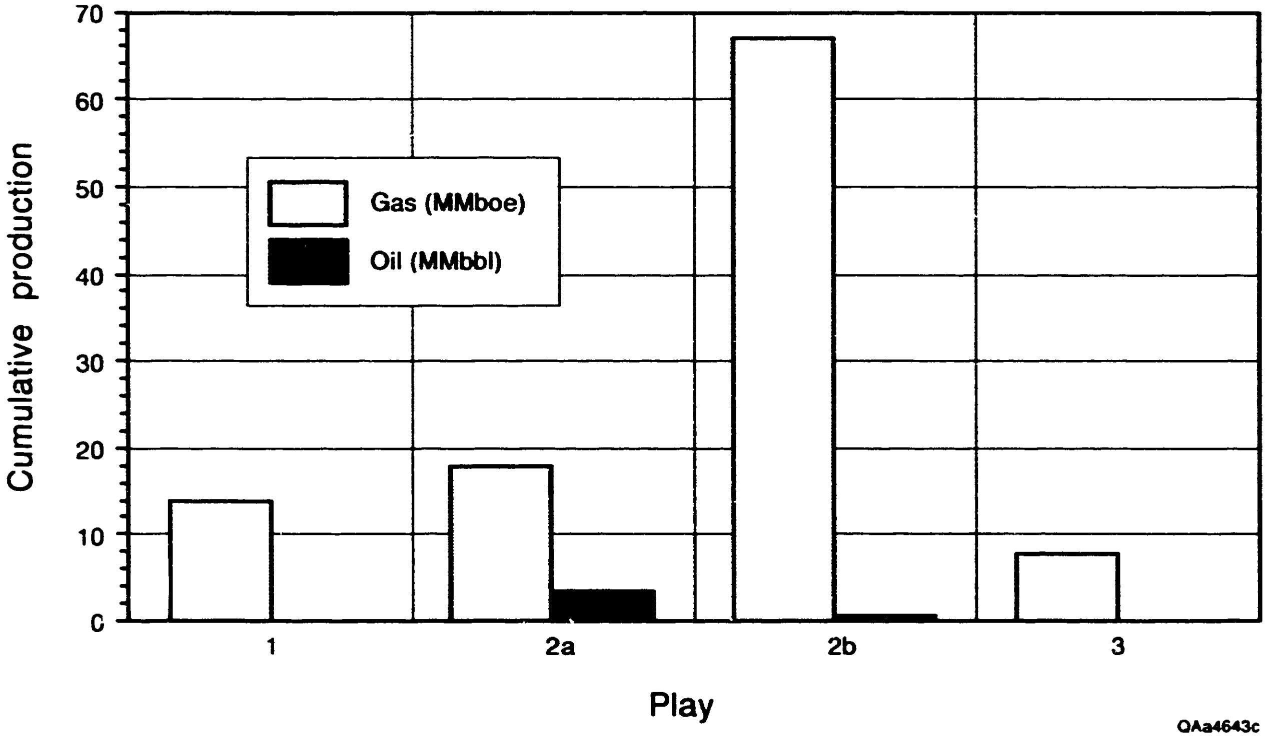

Figure 2. Histogram Showing Cumulative Production and Hydrocarbon Type for Oligocene Frio–Anahuac Plays

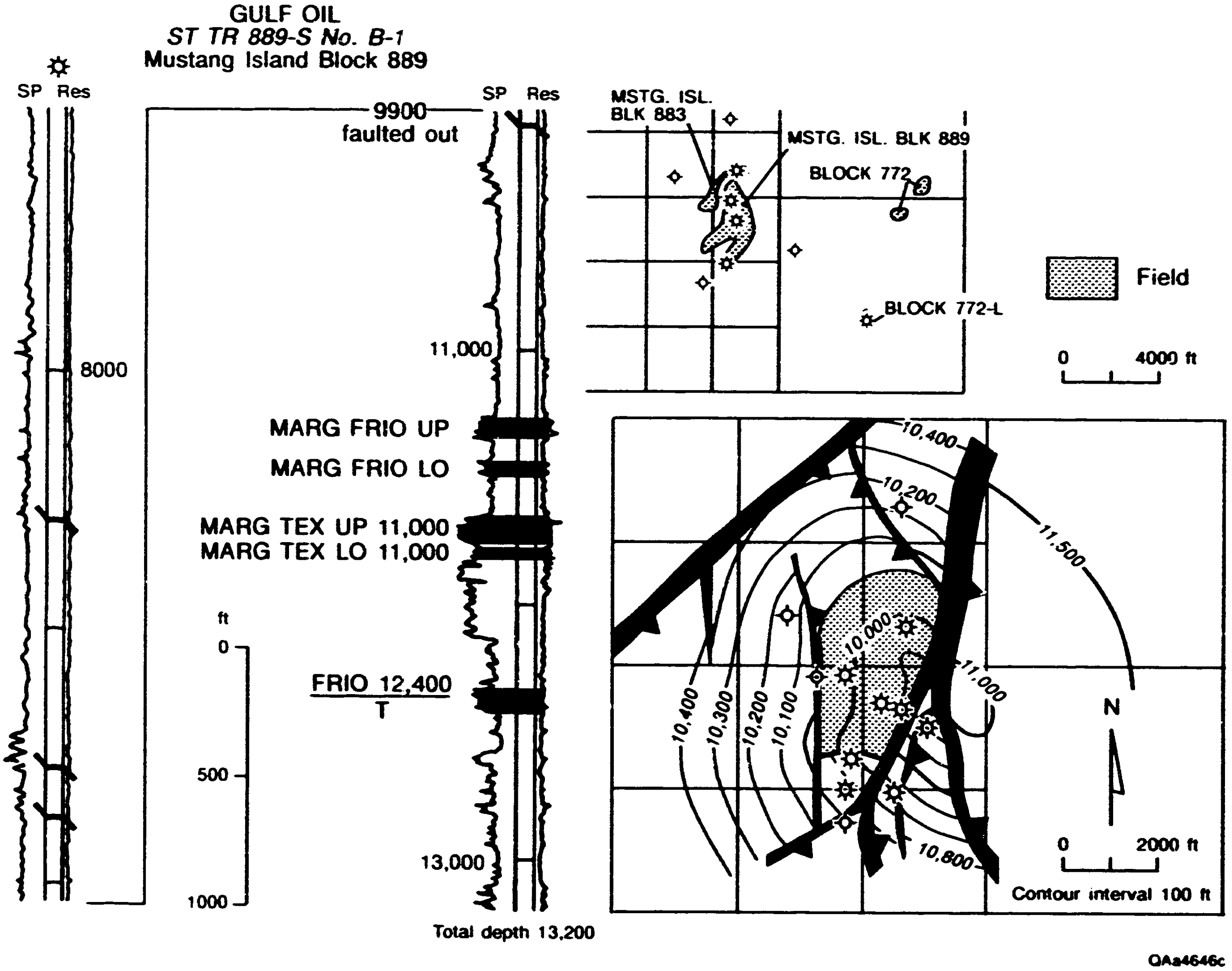

Figure 3. Geologic Data from Type Field, Mustang Island Block 889, in Frio–Anahuac Play 2b

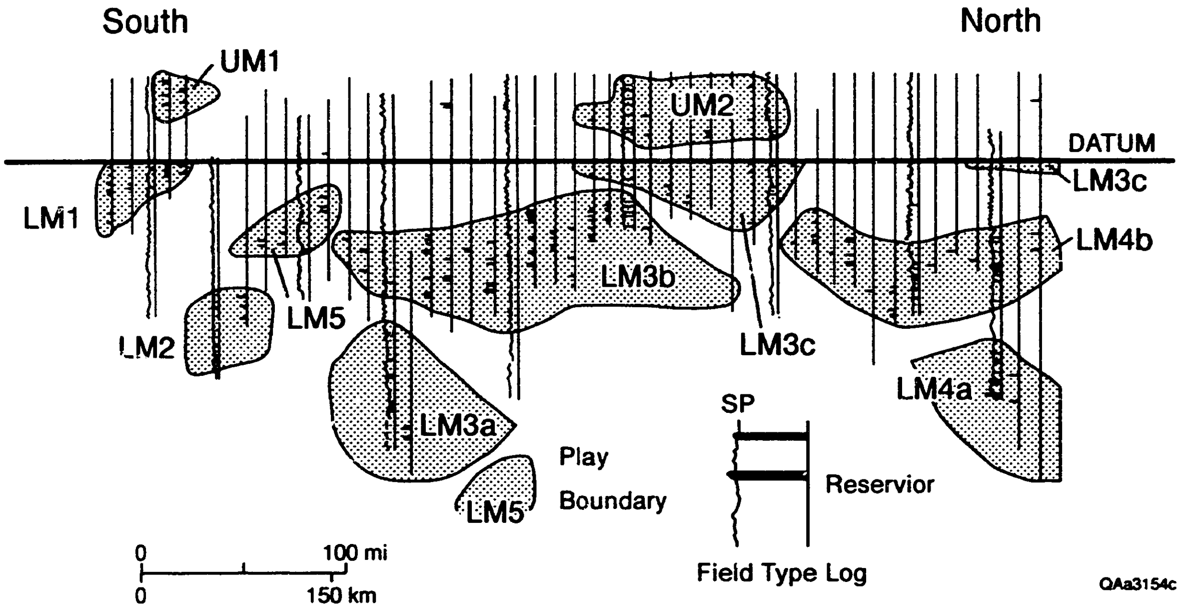

Figure 4. Cross Section of Type Logs from Fields that Produce from Lower Miocene Reservoirs in Texas State Lands

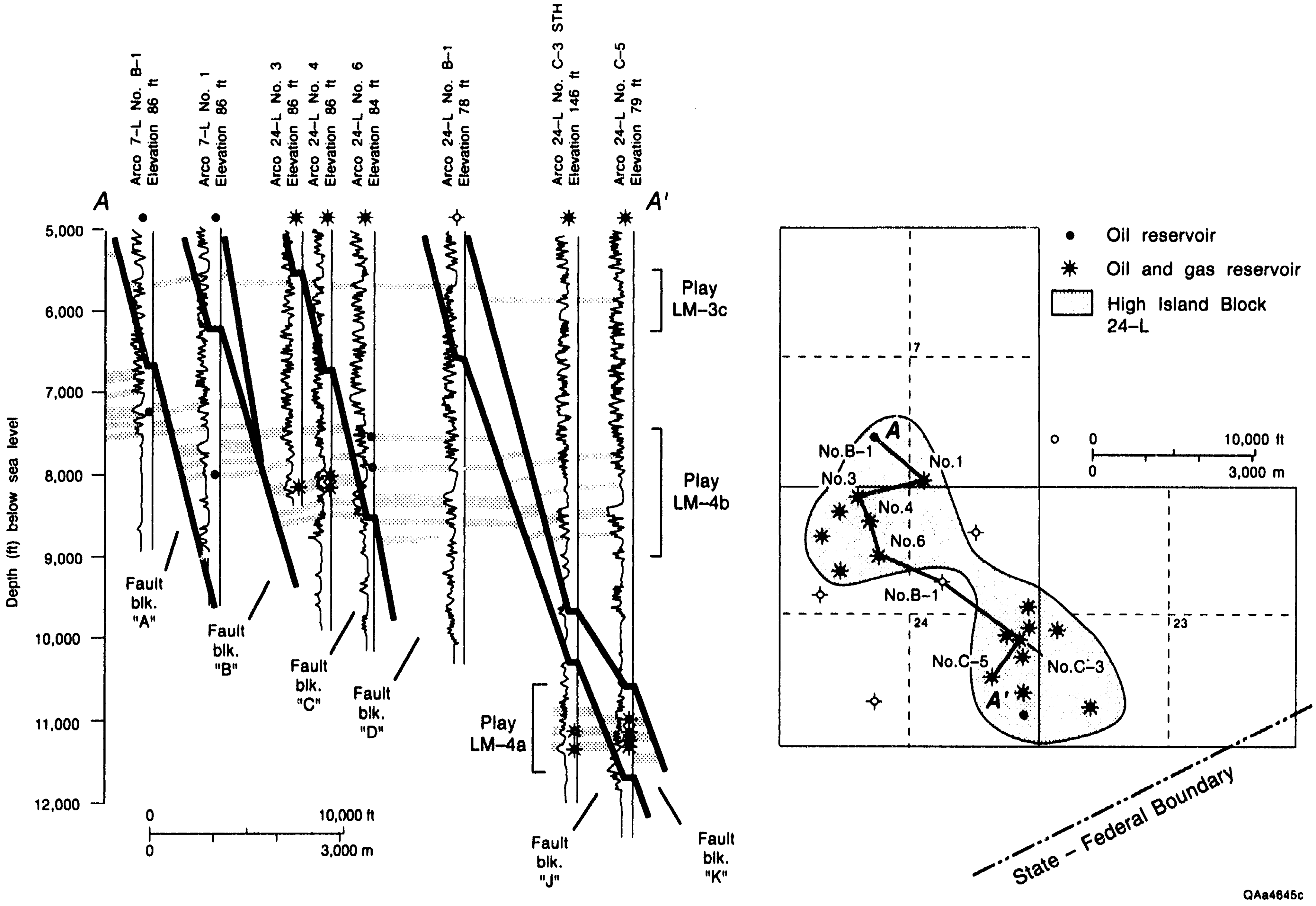

Figure 5. Geologic Data from Type Field, High Island Block 24-L, in Lower Miocene Play 4b

P9 The Synthesis and Characterization of New Iron Coordination Complexes Utilizing an Asymmetric Coordinating Chelate Ligand

CONTRACT INFORMATION

Contract Number	FEW0003
Contractor	Lawrence Livermore National Laboratory L-365 7000 East Avenue Livermore, CA 94550 (510) 422-5717
Contract Project Manager	David Baldwin
Principal Investigators	Bruce E. Watkins Joe H. Satcher
METC Project Manager	Rodney D. Malone
Period of Performance	Open

Objectives

We are investigating the structure/activity relationships of the bacterial enzyme, methane monooxygenase, which catalyzes the specific oxidation of methane to methanol. We then utilize this information to design and synthesize inorganic coordination complexes that mimic the function of the native enzyme but are more robust and have higher catalytic site density. We envision these catalysts to be useful in process catalytic reactors in the conversion of methane in natural gas to liquid methanol.

Background Information

The catalytic oxidation of light hydrocarbons, especially methane derived from natural gas, is an important research area attracting considerable attention. The potential for methane processing will depend on the development of catalyzed routes directly converting methane to higher valued products (heavier hydro-carbons, olefins, and alcohols). However, methane is chemically quite inert and has not proved easy to convert to liquid hydrocarbons. Modeling studies suggest that a theoretical ceiling in overall yield exists as the rate constant of a catalyst is increased[1]. The rate constant of the catalyst must be sufficient to overwhelm the non-specific gas phase reactions but low enough to prevent over oxidation. In theory this limits the yield to about 35%. As a result, no technologies are currently available to process methane economically.

It is well-known that a select group of aerobic soil/water bacteria called methanotrophs can efficiently and selectively utilize methane as the sole source of their energy and carbon for cellular growth.[2] The first reaction in this metabolic pathway is catalyzed by the enzyme methane monooxygenase (MMO) forming methanol. Methanol is a technologically important product from this partial oxidation of methane since it can be easily converted to liquid hydrocarbon transportation fuels, used directly as a liquid fuel itself, or serve as a feedstock for fine chemicals production.

Microorganisms can produce MMO in two distinct forms: a membrane-bound particulate form or a discrete soluble form. The soluble form contains an oxygenase subunit, whose active site includes a binuclear iron center.[3,4,5]. The complete details of the structure of the active site are not known, however, the general description of the iron site in the soluble form is a binuclear cluster containing some type of μ-oxo ligand between the iron atoms. The remaining ligands are derived from adjacent amino acid residues and the Fe-Fe distance is 3.4 Å. The best description of the amino acids coordinating the binuclear iron center is surmised by the close amino acid sequence homology between MMO and ribonucleotide reductase[6], an enzyme containing a binuclear iron center whose X-ray crystal structure has been determined[7]. Recent Mossbauer and EPR studies on soluble MMO[8] have demonstrated that coordination number asymmetry occurs about the two metal centers similar to that found in the related binuclear iron oxygen transport enzyme, hemerythrin. X-ray crystallography has clearly shown a 5,6 coordination sphere about the iron atoms in hemerythrin and reaction studies reveal that oxygen binding occurs at the five coordinate iron.[9]

It is speculated that the active site of particulate form of the enzyme is similar to the soluble form, except that the coordinated metal is copper. We have previously reported on the synthesis of asymmetrically coordinated copper complexes and their ability to catalyze the oxidation of cyclohexane to a mixture of cyclohexanol and cyclohexanone[10].

Project Description

Our work centers on the synthesis and characterization of inorganic/organic chemical models of the active site of MMO. We have focused on the synthesis of an asymmetrical, binuclear chelating ligand possessing an alkoxo group that can serve as a bridging μ-oxo ligand. The advantage of such a ligand system is twofold: (a) metal complexes of an asymmetric binucleating ligand will provide coordinative unsaturation at only one metal resulting in focused substrate reactivity at that site and (b) a single ligand with binuclear coordination provides a more robust environment for metal oxidation state changes and accompanying chemical reactivity.

We report here the synthesis of new prototype asymmetric iron complexes, and characterization of oxidized chelate compounds. This work provides the first proof-of-concept for the formation of binuclear iron complexes with different coordination at each metal ion. Such complexes are relevant to the development of model systems for the active site of MMO.

Results

Synthesis of the chelating ligand HMeL obtained by a five step procedure has been described previously.[11] When HMeL was allowed to react with two equivalents of iron(III) nitrate and excess sodium acetate in acetone/water (1:1), red crystals of (1) were deposited in 70% yield. The structure consists of a 5 coordinate (distorted square pyramidal) iron atom bridged to a 6 coordinate (distorted octahedral) iron atom through an alkoxide bridge supplied by the ligand (Figure 1). The metal-metal separation for this intra-ligand pair of iron atoms is 3.530Å which is similar to reported alkoxo bridged complexes.[12] The reported tetranuclear complex is further bound to an identical binuclear unit through an inversion center in which the 5 coordinate iron atom is bridged to the 6 coordinate iron through an oxo and a bidentate carboxylato bridge, the metal-metal separation for this inter-ligand pair being 3.224Å. This compound represents a proof-of-concept for the generation coordination asymmetry about two metals of a binuclear system.

Complex (2) results from the reaction of methanolic iron(II)tetrafluroborate, sodium benzoate and HMeL under anaerobic conditions (65% yield). Under these conditions a discrete binuclear complex is generated as the tetrafluoroborate salt (Figure 2). In the crystal structure one iron is five coordinate (distorted trigonal bipyramidal) utilizing three nitrogen donor atoms and an alkoxy oxygen atom from the chelate and an oxygen atom from a bridging benzoate group. The other iron atom is six coordinate (distorted octahedral) with nitrogen and oxygen donation from chelate and benzoate moieties and an additional donation from two methanol solvent molecules making a 5,6 coordinate pair. The ease of solvent removal (confirmed by elemental analysis) indicates that the molecule may be more appropriately considered 5,4 coordinate system. Initial attempts to exploit the coordinative unsaturation have led to two additional compounds: the bis-thiocyanato complex (3) and a bis-phosphato complex (4) shown in Figures 3 and 4 respectively. Complex (3), prepared by the addition of two equivalents of ammonium thiocyanate to an acetonitrile solution of (2), still retains coordination number asymmetry by binding both anions to the formerly four coordinate iron. This yields a neutral 6,5 coordinate molecule still bridged by an exogenous benzoate with the nitrogen atoms of two thiocyanate anions replacing the solvent groups. Complex (4) is formed when two equivalents of $(n\text{-}Bu_3N)_2HPO_4$ are added to a methanol/acetonitrile solution of (2). In this case one equivalent replaces the bridging benzoate in a bidentate binding mode and the second binds in a monodendate "end-on" fashion to a single iron atom. This leaves a 5,5 coordinate system in which coordination asymmetry is not preserved, yet coordinate unsaturation still exists. The reaction of both compounds (3) and (4) with molecular oxygen is currently being explored.

The oxidation of complex (2) with molecular oxygen in acetonitrile was found to conform to a 1:1 stoichiometry. When an acetonitrile solution of (2) is exposed to air and subsequently layered with ether a crystalline material (5) is formed (Figure 5). The structure reveals a tetrameric iron(III) unit supported by an alkoxo oxygen (intra-molecular) and two oxo (inter-molecular) bridges, the bridging benzoate moiety has been eliminated. In addition there is a terminal hydroxy anion bound to two of the iron centers making all iron atoms six coordinate. It has not been determined at this point if the oxygen bridges are formed from molecular oxygen. The lack of a benzoate bridge in this structure led to the investigation of the oxidation behavior in the presence of excess sodium benzoate. When an acetonitrile solution of (2) and five equivalents of sodium benzoate is exposed to air single crystals of (6) were formed (Figure 6). In this case the binuclear system remains intact supported by an endogenous alkoxo and two exogenous bidentate benzoate bridges. There is also a monodentate benzoate bound to one iron atom again making a 6,6 coordinate pair of metals. The crystal structure difference map shows only one tetrafluoroborate anion in the unit cell leading to Fe(II)/Fe(III) oxidation state assignment for charge balance. In both of the above oxidation structures the central core of the ligand remains intact and the metal:ligand ratio remains constant. Finally, if the oxidation reaction is carried out in a large excess of tetrabutylammonium perchlorate in acetonitrile, crystals of (7) are formed (Figure 7) in which the metal:ligand ratio has been increased to 3:1.

Conclusions

A binuclear, unsymmetric coordinating ligand that is an effective metal chelator has been designed and synthesized. The new ligand has been shown to react readily with iron(II)/(III) forming a variety of coordination complexes. The binuclear complexes are of significant interest since they represents proof-of-principle for the development of coordinatively asymmetric, binuclear metal chelate compounds. Although this structural type of chelator now appears to be common in biological systems, it has not been previously described for inorganic coordination chemistry. The isolation of oxidation products will be helpful in establishing reaction mechanism(s) of these complexes with molecular oxygen. It is expected that this ligand and derivatives of it will play an important role in the development of bioinorganic complexes that aim to mimic enzyme active sites that function by substrate interaction at only one metal site of a multimetal active site.

Acknowledgement

Work performed under the auspices of the US Department of Energy by the Lawrence Livermore National Laboratory under contract No. W-7405-ENG-48

References

1. Hair, L.M., Pitz, W.J.; Droege, M.W.; and Westbrook, C.K. Preprint, ACS National Meeting, April 6-10, 1992, San Francisco, CA

2. Dalton, H. *Adv. Appl. Microbiol.* 1980, *26*, 71-87.

3. (a) Woodland, M.P.; Dalton, H. *J. Biol. Chem.* 1984, *259*, 53-59. (b) Green, J.; Dalton, H. *J. Biol. Chem.* 1985, *260*, 15795-15801. (c) Fox, B.G.; Froland, W.A.; Dege, J.E.; Lipscomb, J.D. *J. Biol. Chem.* 1989, *264*, 10023-10033.

4. (a) Woodland, M.P.; Patil, D.S.; Cammack, R.; Dalton, H. *Biochim. Biophys. Acta* 1986, *873*, 237-242. (b) Fox, B.G.; Surerus, K.K.; Munck, E.; Lipscomb, J.D. *J. Biol. Chem.* 1988, *263*, 10553-10556.

5. Prince, R.C.; George, G.N.; Savas, J.C.; Cramer, S.P.; Patel, R.N. *Biochim. Biophys. Acta* 1988, *952*, 220-229.

6. Ericson, A.; Hedman, B.; Hodgson, K.O.; Green, J.; Dalton, H.; Bentsen, J.G.; Beer, R.H.; Lippard, S.J. *J. Am. Chem. Soc.* 1988, *110*, 2330-2332.

7. Pilkington, S.J.; Salmond, G.P.C.; Murrell; Dalton, H. FEMS Microbology Letters 1990, 72, 345-348.

8. Nordlund, P.; Sjöberg, B.-M.; Eklund, H. Nature 1990, 345, 593-598.

9. (a) Stenkamp, R.E.; Sieker, L.C.; Jensen, L.H. *Proc Natl Acad Sci. U.S.A* 1976, *73*, 349. (b) Stenkamp, R.E.; Sieker, L.C.; Jensen, L.H. *J. Mol. Bio.* 1978, *126* , 457.

10. B.E.Watkins, M.W. Droege, R.T. Taylor, and J.H. Satcher Biommimetic methane oxidation, Preprint, IGRC meeting, Orlando, FL, November 16-19, 1992.

11. Droege, M.W.; Satcher, J.H.; Reibold, R.A.; Weaklely, T.J.R. Preprint, ACS National Meeting, April 6-10, 1992, San Francisco, CA.

12. Fox, B.G,; Hendrich, M.P.; Surerus K.K.; Andersson K.K.; *J Am Chem Soc* 1993 , *115*, 3688-3701.

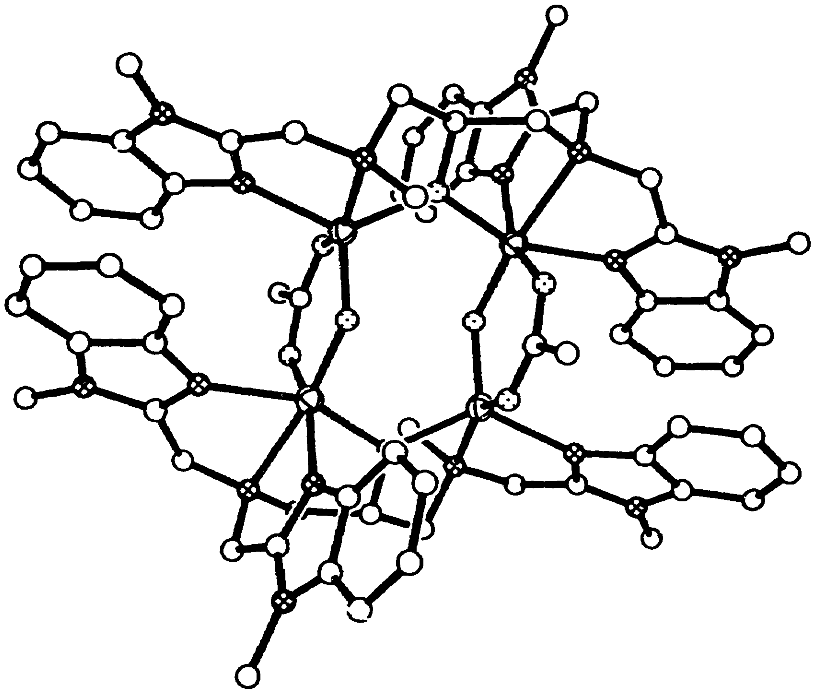

Figure 1. Cation of $(Fe_4(MeL)_2(OAc)_2(O)_2]$ $(NO_3)_4$ Hydrogen atoms omitted for clarity
50% thermal elipsoids: Fe / open circles: C / cross-hatched circles: N / dotted circles: O

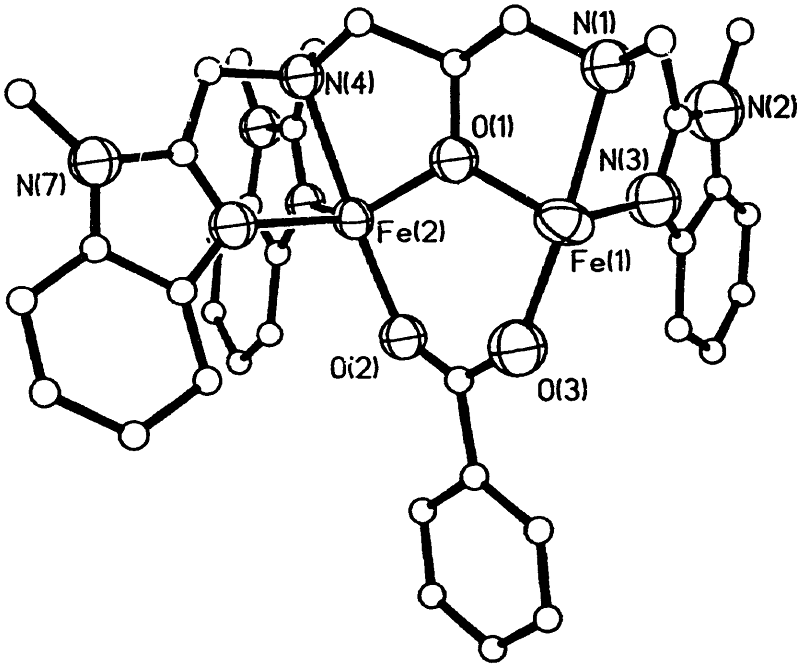

Figure 2. Cation of $[Fe_2(MeL)(O_2CPh)]$ $[BF_4]_2$ Bound solvent and hydrogen atoms omitted for clarity

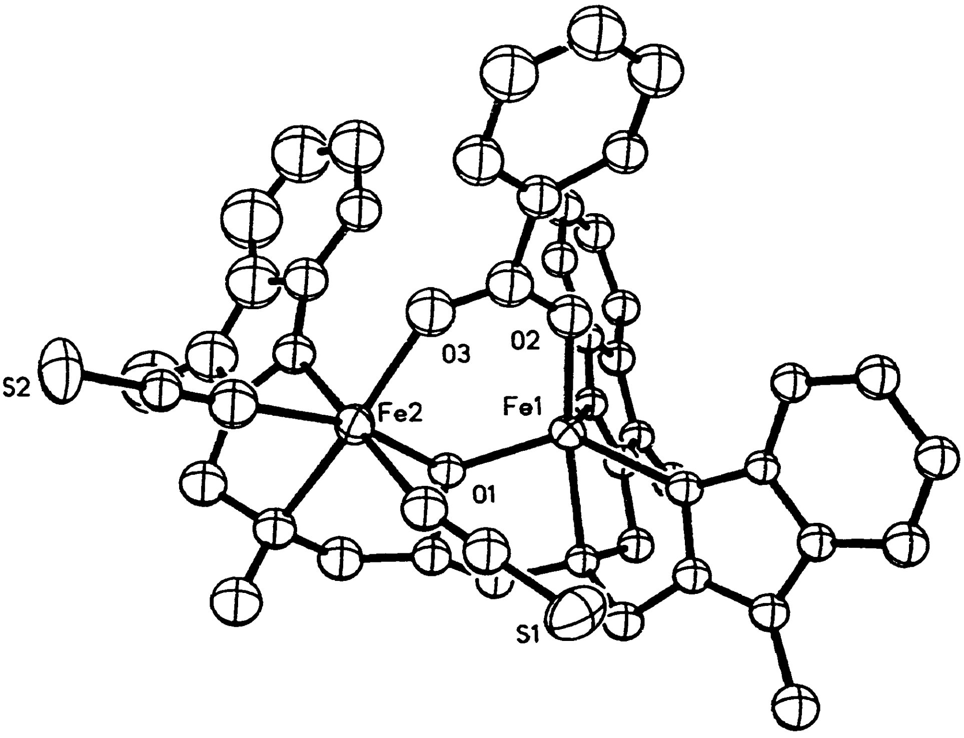

Figure 3. [$Fe_2(MeL)(O_2CPh)(SCN)_2$] Hydrogen atoms omitted for clarity

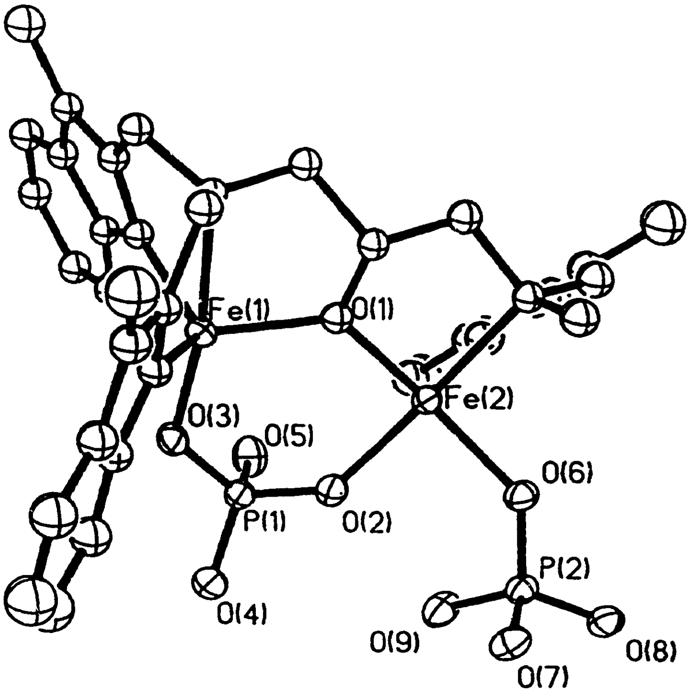

Figure 4. [$Fe_2(MeL)(H_2PO_4)(HPO_4)$] Hydrogen atoms omitted for clarity

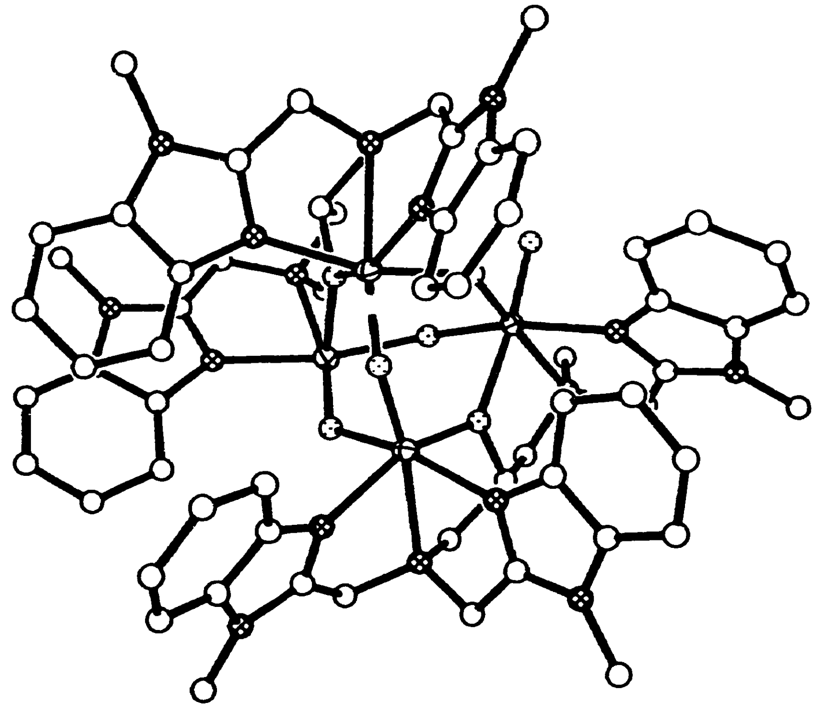

Figure 5. Cation of [$Fe_4(MeL)_2(O)(OH)_5$] [BF_4]$_3$ Hydrogen atoms omitted for clarity
50%thermal elipsoids: Fe / open circles: C / cross-hatched circles: N / dotted circles: O

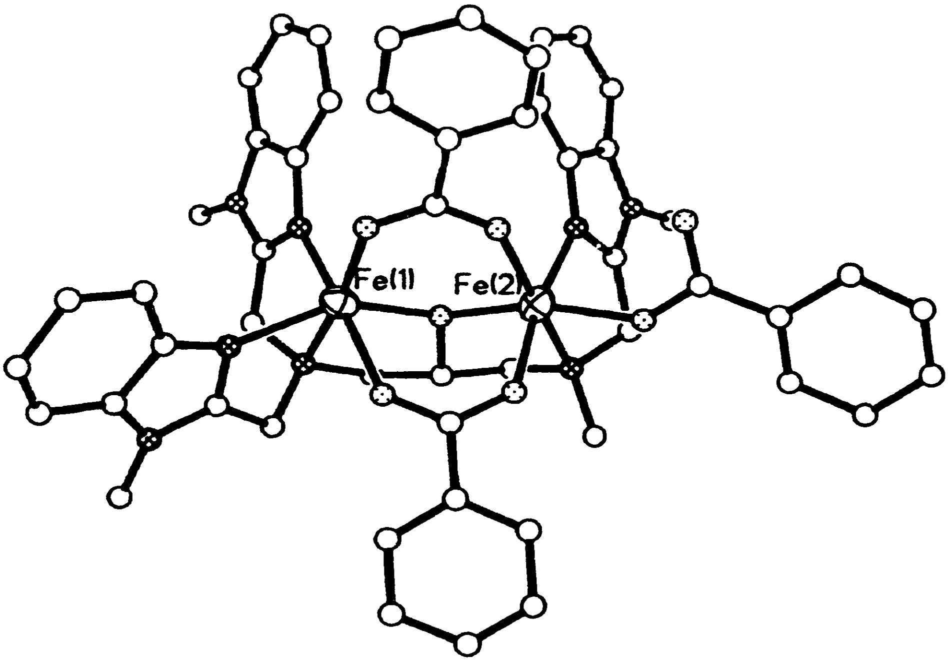

Figure 6. Cation of [$Fe_2(MeL)(O_2CPh)_3$] [BF_4] Hydrogen atoms omitted for clarity
50%thermal elipsoids: Fe / open circles: C / cross-hatched circles: N / dotted circles: O

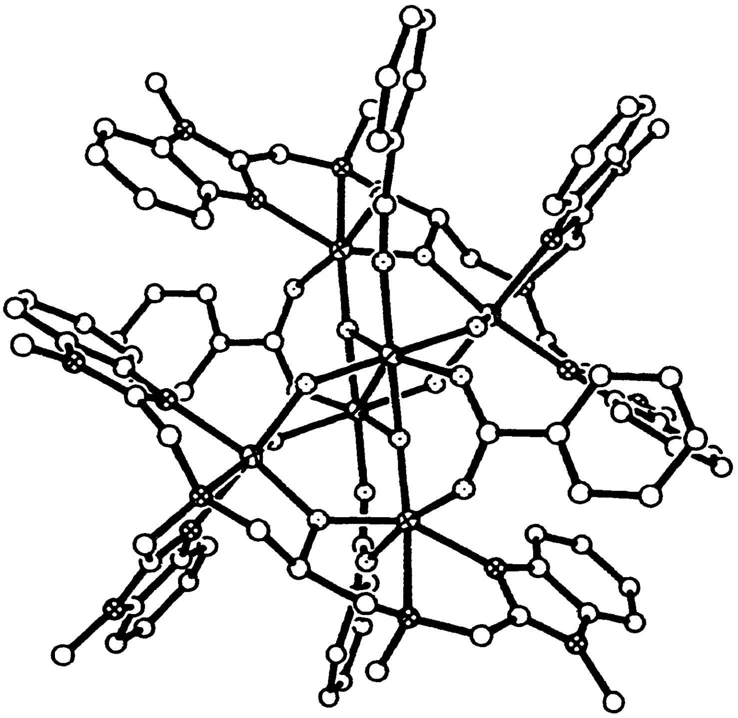

Figure 7. Cation of $[Fe_6(MeL)_2(O_2CPh)_4(O)_2(OH)_4]$ $[ClO_4]_4$ Hydrogen atoms omitted for clarity 50% thermal elipsoids: Fe / open circles: C / cross-hatched circles: N / dotted circles: O

P10 Analysis of Deep Seismic Reflection and Other Data From the Southern Washington Cascades

CONTRACT INFORMATION

Contract Number	DE-AT21-92MC2967
Interagency	U.S. Geological Survey Box 25046, MS964 Denver Federal Center Denver, CO 80225 303-236-1328
Agency Project Manager	William D. Stanley
Principal Investigators	William D. Stanley and Samuel Y. Johnson
METC Project Manager	William J. Gwilliam
Period of Performance	Oct. 1, 1992-Dec. 31, 1993
Schedule and Milestones	

FY93-94 Program Schedule

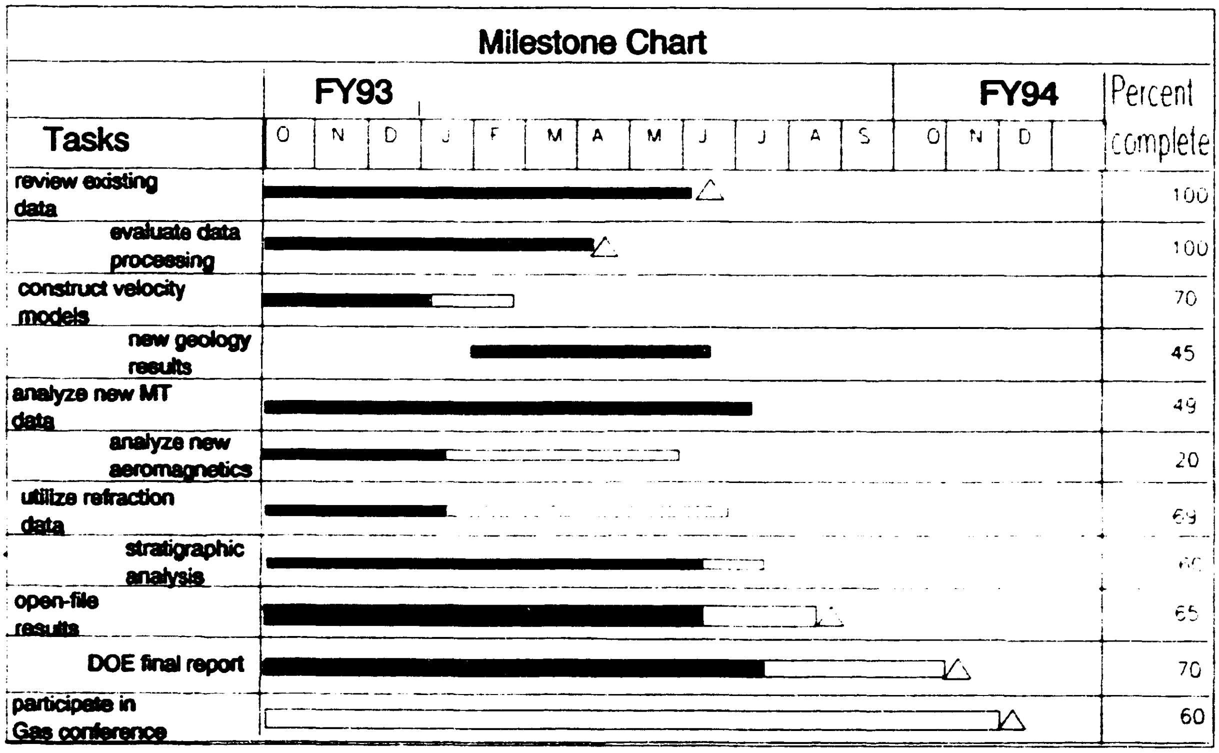

ABSTRACT

Limited possibilities exist for new hydrocarbon exploration regimes in the Pacific Northwest. Extensive geophysical studies have been used to outline a proposed sedimentary basin hidden beneath volcanic rocks of the Cascades region of southwestern Washington (Stanley et. al, 1992, AAPG Bull. 76, 1569-1585). Electrical geophysical imaging using the magnetotelluric (MT) method first detected thick, electrically conductive sequences believed to represent late Cretaceous to Oligocene marine sedimentary rocks. The conductive section occurs at depths from about 1 km to 10 km in the area west of a line between Mt. Rainier and Mt. Adams, extending westward to a line between Mt. St. Helens and just west of Morton, WA. The conductive rocks reaches thicknesses as great as 10 km. The anomalous rocks appear to be very near the surface in the axis of anticlines that bring Eocene marine shales to shallow depths. Careful consideration of physical properties and the correspondence of the morphology of the units to known fold sets suggests that the high conductivities are related to lithologic/stratigraphic units rather than to variations in physical properties. Our preference for the lithology of the anomalous section, based upon a study of regional geology and structure, is one dominated by marine shales of Eocene and older age. Other possible lithologies that have been evaluated for the conductive section include nonmarine sedimentary units of Tertiary age, highly altered volcanic flows, and pre-Tertiary metasedimentary rocks with large percentages of graphite. We refer to this anomalously conductive region as the southern Washington Cascades conductor (SWCC).

INTRODUCTION

Based upon magnetotelluric evidence for a possible hidden basin in the southern Washington Cascades (Figure 1), a large scale seismic reflection program was implemented by the Department of Energy (Figure 1). The DOE program used a 1000-channel sign-bit recording system with five Vibroseis source units as energy. Downsweeps of the vibrators was employed with recording out to 15 seconds, although the data contained very little useable information below about four seconds two-way travel time. The data have been released on CD-ROM as USGS Open File Report 92-714. In addition, a high-resolution aeromagnetic survey of the suspected marine basin region has been completed (Figure 2) and is available as USGS Open-File Report No. 92-251. Although no new gravity data have been acquired, modeling of existing data has proved useful in examining certain aspects of the geology in the region.

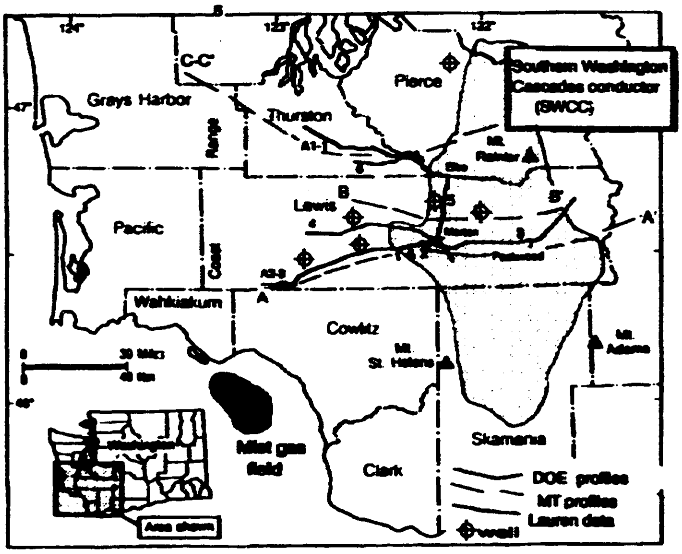

Figure 1-Index map of SWCC region, with the location of DOE seismic data, Lauren Corporation seismic data, and MT profiles shown.

The region in question has been examined using several types of data in addition to MT, seismic, magnetic, and gravity. We have undertaken a synthesis of this geophysical data and ongoing geological mapping in the region being done by the USGS. Prior to initiation of the synthesis, all available existing data have been catalogued and utilization made of the seismic reflection CD-ROM. Processing of DOE reflection profiles 1-3 was done with direct involvement of the principal investigators, but processing of lines 4-6 needed to be reevaluated as regards the state of processing. Some minor reprocessing has been done, involving binning of CDP data, but mainly limited to band and low-pass filtering, normalization, and color amplitude displays.

Velocity models have been constructed for synthetic seismograms, although some work had earlier been completed in this area by West Virginia University. Profile velocity models in 3D form were constructed for parts of the data set to study side-swipe and other effects in the data. There are being utilized to construct synthetic, 3D model sections.

Specific geological mapping tasks have been completed through funding by the Department of Energy and the USGS in the western part of the proposed basin near Morton, WA. Other regional geological studies using wells and outcrops done as part of the USGS Evolution of Sedimentary Basins program have added information that constrain the possible nature of the SWCC rocks and their tectonic setting. Recently, evaluation of patterns of seismicity in the SWCC region has demonstrated the likelihood of several parallel and step-over strike-slip faults, which may have produced the proposed basin or altered its geometry. In addition, the seismicity patterns trace the axis of key anticlinal structures and thrusts. Results from this seismicity study are shown in the poster for this project.

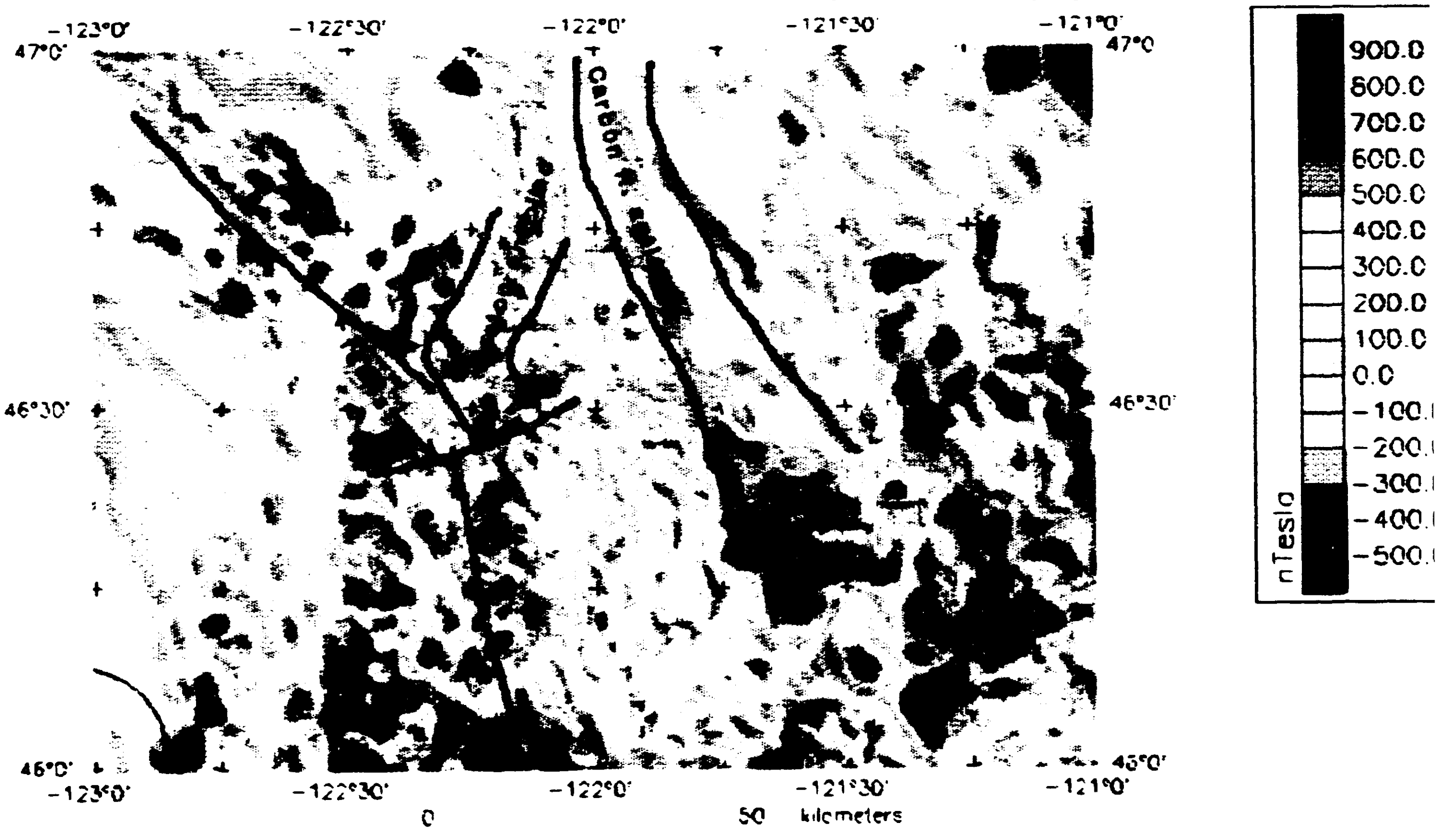

Figure 2-High resolution aeromagnetic data acquired under DOE funding. The location of the Morton and Skate Mtn.-Carbon River anticline systems are shown, as well as key faults associated with the St. Helens seismic zone (SHZ) and other features noted.

GEOLOGY OF THE SWCC

The nature of the SWCC is still largely a mystery in spite of our inferences about the rock types, as well as other factors that are important in evaluating the region for hydrocarbon potential. Tracing the conductive rocks to the surface in the area near Morton, WA, and close to the surface just west of Mount Rainier (Figure 3) suggests a correlation of the anomalous units with rocks like those of the Raging River, Carbonado, and McIntosh Formations, all of middle Eocene age.

The Morton anticline near Morton, WA, a main structure within the SWCC, is cored with Eocene sedimentary rocks of the Puget Group, which are interpreted to be several kilometers thick based on surface sections, MT models, and seismic reflection data. The Puget Group was deposited in a series of interconnected basins east of the terrane boundary between the Coast Range province (underlain by an Eocene basaltic basement) (Figure 4) and the Cascades/Pre-Tertiary province (underlain by a diverse basement of pre-Tertiary rocks). Puget Group strata exposed in the core of the anticline are deltaic in origin and consist of alternating intervals of nonmarine and shallow marine rocks. Elsewhere in the region, the Puget Group rocks are underlain by fine-grained marine strata of the Raging River Formation (Johnson, 1992, USGS Open-File Rept. 92-581); similar rocks probably underlie the Morton area.

SOURCE ROCKS AND MATURATION

Samples of the Raging River Formation contain significant amounts of organic matter, but are overmature and do not yield reliable petroleum source-rock data. Occurrence of numerous coals in the Morton anticline area indicates some possibility for methane derived from the coals. We infer that rocks similar to the Raging River, McIntosh, and Carbonado Formations (Figure 4) make up a significant portion of the SWCC, in addition to older sedimentary rocks of Paleocene or Cretaceous age.

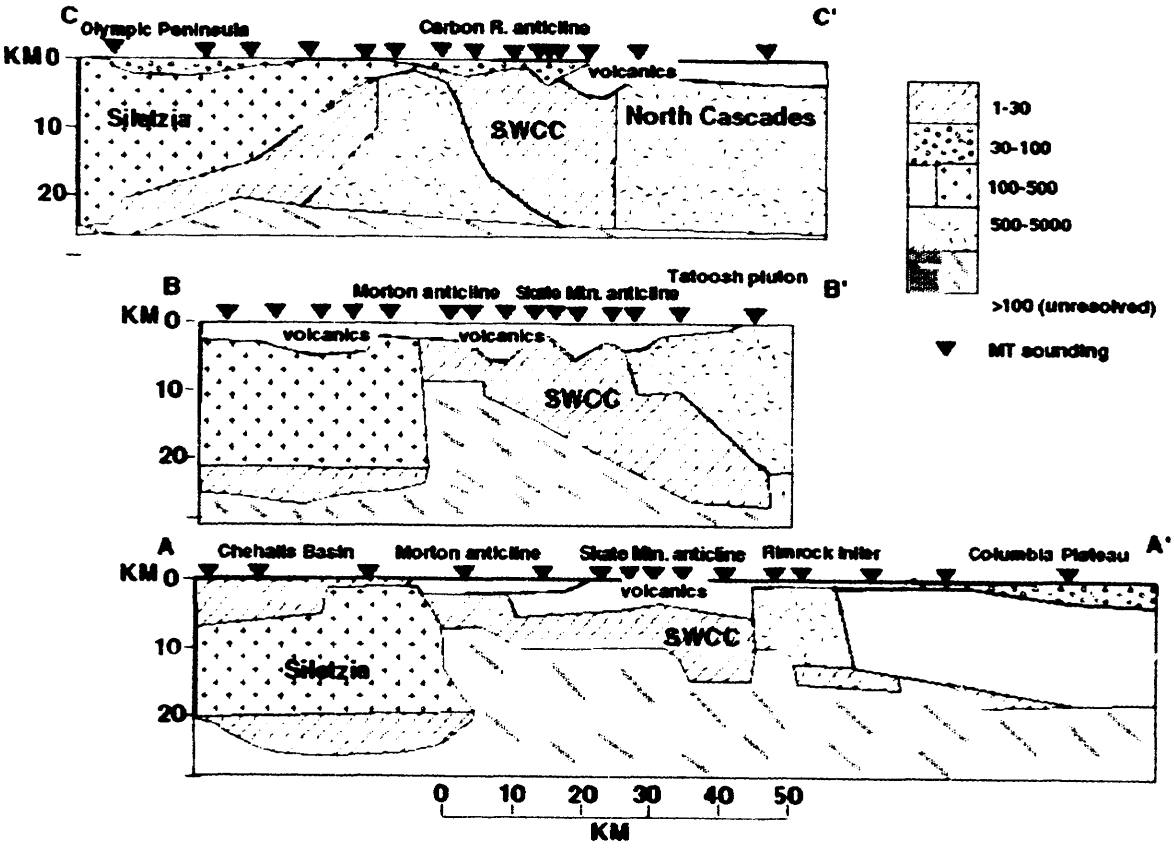

Figure 3-MT models for the three profiles indicated in Fig. 1.

Vitrinite reflectance data from an AMOCO stratigraphic test well in the Morton anticline range from $R_0=1.34$ to 0.96 percent (depths of 524 m and 171 m, respectively). Samples from two surface sections on the west flank of the anticline have R_0 values of 0.59 to 0.78 percent. Samples from a section in Coal Canyon on the east flank of the anticline have values ranging from 0.40 to 0.52 percent. Samples collected adjacent to small intrusions have elevated vitrinite reflectance values ranging up to 2.21 percent. Coal-rank data (Walsh and Lingley, 1991, Washington Dept. of Natural Resources, Rept. 91-2.) show predictable increases in maturation eastward across the region towards the Cascades magmatic arc.

Preliminary petrographic analysis indicates that sandstones from the Morton anticline are largely plagioclase-rich, arkosic arenites, with variable porosity controlled by calcite cement and clay minerals. Unsubstantiated reports of secondary porosity in Puget Group units mapped in mines in the Morton area may be an indication of possible reservoir potential. However, extensive evidence for transpressive deformation, fracturing, and faulting of the Morton anticline must be considered negative factors for the occurrence of a suitable reservoir. Such considerations, along with the limited evidence for adequate source rocks, make the Morton anticline area a high-risk exploration target, but possibly one of the few remaining to be tested in western Washington.

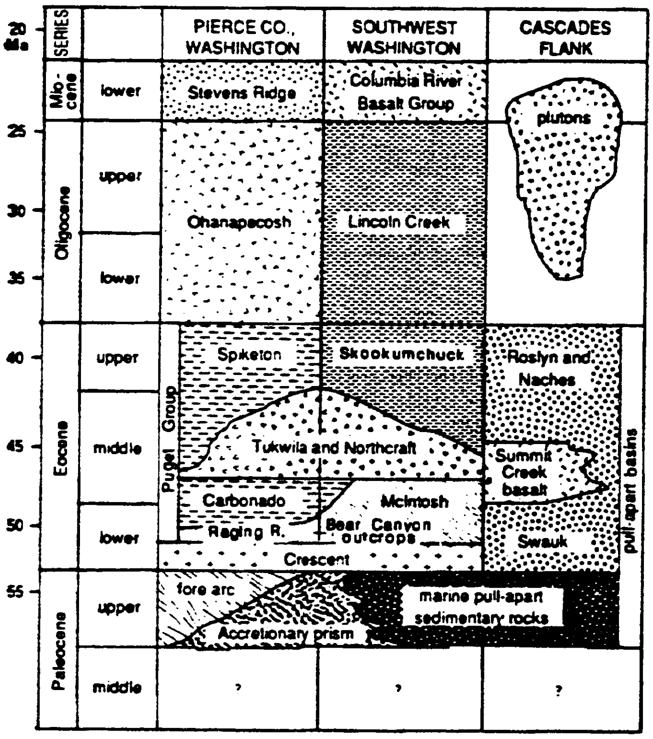

Figure 4-Stratigraphic chart for the SWCC region.

SEISMIC STRATIGRAPHIC ANALYSIS

Details of the seismic reflection data are indicated in the poster session for this meeting and will be included in the contract final report, but displays of data from lines 1/2 and line 3 are shown in Figures 5 and 6. Figure 5 indicates the key seismic-stratigraphic elements in the data: the Crescent Fm. basement, a highly layered zone within the SWCC, and upper zones coinciding with non-marine parts of the Puget Group sequences and the uppermost volcanic section. The location of a proposed 12,000' deep stratigraphic test to be drilled by Hunt Oil Co. in 1994 is indicated near the crest of the Morton anticline. Figure 6 shows reprocessed data from line 3, indicated a thick pile of reflective volcanics in a large syncline east of Packwood, WA. This syncline developed during the volcanic activity as indicated by the onlap nature of most of the flows. The syncline involved thick (up to 10 km) of layered, presumed sedimentary rocks that comprise the SWCC and are probably basal Puget Group and older basin sediments. The units are thrust over unfolded rocks of similar age west of the Skate Mtn. Anticline. This thrust is seismically active, as indicated in the poster display for this project.

Work is continuing on stratigraphic analysis of all of the DOE data, combined with several proprietary reflection profiles from Lauren and Voyager Corporations, and relying upon new geological mapping and well studies being done in conjunction with this projects and others.

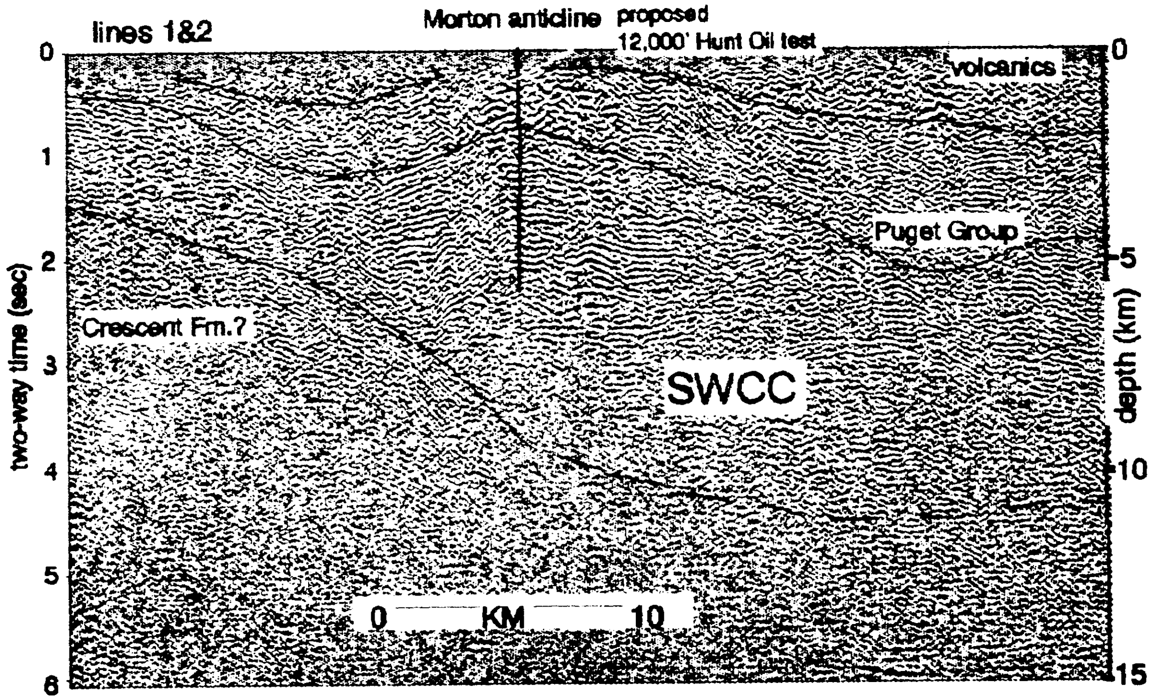

Figure 5-Reprocessed and combined data for DOE lines 1 and 2. A constant velocity of 5 km/s was assumed for the depth scale.

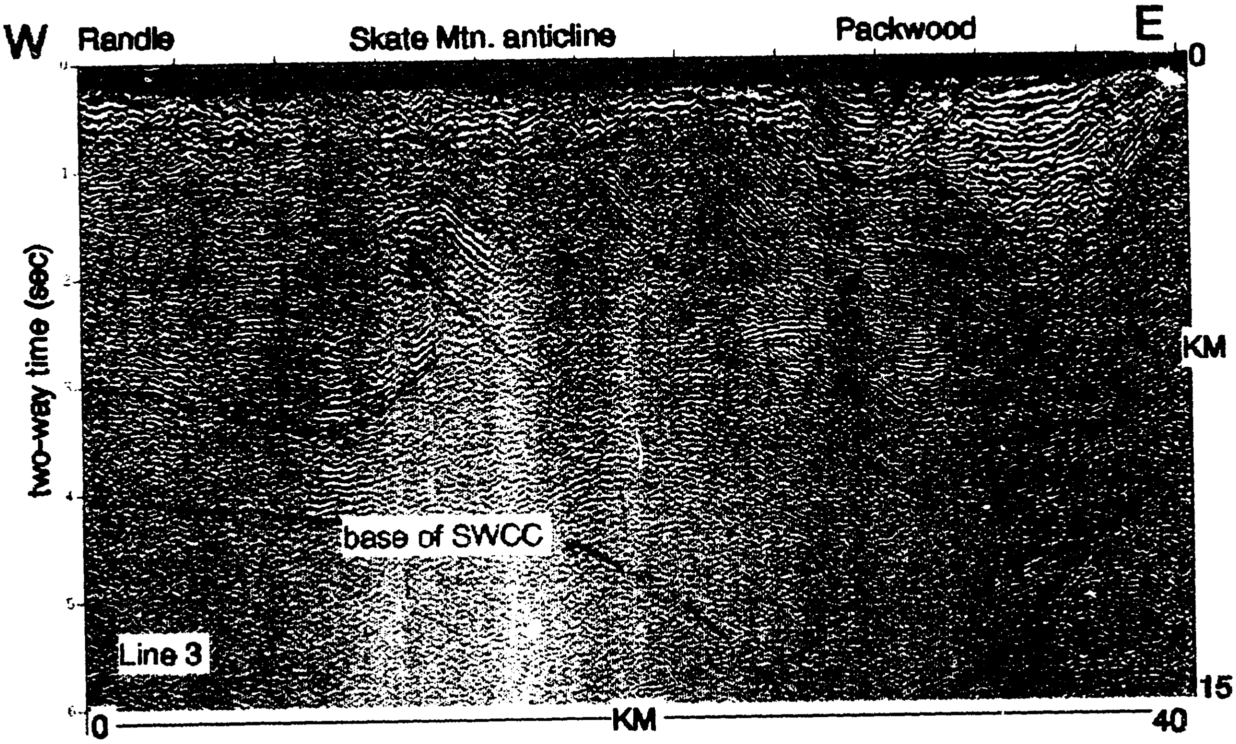

Figure 6-Reprocess data with minor interpretive details for DOE line 3. A constant velocity of 5 km/s was assumed for the depth scale.

P11 Analysis and Evaluation of Gas Hydrate on Alaska's North Slope

CONTRACT INFORMATION

Contractor	U.S. Geological Survey Denver Federal Center Box 25046, MS-940 Denver, Colorado 80225 (303) 236-5731
Contractor Project Manager	Timothy S. Collett
Principal Investigators	Kenneth J. Bird Robert C. Burruss Myung W. Lee
METC Project Manager	Rodney D. Malone
Period of Performance	October 1, 1983 to September 30, 1993

ABSTRACT

The primary objective of this project is to assess the production characteristics and economic potential of continental gas hydrates. Because of national interest and the abundance of geologic data, our research has focused on assessing the gas hydrates within northern Alaska. This project has been designed to obtain a clear understanding of the gas hydrate resource potential in northern Alaska and to develop the extraction technology necessary to economically produce gas hydrates. This study has resulted in the discovery of an estimated 40 tcf of gas trapped as gas hydrates, or about twice the volume of conventional gas in the Prudhoe Bay field. On the North Slope, the zone in which methane hydrates may exist is areally extensive beneath most of the Arctic coastal plain and extends to depths greater than 1,000 m in the Prudhoe Bay area. Gas hydrates have been conclusively identified and tested in a Prudhoe Bay field well and are inferred to occur in a series of discrete reservoirs overlying the eastern part of the Kuparuk River field, the southern part of the Milne Point field, and the western part of the Prudhoe Bay field. Recently, multichannel seismic data from northern Alaska has revealed the first ever observed onshore gas hydrate surface simulating reflector (SSR). This prominent reflector in the Prudhoe Bay area coincident with the base of the gas hydrate stability zone is postulated to be the result of free-gas trapped stratigraphically downdip below gas-hydrate-bearing sediments. The discovery of this SSR confirms the occurrence of gas hydrates on the undrilled offshore Alaskan continental shelf. The presence of free-gas trapped below the gas hydrates in the Prudhoe Bay area is analogous to the Messoyakha gas-hydrate/free-gas accumulation in western Siberia from which ≈70 bcf of gas has been produced from hydrates alone. The production history of the Messoyakha field has demonstrated that gas hydrates are an immediate producible source of natural gas and that production can be started and maintained by conventional methods. The geologic comparison of the Messoyakha and Prudhoe Bay-Kuparuk River gas hydrate accumulations suggests that the Alaskan gas hydrates may also be a producible source of natural gas.

At present, North Slope conventional gas reserves are being used for electrical power generation, reservoir pressure maintenance, gas-lift operations, and a myriad of other purposes.

However, the demand for gas in northern Alaska is out-pacing the available supplies. In the future, as conventional oil production declines, additional sources of gas will be needed to fuel numerous EOR projects. For example, the West Sak, Ugnu, and Schrader Bluff reservoirs, which may contain 40 billion bbl of in-place low-gravity oil, will likely be subjected to immiscible gas and water floods, and energy intensive steam floods. Hydrates may represent an important source of natural gas, which may be utilized to fulfill the steadily increasing demand for gas in northern Alaska. The need for additional gas reserves in northern Alaska has stimulated the development of a three-year joint industry-government project to evaluate the economic and engineering feasibility of natural gas recovery from in-situ natural gas hydrates on the North Slope. This project will be ran by a multi-disciplinary team with expertise in well logging, horizontal-drilling, formation fracturing, reservoir engineering, and production modeling. Potential project participants include ARCO Alaska, British Petroleum Exploration, Exxon Company, Conoco, Halliburton, IIT Research Institute, U.S. Department of Energy, and the U.S. Geological Survey.

Other ongoing gas-hydrate-related studies in the USGS have focused on (1) the potential geologic hazards of Arctic gas hydrates and (2) the relation between atmospheric methane, a greenhouse gas, and destabilized in-situ gas hydrates. United States, Canadian, and Soviet researchers have described numerous drilling and production problems attributed to the presence of gas hydrates, including uncontrolled gas releases during drilling, collapsed casings, and gas leakage to the surface. In several reports we have documented geologic problems attributed to the presence of gas hydrates. Analysis of gases trapped in ice cores indicates that contemporary atmospheric methane concentrations and their rate of increase are unprecedented over the last 160,000 years. Numerous researchers have suggested that destabilized gas hydrates may be contributing to this buildup in atmospheric methane. One of the areas of greatest concern is the thermally unstable continental shelf of the Arctic Ocean. Since little is known about the geology of the Arctic Shelf, our onshore Alaska gas hydrate studies are being used to develop geologic analogs for potential Arctic Shelf gas hydrate occurrences.

PUBLICATIONS

This project has been responsible for the publication of 110 professional and administrative reports, listed below are several of our most significant contributions.

Collett, T.S., and Kvenvolden, K.A., 1990, Exploration for gas hydrates: United Nations Seminar on Petroleum Geology and Geochemistry, May 31-June 6, 1989, Kiev, U.S.S.R., Proceedings, 6 p. [Also published in the Geological Magazine of Ukrainian USSR Academy of Sciences, v. 1, p. 8-14.]

Collett, T.S., Kvenvolden, K.A., and Magoon, L.B., 1990, Characterization of hydrocarbon gas within the stratigraphic interval of gas-hydrate stability on the North Slope of Alaska: Applied Geochemistry, v. 5, p. 279-287.

Collett, T.S., 1992, Potential of gas hydrates outlined: Oil and Gas Journal, June 22, p. 84-87.

Yakushev, V.S., and Collett, T.S., 1992, Gas hydrates in permafrost regions--the risk to drilling and production operations: Second International Offshore and Polar Engineering Conference, June 14-19, 1992, San Francisco, California, Proceedings, v. 1, p. 669-673.

Collett, T.S., 1993, Natural gas hydrates of the Prudhoe Bay and Kuparuk River area, North Slope, Alaska: American Association of Petroleum Geologist Bulletin, v. 77, no. 5, p. 793-812.